

Diagnostyka

Diagnostics and Structural Health Monitoring

Rok założenia 1990

ISSN 1641-6414



Nr 4(60)/2011

RADA PROGRAMOWA / PROGRAM COUNCIL

PRZEWODNICZĄCY / CHAIRMAN:

prof. dr hab. dr h.c. mult. **Czesław CEMPEL** *Politechnika Poznańska*

REDAKTOR NACZELNY / CHIEF EDITOR:

prof. dr hab. inż. **Ryszard MICHAŁSKI** *UWM w Olsztynie*

CZŁONKOWIE / MEMBERS:

prof. dr hab. inż. **Jan ADAMCZYK**

AGH w Krakowie

prof. **Francesco AYMERICH**

University of Cagliari – Italy

prof. **Jérôme ANTONI**

University of Technology of Compiègne – France

prof. dr. **Ioannis ANTONIADIS**

National Technical University Of Athens – Greece

dr inż. **Roman BARCZEWSKI**

Politechnika Poznańska

prof. dr hab. inż. **Walter BARTELMUS**

Politechnika Wroclawska

prof. dr hab. inż. **Wojciech BATKO**

AGH w Krakowie

prof. dr hab. inż. **Adam CHARCHALIS**

Akademia Morska w Gdyni

prof. **Li CHENG**

The Hong Kong Polytechnic University – China

prof. dr hab. inż. **Wojciech CHOLEWA**

Politechnika Śląska

prof. dr hab. inż. **Zbigniew DĄBROWSKI**

Politechnika Warszawska

Prof. **Charles FARRAR**

Los Alamos National Laboratory – USA

prof. **Wiktor FRID**

Royal Institute of Technology in Stockholm – Sweden

dr inż. **Tomasz GAŁKA**

Instytut Energetyki w Warszawie

prof. **Len GELMAN**

Cranfield University – England

prof. **Mohamed HADDAR**

National School of Engineers of Sfax – Tunisia

prof. dr hab. inż. **Jan KICIŃSKI**

IMP w Gdańsku

prof. dr hab. inż. **Daniel KUJAWSKI**

Western Michigan University – USA

prof. **Graeme MANSON**

University of Sheffield – UK

prof. dr hab. **Wojciech MOCZULSKI**

Politechnika Śląska

prof. dr hab. inż. **Stanisław RADKOWSKI**

Politechnika Warszawska

prof. **Bob RANDALL**

University of South Wales – Australia

prof. dr **Raj B. K. N. RAO**

President COMADEM International – England

prof. **Massimo RUZZENE**

Georgia Institute of Technology – USA

prof. **Vasily S. SHEVCHENKO**

BSSR Academy of Sciences Mińsk – Belarus

prof. **Menad SIDAHMED**

University of Technology Compiègne – France

Prof. **Tadeusz STEPINSKI**

Uppsala University - Sweden

prof. **Wiesław TRĄMPCZYŃSKI**

Politechnika Świętokrzyska

prof. dr hab. inż. **Tadeusz UHL**

AGH w Krakowie

prof. **Vitalijus VOLKOVAS**

Kaunas University of Technology – Lithuania

prof. **Keith WORDEN**

University of Sheffield – UK

prof. dr hab. inż. **Andrzej WILK**

Politechnika Śląska

dr **Gajraj Singh YADAVA**

Indian Institute of Technology – India

prof. dr hab. inż. **Bogdan ŻÓŁTOWSKI**

UTP w Bydgoszczy

WYDAWCA:

Polskie Towarzystwo Diagnostyki Technicznej
ul. Narbutta 84
02-524 Warszawa

REDAKTOR NACZELNY:

prof. dr hab. inż. **Ryszard MICHAŁSKI**

SEKRETARZ REDAKCJI:

dr inż. **Sławomir WIERZBICKI**

CZŁONKOWIE KOMITETU REDAKCYJNEGO:

dr inż. **Krzysztof LIGIER**

dr inż. **Paweł MIKOŁAJCZAK**

ADRES REDAKCJI:

Redakcja Diagnostyki
Katedra Budowy, Eksploatacji Pojazdów i Maszyn
UWM w Olsztynie
ul. Oczapowskiego 11, 10-736 Olsztyn, Poland
tel.: 89-523-48-11, fax: 89-523-34-63
www.diagnostyka.net.pl
e-mail: redakcja@diagnostyka.net.pl

KONTO PTD:

Bank PEKAO SA O/Warszawa
nr konta: 33 1240 5963 1111 0000 4796 8376

NAKLAD: 500 egzemplarzy

Spis treści / Contents

Piotr KOHUT, Krzysztof HOLAK, Tadeusz UHL – AGH University of Science and Technology in Kraków	3
Prototype of the vision system for deflection measurements <i>Prototyp systemu wizyjnego do pomiarów ugięć</i>	
Paweł MIKOŁAJCZAK – UWM Olsztyn	13
Prediction of changes in the technical condition using discriminant analysis <i>Prognoza parametrów diagnostycznych z wykorzystaniem analizy dyskryminacyjnej</i>	
Mateusz MARZEC, Tadeusz UHL, Tomasz BARSZCZ – AGH University of Science and Technology in Kraków	21
Application of UML modelling for analysis of safety integrity level in railway traffic control systems <i>Zastosowanie języka UML do badania poziomu nienaruszalności bezpieczeństwa systemów sterowania ruchem kolejowym</i>	
Czesław CEMPEL – Poznan University of Technology	27
Singular values of symptom observation matrix of a system in operation as indicators of system damage <i>Wartości szczególne symptomowej macierzy obserwacji eksploatowanego systemu mechanicznego jako wskaźniki zużycia</i>	
Dariusz BRODA, Tomasz BARSZCZ – AGH University of Science and Technology in Kraków	39
Description of varying operational conditions in wind turbines <i>Opis zmienności warunków operacyjnych turbin wiatrowych</i>	
Jędrzej MĄCZAK – Warsaw University of Technology	47
Application of the local meshing plane in detecting assembly and manufacturing errors of gears <i>Wykorzystanie lokalnej płaszczyzny przyporu w wykrywaniu błędów wykonania i montażu przekładni zębatych</i>	
Adam CHARCHALIS, Mirosław DERESZEWSKI – Gdynia Maritime University	53
Monitoring of instantaneous angular speed of the crankshaft for control of the ship engine performance changes <i>Monitorowanie chwilowej prędkości kątowej wału korbowego w celu kontroli zmian jakości pracy silnika okrętowego</i>	
Maciej KLEMM, Maciej TABASZEWSKI – Poznan University of Technology	59
Agent approach in machine diagnosis <i>Podejście agentowe w diagnostyce maszyn</i>	
Bogdan POJAWA – Polish Naval Academy	65
Tests of LM2500 naval gas turbine with the objective of determining its operating characteristics <i>Badania okrętowego turbinowego silnika spalinowego LM2500 w aspekcie wyznaczenia charakterystyk obrotowych</i>	
Stanisław RADKOWSKI, Robert GUMIŃSKI – Warsaw University of Technology	71
Use of Hough's transform for designing the decision-making module of a proactive operations system <i>Wykorzystanie transformacji Hough'a w projektowaniu modułu decyzyjnego systemu proaktywnej eksploatacji</i>	
Warto przeczytać / Worth to read	77
Lista recenzentów artykułów opublikowanych w czasopiśmie Diagnostyka w 2012 roku	78

PROTOTYPE OF THE VISION SYSTEM FOR DEFLECTION MEASUREMENTS

Piotr KOHUT, Krzysztof HOLAK, Tadeusz UHL

AGH University of Science and Technology, Department of Robotics and Mechatronics
Al. A. Mickiewicza 30, 30-059 Krakow, tel. 12 6173396
pko@agh.edu.pl, holak@agh.edu.pl, tuhl@agh.edu.pl

Summary

The vision-based method of civil engineering construction's in-plane deflection measurements was developed. Displacement field of the analyzed structure resulting from load was computed by means of digital image correlation coefficient. The application of homography mapping enabled the deflection curve to be computed from two images of the construction acquired from two distinct points in space. The shape filter and rectangular marker detector were implemented to provide higher level of automation of the method. There are discussed developed methodology, created architecture of software tool as well as experimental results obtained from tests made on lab set-ups.

Keywords: digital image correlation, image registration, vision systems, deflection measurement.

PROTOTYP SYSTEMU WIZYJNEGO DO POMIARÓW UGIĘĆ

Streszczenie

W pracy przedstawiono opracowany prototyp systemu wizyjnego do pomiarów dwuwymiarowych deformacji konstrukcji. Pole przemieszczeń analizowanego obiektu, powstałe pod wpływem działających obciążeń, wyznaczono przy pomocy znormalizowanego współczynnika korelacji. Zastosowanie przekształcenia homograficznego umożliwiło wykonanie pomiarów ugięcia konstrukcji na podstawie jej dwóch obrazów zarejestrowanych z dwóch różnych punktów przestrzeni. Zaimplementowany filtr kształtów oraz detektor znaczników referencyjnych umożliwił zwiększenie automatyzacji procesu pomiarowego. W artykule przedstawiono opracowaną metodykę, architekturę stworzonego oprogramowania oraz wyniki testów eksperymentalnych systemu na stanowisku laboratoryjnym.

Słowa kluczowe: korelacja obrazów, nakładanie obrazów, systemy wizyjne, pomiary ugięcia.

1. INTRODUCTION

Structural Health Monitoring methods can be divided into two main categories: local methods and global methods. The latter are applied if a global change in the geometry or motion of a structure under the loads can be observed. On the other hand, local methods make use of the physical phenomena acting locally within a small area of the construction. Vision-based techniques belong to the group of contactless global SHM methods which enable global measurements of static deformations as well as dynamic processes to be carried out. They allow damage detection to be performed by means of a change in the geometry of a structure analysis, such as deflection curve or mode shapes of vibrations. In diagnostics of civil engineering structures, displacements' measurements are the major aspect of constructions' static states and dynamic characteristics evaluation. In this area, the analysis of deflection shapes of structures has become more significant and accurate than other methods of the analysis [1-6].

Nowadays, the increase of availability of vision systems for the measurement of motion and three-dimensional geometry of objects is noticed on the world markets. However their number is still small in the field of measurement of deformations and low-frequency vibration of structures.

In this paper, the developed prototype of vision based system, for in-plane measurement of civil engineering structures displacement fields' is presented. The system provides monitoring of static states of civil engineering constructions such as displacements, deflections and deformations. The system consists of one or more high resolution digital cameras mounted on a head or on portable tripods, the software embedded in MS-Windows operating system, lighting system and the set of special markers placed on the construction. Calibration patterns which enable computation of the scale coefficient and lens distortions are also parts of the system.

Deflection curve is obtained from two images of the construction: reference one and the one acquired after application of a load. The principle of the

method is calculation of object's points displacement by means of normalized cross correlation coefficient. Image registration techniques were introduced in order to increase flexibility and accuracy of the method. Perspective distortions of the construction's image are removed by means of homography mapping, which allows two photographs of the object to be taken from two distinct points in space. In order to calculate correspondences between matching features on both images, new technique of markers detection and shape filtering, as well as sub-pixel corner detection are introduced.

2. VISION MEASUREMENT SYSTEMS CURRENTLY AVAILABLE ON THE MARKET

Nowadays, there are a lot of optical systems for three-dimensional structure and motion measurements. These systems allow for considerable shortening of a time needed for carrying out phenomena analysis, as well as getting three-dimensional structures of inspected objects. In this paper, optical measuring systems available on the market were listed, their most important features were described and they were divided into groups on account of the principle based on which they operate. The most important companies offering vision measurement systems existing at present on the market are: Correlated Solution, GOM, LIMESS Messtechnik & Software, Dantec Dynamics, Metris (Krypton 9000) [7-24].

There are following systems for the measurement of three dimensional motion available: PONTOS/TRITOP (GOM), Vic 2D/Vic 3D (Correlated Solution/LIMESS). Accuracies of these systems vary in the range from 1/50 to 1/100 pixels, whereas sizes of measured object depend on the configuration of the system: from a few mm up to 10 m. Available frequencies of images acquisition are in the range from a few to a few hundred thousand frames per second, depending on the used resolution and the field of view. For example in the PONTOS system, carrying out measurements requires placing special markers on examined structures. An acquisition of vibration of the structures with the help of the pair of high-frequency cameras is the next step of the measurement. A course of the displacement of particular points of the object is the analysis result.

The systems PONTOS ARAMIS/ (GOM), Vic 2 D/Vic 3 D (Correlated Solution/LIMESS) or Q- 400 - II (Dantec Dynamics) can be applied to measurements of displacements, deformations and stresses of the structure. ARAMIS (GOM) is an example of systems of this type, which enable analysis of the deformation and stresses of objects with complicated geometry, deformed under the load. The system uses the method of three-dimensional correlation and high resolution digital cameras. A stochastic or regular pattern is placed on

the inspected structure. The object under the load is observed by one or more digital cameras. The visualization of three-dimensional deformations of the structure is obtained as a result of the analysis.

Systems ATOS, TRITOP (GOM), and 3 D-Cam (Correlated Solution/LIMESS) are used in the reverse engineering for the measurement of the three-dimensional shape of objects. ATOS is the active vision system, which means that a shape of the light pattern projected onto the examined surface is analyzed. The scanner works on the principle of a triangulation, two cameras are observing courses of stripes on the measured detail which enables three-dimensional coordinates of all points of interest to be determined. Measurements requires placing round markers with a known diameter on the analyzed structure. In the next step, the prepared object is registered by a photogrammetric camera from a few different points of view. The software allows for finding coordinates of all markers.

Three-dimensional measurements of geometry using three cameras are carried out by the following devices: Krypton of K series (Metris) and OPTIGO (Cognitens). Krypton system uses 3 linear cameras, additionally it has a possibility of tracking the markers put on the structure, whereas OPTIGO uses 3 matrix cameras for the measurement of a geometry. Active interferential techniques are offered by systems: ESPI SD-30 / SD-10S systems (GOM); Shearwin NT (Correlated Solution /LIMESS), or Q-810 (Dantec Dynamics) can be applied for the measurement of the deformation. Measurement methods are based on phenomena of interference and they concern little objects [7 - 24].

3. MEASUREMENT METHOD

The method of non-contact measurement of civil engineering constructions' in-plane deflection consists of three major steps [1-4]. In the first step, a rectification [25],[26] of images acquired from distinct points of view, not coincident with the reference one which can be chosen by an user, is performed by means of homography matrix \mathbf{H} . In the following step, the deflection of a construction is calculated using the normalized cross correlation coefficient (NCC). Sub-pixel feature detection techniques were introduced in order to increase the accuracy of the measurement. In the final step, the scale coefficient is computed with the help of a circular intensity pattern with a known diameter. The developed algorithm is presented on figure 1.

Image registration [30] is a method of stitching two or more images taken at different times, from distinct points of view or by using different imaging devices. In this work, homography mapping was introduced to align two images acquired from distinct points of view.

Image rectification [1-4],[25],[26] is a process of projective distortions reduction by means of homography transformation. Four pairs of coplanar corresponding points are sufficient for the

computation of matrix **H** if none three of them are collinear.

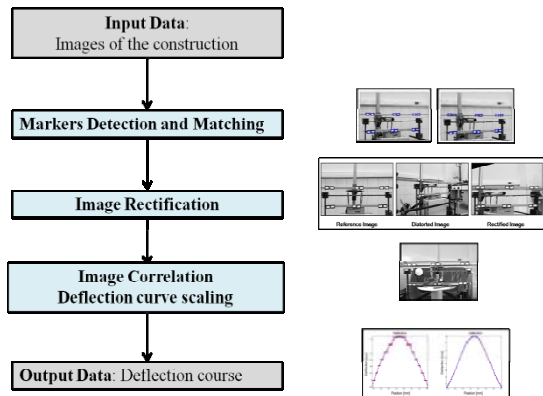


Fig. 1. Developed algorithm of the in-plane deflection measurement

The set of corresponding points used for the homography computation consist of vertices of rectangular markers, which are placed on the structure. Markers must be coplanar with the plane of the construction and can't change their position as it deforms [1-4]. Coordinates of the corresponding points on both images are calculated by automatic corner detector. In the first step, rectangles are detected on images by means of contour processing and shape filtering methods. Exact positions of each of markers' vertices are determined by the sub-pixel improvement of the detector. Vertices' positions are expressed in polar coordinates in the coordinate frame with the origin at the center of mass of markers' set. Markers are sorted by comparison of their corners' polar angles and distances from the origin. As the alternative for the aforementioned method of feature matching, image patch correspondence matching based on binary codes recognition has been developed. When the homography mapping between two images of a construction is calculated, projective distortions of the particular plane of the object are removed from the image.

The normalized cross correlation coefficient [25,26] (NCC) is applied for the computation of the in-plane displacement field. In the developed method, the reference image of unloaded construction is divided into intensity patterns whose position are computed by means of the NCC coefficient. The displacement vector for each of the measurement points is computed as a difference between positions of the pattern on two images of the construction: taken before and after application of a load. [1-4].

In order to express a deflection curve in metric units, calibration of the system is necessary. It is performed by a circular intensity pattern with a known diameter. Optionally, full camera calibration is performed in order to obtain intrinsic parameters, which are necessary for reduction of radial and tangential lens distortions [1-4].

4. FEATURE POINT DETECTION AND MATCHING

The higher level of automation was provided by development of novel markers' detection and matching algorithm. Two sets of rectangles are detected on two images by means of binary image processing, contour detection and shape filtering. The set of corresponding points positions necessary for homography computation, consisting of vertices of rectangles, are calculated by Harris corner detector with a sub-pixel improvement of the accuracy. Markers are expressed in polar coordinates and sorted with respect to marker set's center of the mass.

The binary image *I* of resolution *M* by *N* is the image which consist of two kind of pixel areas: *A* – the foreground and *B* – the background where *A* and *B* are two sets of pixels defined as [27-29]:

$$A = \{(x, y) : 0 \leq x \leq M, 0 \leq y \leq N \text{ and } I(x, y) = 1\} \quad (1)$$

$$B = \{(x, y) : 0 \leq x \leq M, 0 \leq y \leq N \text{ and } I(x, y) = 0\}$$

Let D_8 be the 8-neighbourhood [27-29] of a pixel $p_i = (x, y)$. A closed contour (or a boundary) of a foreground region *A* on a binary image is a set of pixels defined as follows:

$$cc = \{p_{i=1,2,\dots,n} \in A : (\forall p_i \exists p \in (B \cap D_8(p_i)) \text{ and } p_i = p_N)\} \quad (2)$$

The first step of the algorithm is binarization of a grayscale image. The threshold value is obtained by analysis of an intensity histogram of an image. In the next step, contours enclosing all foreground object are detected [27-29] on both of images. Contours are transformed to the chain polygon representation in which only endpoints of the line elements approximating the contour are stored. In the case of the implementation of the method in described software, the set of points consist of vertices of rectangular markers. Contours are filtered by the shape filter whose response is the strongest for convex, rectangular contours with user defined ranges of: area enclosed by the boundary, width to height ratio and angle between sides of the quadrilateral. Obtained vertices positions are refined by Harris corner detection algorithm with the sub-pixel accuracy improvement. The example of application of the method is illustrated on figure 2.

It is assumed that there is no rotation about the optical axis of the camera coordinate frame from which the reference image was obtained. In the first step, the center of mass of set of markers' vertices is computed. The calculated point becomes the origin of the new coordinate frame. All of the points have to be expressed in this new coordinate frame in the polar representation. Next, the sorting of points is performed. Points' polar angles and radial distances from the origin are input to the comparison function passed to the sorting algorithm. The sorting is

carried out on sets of markers on both images of the construction.



Fig. 2. Example of the application of rectangle detection algorithm

In the second method, the position and orientation of the camera is not constrained by the requirement of no rotation described above. The image patches which are matched on two images are coded markers. The marker consists of N rows and N columns of small squares arranged in chessboard-like pattern. Each of the squares can be black which represents logic 1 or white which represent logic 0. The innermost 2×2 pattern of the marker is the same for all markers and resemble letter 'L' (see figure 3). The outer part of the chessboard pattern is different for each marker and encodes the number. The position of each square marker on the image is detected by means of algorithm described previously. Next, the homography mapping is applied to remove the perspective distortions from the image of the marker. Image patch is rectified using data from marker model which is specified by the user. The marker orientation is decoded from the innermost 'L' shaped pattern of the marker. In the last step, the image patch is encoded as $N \times N$ array of logical values. In the pattern matching step, actual images of markers are not compared with each other, but instead their code representations are. The process is much faster than image pattern matching methods.

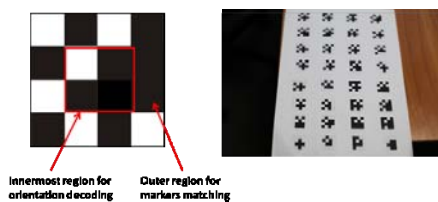


Fig. 3. Example of marker used for pattern matching and set of markers on real photograph

The matching of markers by means of their code representations' comparison can be applied in problems like image rectification, image registration method (image stitching, mosaicing) as well as in 3D structure and motion reconstruction techniques based on epipolar geometry [25,26] and fundamental matrix (corresponding set of points needed for F matrix computation can be encoded as the chessboard pattern markers).

5. DEVELOPED SOFTWARE

The main purpose of the software is construction's continuous monitoring and diagnostics. As a standalone system (operating in on-line mode) can immediately evaluate changes of static states of structure and send them to a diagnostic center.

Application provides advanced operations on camera devices like live preview mode or remote modification of camera parameters. System's IO Handler module allows multiple picture acquisition devices to operate in the real-time. Application supports popular SLR cameras with available driver libraries used for device management from system.

Calibration module (figure 4) allows calculating calibration data based on images of a planar chessboard pattern with a known geometry (odd row and even column count). Calibration process results contains intrinsic and extrinsic camera parameters. Calibration data is necessary for identification of camera's position and orientation with respect to the examined object. The intrinsic camera parameters can be used for reduction of radial and tangential distortions from acquired images.

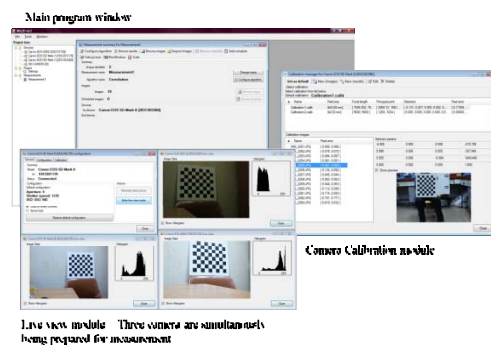


Fig. 4. Software modules: main window, live preview, camera parameter setting module and camera calibration module

Camera configuration is accessed and modified from configuration window. Common modifiable camera parameters consists of shutter speed, aperture value and ISO speed. Configuration window provides also specific camera parameters: live view zoom and information about battery level. Enabling live view mode allows quick check on how modified parameters affect camera's work. It's possible to store camera configuration. Such stored configuration can be loaded into camera manually or automatically after connection (depending on settings).

The developed software tool provides a high level of measurement process automation, accomplished by automated operations like image acquisition, image preprocessing and algorithm calculation (Figures 4,5). Although the system is suitable for online work using data acquisition

devices, it's also possible to perform offline measurements using existing images.

Correlation algorithm provided with software tool is fully customizable: user can modify start/end point for measured line on calculated images, search window size and window count. During configuration it's possible to test algorithm on measurement images in order to fine-tune algorithm parameters. User can make algorithm work automatically whenever new image has been added to measurement. This feature combined with possibility of creating scheduled sequences of picture taking makes it possible for software to automatically execute data acquisition and calculation.

Rectification algorithm provides functionality on generating perspective transformation for images based on image markers' location on image. In rectification window user can modify rectification parameters and see preview images: original image, original image with drawn image markers' locations, transformed image and reference image. Rectification parameters are stored in the measurement configuration.

Scale algorithm is used for converting pixel values into real length unit. In order to calculate scale coefficient user has to load image containing circular marker and provide information about its size. After scale coefficient has been calculated, analyzed images results will be shown in millimetres instead of pixels.

The system warns the user when a critical level of measurement estimates has been exceeded. A message is sent by e-mail or text message. It's possible to send data to external monitoring and diagnostics systems using TCP/IP. Data generated by the application can be exported to external data sheets in popular formats e.g. Excel spreadsheet, PDF and HTML

The software architecture is shown in figure 6. The drivers (DRV) are the modules that provide data acquisition from cameras: configuration, remote picture taking and downloading. Drivers are coordinated by an IO Handler (IO HDLR) responsible for device data transfer synchronization to ensure no conflicts in the driver's work. The data processor (DATA PROC) performs all image calculations such as vision algorithms and preprocessing methods. The database server (DBS) is used for storing various project data – downloaded images, algorithm results and configuration. The limit checked module (ALM) checks if measurement estimates are within allowed limits. The messenger (MSGR) is responsible for sending messages when the estimate crosses limit values. The configuration server (CFGS) is a separate storage module used for storing system configuration. The watchdog (WDG) controls a system's performance.

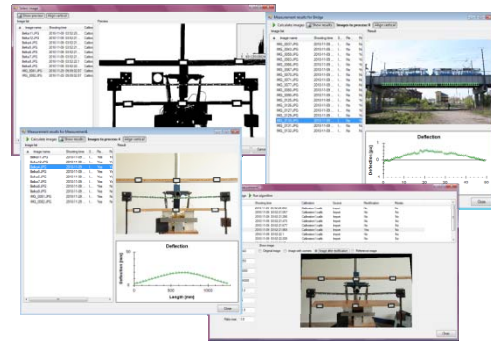


Fig. 5. Software modules: Measurement module, rectification module, image correlation module and result browsing module

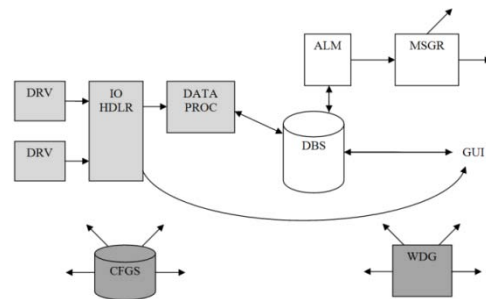


Fig.6. Software Tool Architecture

6. LAB TESTS OF THE DEVELOPED SOFTWARE

In the first examination, the system performance was tested on the lab-setup consisting of steel frame fixed at one end, loaded by the single weight (Figure 7,8). The point of application of the force could be moved along the length of the vertical part of the frame which provided variable loading conditions. Two digital SLR cameras Canon EOS 5D Mark II with a lens with Canon 24-70mm f/2,8L zoom lens with 50 mm focal length adjustment were placed in two points on the scene. The first one was positioned in such a way that its optical axis was perpendicular to the construction's plane. The second one was placed at the same distance from the construction as the first one, but its orientation was changed – the angle between its optical axis and the direction perpendicular to the frame's plane was 50 degrees. During the investigation, the load was moved along the length of the vertical part of the frame. The set of its positions (d [mm]) has been presented in table 1. For each of the load positions, 30 images were captured by both cameras. The mean value of the measured maximum deflection (in free endpoint of the beam) and its standard deviation were computed for deflection curves obtained by both cameras, for each of the positions of the load. The difference between the corresponding values of statistical parameters (mean value of maximum deflection) calculated from the data captured by the first camera and the second one was a measure of the error

introduced to the system by the rectification algorithm. Additionally, the noise of the method resulting from the lighting conditions as well as inaccuracy of correlation algorithm were investigated. The scale coefficient value in the examination was 0.174 mm/pixel.

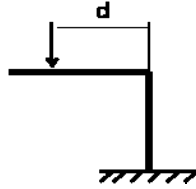


Fig. 7. The lab set-up



Fig. 8. The photograph of the first lab set-up

In next experiment, the developed software was tested by performing the continuous vision monitoring of the structure under the load. The wooden beam of the length of 180 cm supported at two ends was inspected construction (figure 9). The beam was loaded by a point force acting in the middle of its length. There was no artificial speckle pattern on the plane of the structure, natural texture of the material was used as an intensity pattern in correlation method. The measurement was verified with the help of the laser distance sensor Disto D5. The conducted experiment was divided into continuous measurement sessions of 30 photographs, separated by 10 minutes breaks. The continuous change of the deflection in the point of maximum deflection during investigation was observed (figure 13). It was confirmed on the basis of the measurement with the laser distance sensor.



Fig. 9. The photograph of the second lab set-up

The position of the camera with respect to the construction as well as its orientation were changed during the investigation. The measurement of the noise of the method was carried out to examine the influence of the lighting conditions on the method. The digital SLR camera Canon EOS 5D Mark II with Canon 24-70mm f/2,8L zoom lens with 45mm focal length adjustment was used. There were no artificial lights present on the scene. The measurement points from which images were acquired are shown on figure 10.

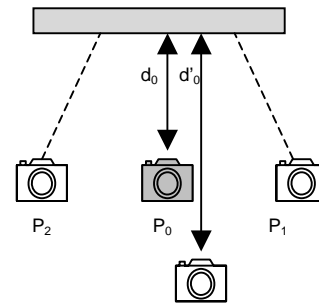


Fig. 10. The points of space from which images were acquired

7. RESULTS OF THE EXAMINATION

In the first examination, the mean value of the noise of the method for the natural lighting conditions was 0.002 mm (0.015%). For the images captured from one point in space, the standard deviation of calculated displacement value in the point of maximum deflection (repeatability of the method) was not affected by the change of position of the load and had value about 0.004 mm. Introduction of the rectification algorithm increased the error of the method. The maximum value of the difference between displacement calculated from the reference point and from the second position was about 0.15 mm. The relative error induced by the rectification calculated as the ratio between difference Δx (table 1) and the displacement computed from the reference image was in a range between 0.001% to 0.2%. The results of the examination are shown in the table 1. The examples of curves of deflection for different positions of load are presented on figure 10.

In the second experiment, when there was no artificial speckle pattern on the object because of that value of the measurement noise (its standard deviation obtained from a series of 30 images) of the method induced by variable illumination condition turned out to be 0.04 mm (Fig. 11). The standard deviation of the measured value of the deflection in the point of maximum deflection was 0.03 mm for the case of the images acquired from the same point in space, however the standard deviation of the measurement after application of rectification reached value of 0.19 mm.

Table 1. The results of examination. The first column – position of a load with respect to the fixed end of the frame (Figure 10). The columns 2 - 5 – results (mean value from 30 images and standard deviation) of deflection computation in point of maximum deflection for camera 1 and 2. The column 6 – difference between results obtained from two cameras, in mm, column 7 – the relative difference with respect to the first camera, in percents.

d[mm]	Camera 1		Camera 2		Δx	$\Delta x\%$
	mean	std	mean	std		
-	0.002	0.003	0.012	0.092	0.119	-
550	18.306	0.003	18.147	0.105	0.159	0.008
360	10.794	0.005	10.686	0.089	0.108	0.01
200	4.114	0.004	4.138	0.093	0.020	0.005
600	20.937	0.004	20.907	0.129	0.030	0.001
-	0.002	0.005	0.011	0.093	0.109	-

Results of measurement are shown on figure 12. In figure 13, an increase of the average value of beam's displacement in the maximum point of deflection resulting from the increasing deformation can be noticed. In figure 14, the change of the standard deviation resulting from application of the rectification algorithm was shown.

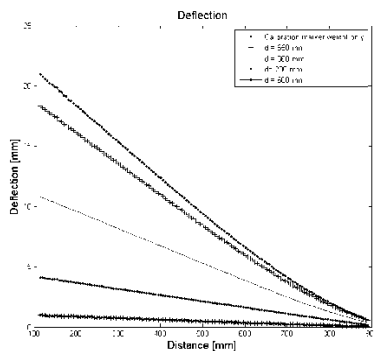


Fig. 10. Deflection courses for different cases of the loading (table 1). Results obtained from the reference camera

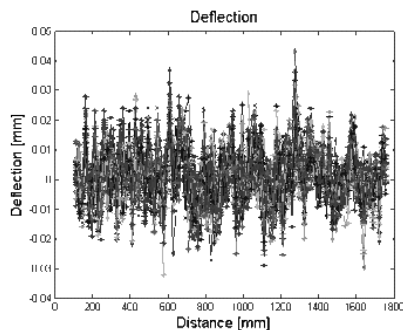


Fig. 11. The noise of the method in the case of object without artificial speckle intensity pattern

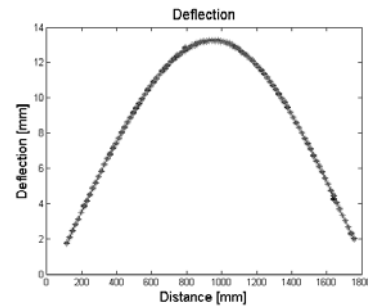


Fig. 12. Deflection curve family (from 30 images) calculated from images acquired from the Point P₀

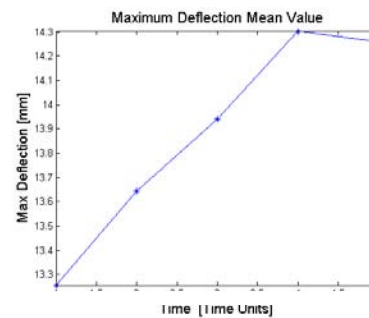


Fig. 13. Increase of the mean value of the displacement in the point of maximum deflection. Time interval between each point is 10 minutes.

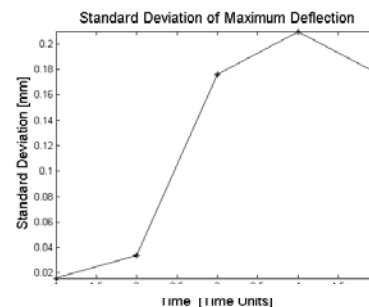


Fig. 14. Increase of the standard deviation of the displacement values calculated from the series of 30 images after application of rectification. Time interval between each point is 10 minutes

8. CONCLUSIONS

SHM vision-based measurement system enables structure static and quasi-static states assessments during inspections and on-line continuous state monitoring to be performed by means of analysis of changes in the geometric properties of the structure, such as a shape of the deflection curve. The introduction of image registration techniques has improved the flexibility, universality and accuracy of this method. The technique of in-plane deflection measurement, with application of image registration methods, presented in this article enables images of the construction to be taken from different points of view during examination. The lab tests revealed that the influence of the lighting on the performance of

the method was negligible (measurement noise value 0.03%). The standard deviation of the deflection computation, in the case of images obtained from the same point in space amounted to 0.004 mm. When the rectification algorithm was applied, the standard deviation of maximum deflection was located in the range between 0.03 mm to 0.15 mm for specimens with artificial speckle pattern and up to 0.2 mm for the objects without special texture. The developed techniques of marker detection and matching make it possible to create an application with fully automatic vision structure's on-line monitoring systems in which the construction can be examined during its everyday use. On the other hand, the developed methods can be applied in an user-friendly software which can help one to quickly assess the state of the construction during inspection. The system has employed easily available digital SLR camera as the measuring sensor for the measurement of static or quasi-static states of structures. It can be applied to the structures with an artificial texture in the form of the optical noise, natural texture of materials and when special geometric markers are available. The system has provided high measurement density without use of active optical methods. It can be employed to various civil engineering structures like bridges, footbridges, chimneys, viaducts, girders, ceilings, halls, masts, wind turbines, buildings, machines and devices.

ACKNOWLEDGEMENTS

Reported research realized within confines of OPIE project No: 01.01.02-00-013/08 co-financing by ERDF within a frame of Operational Program Innovative Economy.

BIBLIOGRAPHY

- [1] Kohut P., Holak K., Uhl T.: *Application of image correlation for SHM of steel structures*, Structural Health Monitoring 2008: proceedings of the fourth European workshop, Cracow, Poland, , July 2-4 2008, pp. 1257–1264
- [2] Uhl T.: *SHM of civil structures – methods, tools and applications*, Proceedings of the international conference on Experimental Vibration Analysis for Civil Engineering Structures EVACES'09, Dolnośląskie Wydawnictwo Edukacyjne, Wrocław 2009
- [3] Uhl T., Kohut P., Holak K.: *Construction deflection examination by means of correlation coefficient*, Proceedings of the 13th School of Modal Analysis, Cracow, Poland 2009,
- [4] Uhl T., Kohut P., Szwedo M., Holak K.: *Static and dynamic optical measurement in SHM of civil structures*, Proceeding of the 7th international workshop on Structural Health Monitoring, DESTech publications, Lancaster 2009
- [5] Kohut P., Kurowski P.: *The integration of vision based measurement system and modal analysis for detection and localization of damage*, Engineering achievements across the global village, The International Journal of INGENIUM, Cracow , 2005, pp.391-398
- [6] Kohut P., Kurowski P.: *The integration of vision system and modal analysis for SHM applications*, Proc. Of the IMAC-XXIV a conference and exposition on structural dynamics, January 30-February 02 St. Louis, 2006, pp. 1-8
- [7] Lee, M., Precht, M., Tyson, J., Schmidt, T.: *Application of 3D Measurement System with CCD Camera in Microelectronics, Advanced Packaging*, November 2003.
- [8] Schmidt, T., Tyson, J., Galanulis, K.: *Full-Field Dynamic Displacement and Strain Measurement Using Advanced 3D Image Correlation Photogrammetry*, Experimental Techniques, Vol.27, No.3, pp.41-44, May/June 2003.
- [9] Johnson, E., Woodard, N.: *Low-Cost Electrical Resistance Spot Welding Technique for Micro-Optical Component Mounting with Sub-Micron Tolerance*, Proceedings of Photonics Packaging Symposium, San Francisco, CA, Aug. 2003.
- [10] Schmidt, T., Tyson, J., Galanulis, K.: *Dynamic Strain Measurement Using Advanced 3D Photogrammetry*, Proceedings of IMAC XXI, Orlando, FL, Feb. 2003
- [11] Tyson, J., Schmidt, T., Shahinpoor, M., Galanulis, K.: *Biomechanics Deformation and Strain Measurements with 3D Image Correlation*, Experimental Techniques, Vol.26, No.5, pp.39-42, Sept./Oct. 2002
- [12] Tyson, J., Schmidt, T., Galanulis, K.: *Advanced Photogrammetry for Robust Deformation and Strain Measurement*, Proceedings of SEM. 2002 Annual Conference, Milwaukee, WI, June 2002
- [13] Hotz, W., Hänggi, P., *Determination of Forming Limit Curves*, 2001. Bergmann, D., Ritter, R., 3D Deformation Measurement in small Areas based on Grating Method and Photogrammetry, 1998
- [14] Alpers, B., Bergmann, D., Galanulis, K., Winter, D.: *Advanced Deformation Measurement in Sheet Metal Forming*, 1999
- [15] Steinchen, W. & Yang, L.: *Digital Shearography, Theory and Application of Digital Speckle Pattern Shearing Interferometry*, SPIE Press, 2003
- [16] Schmidt, T., Tyson, J.: *Pulsed Laser Systems for Wide Field Vibration Analysis*, ASNT Fall Conference, Oct. 2000
- [17] Tyson, J.: *Non-Contact Full-field Strain Measurement with 3D ESPI*, Sensors, Vol. 17 No. 5, pp. 62 - 70, May 2000

- [18] Tyson, J.: *Dynamic Deformation Analysis with Pulsed ESPI*, Society of Experimental Mechanics Conference, June 1999
- [19] Tyson, J.: *Full-field Vibration and Strain Measurement with 3D ESPI*, Sensors, Vol 16 No. 6, pp. 16 - 22, June 1999
- [20] Tyson, J.: *Advanced Brake Squeal Analysis and Vibration Measurement*, 4th International Brake Colloquium, Gramado, Brazil, April 15, 1999
- [21] Tyson, John: *Portable Interferometry Systems for Rapid NDI*, USAF Aircraft Structural Integrity Conference, Dec. 1998
- [22] Tyson, John: *Practical Composite Repair Evaluation*, Proceedings of 41st Int'l SAMPE Symposium, Vol. 41, Book 1, pp. 609-614, March 1996.
- [23] Tyson, John: *Shearography NDE of Rocket Motor Components*, Joint Army-Navy-NASA-Air Force Nondestructive Evaluation Subcommittee Meeting, July 14-16, 1992
- [24] Chu T. C., Ranson W. F., Sutton M. A., Peters W. H.: *Application of digital-image correlation techniques to experimental mechanics*. Exp Mech. 25, September 1985, pp.232-24
- [25] Hartley R., Zisserman A.: *Multiple View Geometry in Computer Vision*, Cambridge University Press, 2004
- [26] Ma Y., Soatto S., Kosetska J., Sastry S.: *An Invitation to 3D Computer Vision*, Springer-Verlag, New York 2004
- [27] Gonzales R., Woods R.: *Digital Image Processing*, Prentice Hall 2002
- [28] Russ J.: *Image Processing Handbook*, CRC Press 1998
- [29] Shapiro L., *Computer Vision*, Prentice Hall, 2000
- [30] Zitova B., Flusser J.: *Image registration methods: A survey*, Image and Vision Computing 21, Elsevier, 2003
- [31] Holak K, Kohut P., Cieřlik J.: *Application of three-dimensional vision techniques in mechanical vibrations measurement (in polish)*, Proceedings of the 8th Workshop of Mechatronics Design, 2008, pp. 63-70
- [32] Uhl T., Kohut P., Holak K.: *Image correlation techniques in structures deflection measurement*, Proceedings of the international conference on Experimental Vibration Analysis for Civil Engineering Structures EVACES'09, Dolnořlaskie Wydawnictwo Edukacyjne, Wrocław 2009
- [33] Bradsky G., Kaebler A.: *Learning OpenCV*, O'Reilly 2008



Tadeusz UHL, Prof. is the head of the Department of Robotics and Mechatronics of AGH University of Science and Technology in Cracow. His scientific interests are diagnostics and Structural Health Monitoring of constructions, dynamics of constructions, modal analysis, control systems and mechatronics. He is the author of 16 monographs and over 500 scientific papers.



Piotr KOHUT, Ph.D. is an adjunct professor at the Department of Robotics and Mechatronics of AGH University of Science and Technology in Cracow. His scientific interests focus on mechatronics, vision systems, methods of image processing and analysis and 3D measurement techniques.



Krzysztof HOLAK, M.Sc. is Ph.D. student at the Department of Robotics and Mechatronics of AGH University of Science and Technology in Cracow. His works are connected with image processing and analysis and vision

PREDICTION OF CHANGES IN THE TECHNICAL CONDITION USING DISCRIMINANT ANALYSIS

Paweł MIKOŁAJCZAK

Katedra Budowy, Eksploatacji Pojazdów i Maszyn. Wydział Nauk Technicznych. UWM w Olsztynie
pawel.mikolajczak@uwm.edu.pl

Summary

Discriminant analysis can be used for identification of variables which identify (discriminate) two or more naturally emerging groups of f.ex. diagnostic symptoms or factors influencing development of particular type of machine part use. The goal in this case is searching for rules for assignment of multidimensional objects to one of many populations of known parameters, at the lowest classification mistake level possible. The idea of discriminant analysis is definition if the groups differ on account of a mean of a variable, and using this variable for appurtenance to a group predicting (f.ex. new cases of diagnostic symptoms, factors influencing the use level). In the following paper, an example of discriminant analysis application to diagnostic parameters choosing and identification of external factors influencing intensity of rolling bearings use in rotary machines is introduced.

Keywords: mutual measures, symptoms, sensitivity analysis, discriminant analysis, technical diagnostics.

PREDYKCJA ZMIAN STANU TECHNICZNEGO Z WYKORZYSTANIEM ANALIZY DYSKRYMINACYJNEJ

Streszczenie

Analizę dyskryminacyjną stosuje się do rozstrzygnięcia, które zmienne wyróżniają (dyskryminują) dwie lub więcej naturalnie wyłaniających się grup np. symptomów diagnostycznych lub czynników wpływających na rozwój danego rodzaju zużycia części maszyn. Stawianym celem w tym przypadku jest poszukiwanie reguł postępowania mającego na celu przyporządkowanie wielowymiarowych obiektów do jednej z wielu populacji o znanych parametrach przy możliwie minimalnych błędach klasyfikacji. Główna idea leżąca u podstaw analizy dyskryminacyjnej to rozstrzygnięcie, czy grupy różnią się ze względu na średnią pewnej zmiennej, a następnie wykorzystanie tej zmiennej do przewidywania przynależności do grupy (np. nowych przypadków symptomów diagnostycznych, czynników wpływających na wartość zużycia). W pracy przedstawiono przykład zastosowania analizy dyskryminacyjnej do wyboru parametrów diagnostycznych i predykcji stanu łożysk tocznych wentylatorów w zależności od czynników wymuszających zmianę tego stanu.

Słowa kluczowe: miary wzajemne, ocena wrażliwości symptomów, analiza dyskryminacyjna, diagnostyka techniczna.

1. MUTUAL MEASURES

Technical diagnostics of objects is, among others, comparing two states – current and standard. Hence, in quality or quantity assessment it is necessary to identify how much the signal analyzed is similar to standard signal. The problem is then creating signals estimators and checking for their mutual similarity. The problem can be solved by creating separate measures for the signal analyzed and the signal standard, and comparing the measures' values in diagnostic process [9].

Another solution is creating shared measures, definition of technical condition with shared measure is assessment of similarity of standard signal to the signal analyzed or comparing separate measures of both signals.

Shared measure describing relation between signal value $x(t)$ in the moment t and the value of the

second signal $y(t)$ in the moment $t+\tau$ is the **function of mutual correlation (intercorrelation):**

$$R_{xy} = \lim_{T \rightarrow \infty} \frac{1}{T} \int_0^T x(t) \cdot y(t+\tau) dt \cong \hat{R}_{xy}(\tau) = \frac{1}{T} \int_0^T x(t) \cdot y(t+\tau) dt = \overline{x(t) \cdot y(t+\tau)} \quad (1)$$

where: $\hat{R}_{xy}(\tau)$ - estimator of mutual correlation function

Normalized mutual correlation function is described with the formula:

$$\rho_{xy}(\tau) = \frac{R_{xy}(\tau)}{\sqrt{R_x(0) \cdot R_y(0)}} = \frac{\overline{x(t) \cdot y(t+\tau)}}{\sqrt{\overline{x^2(t)} \cdot \overline{y^2(t)}}} \quad (2)$$

Value of the function is in the range described with the formula $-1 \leq \rho_{xy}(\tau) \leq 1$ and it is equal to $-1/1$ when the signals are identical. Normalized correlation function can be used for localization of vibro-acoustic signal sources and for definition of signal track.

Normalized mutual correlation function is a local measure of similarity of signal in lag time, which means it shows similarity level between signals separately for each τ . Disadvantage normalized mutual correlation function is that it needs to be identified for signals generated concurrently, i.e. for the same value of object exploitation time Θ . Because of its local character diagnostic state assessment requires not a number but function or a set of numbers defining mutual correlation function [7].

Hence, there is also necessity to identify measures of signals similarity for the signals generated in various time of objects exploitation and given with a one number. The measure discussed is a **normalized mutual correlation function** described with the formula [1]:

$$K_{12}(\beta) = \frac{\int_{-\infty}^{\infty} R_{11}(\tau) \cdot R_{22}(\tau + \beta) d\tau}{\left[\int_{-\infty}^{\infty} R_{11}^2(\tau) d\tau \int_{-\infty}^{\infty} R_{22}^2(\tau) d\tau \right]^{\frac{1}{2}}} \quad (3)$$

Square of the formula presented above, for ($\beta=0$), gives the following result:

$$K_{12} = \frac{\left[\int_{-\infty}^{\infty} R_{11}(\tau) \cdot R_{22}(\tau) d\tau \right]^2}{\int_{-\infty}^{\infty} R_{11}^2(\tau) d\tau \int_{-\infty}^{\infty} R_{22}^2(\tau) d\tau} \leq 1 \quad (4)$$

where: $R_{11}(\tau)$, $R_{22}(\tau)$ – functions of vibro-acoustic signals correlation in the time Θ_1 and Θ_2 of technical object exploitation.

The last formula presents **global measure of signals similarity for various time of exploitation**, thus it is a global measure of object exploitation state similarity.

Using plexus characteristics and Wiener-Chinczyn relation and applying a local kind of normalization in frequency range, normalized mutual correlation function can be described with the following formula [1]:

$$\gamma_{xy}^2(f) = \frac{|G_{xy}(f)|^2}{G_{xx}(f) \cdot G_{yy}(f)} \leq 1 \quad (5)$$

where:

$G_{xx}(f)$, $G_{yy}(f)$ – functions of density of signals $x(t)$ and $y(t)$ power;

$G_{xy}(f)$ – function of mutual density of signals $x(t)$ and $y(t)$ power;

$\gamma_{xy}^2(f)$ – squared coherence function.

Value of coherence function may vary in the range given with the formula $0 \leq \gamma_{xy}^2(f) \leq 1$. For linear configurations with constant parameters $\gamma_{xy}^2(f) = 1$, which means signals $x(t)$ and $y(t)$ are completely coherent. In the case when for a given frequency $\gamma_{xy}^2(f) = 0$, signal $x(t)$ and $y(t)$ are incoherent. If signals $x(t)$ and $y(t)$ are stochastically independent, $\gamma_{xy}^2(f) = 0$ for all frequencies. When coherence function value is in the range given $0 \leq \gamma_{xy}^2(f) \leq 1$ measures results include disturbances, which means that the output signal is influenced not only by the input signal, but also other signals or a configuration combining signals $x(t)$ and $y(t)$ is not linear.

Damage in kinematic couple of technical object set causes changes in vibro-acoustic signal and consequently in coherence function. Thus coherence function measured for various time of object's life detects damage, changes in transmittance and relative changes of signal caused by damage. coherence function, like mutual correlation function, is a local measure of similarity of signals of vibration sources separately for each frequency.

It identifies relative quantity of information concerning input (primary) signal in output signal.

Global measure of vibro-acoustic signals generated in the same moment of object lifetime, in all frequency ranges **similarity** is so called sources similarity level S_{xy}^2 , because at any transmittance of a configuration $S_{xy}^2 = 1$ [1]:

$$S_{xy}^2 = \frac{\int_{-\infty}^{\infty} |R_{xy}(\tau)|^2 d\tau}{\int_{-\infty}^{\infty} R_{xy}(\tau) R_{yy}(\tau) d\tau} = \frac{\int_{-\infty}^{\infty} |G_{xy}(f)| df}{\int_{-\infty}^{\infty} G_{xx}(f) G_{yy}(f) df} \quad (6)$$

Whereas when there are no input or output disturbances $S_{xy}^2 < 1$, these characteristics can be used in diagnostics for identification of vibration and noise sources.

Using the mutual correlation function defined as opposite Fourier's transformation of mutual spectra power of signals density and the definition of correlation function shifted by 90° for one of the signals, the following result can be obtained:

$$\rho_{xy}^2 = \frac{\left[\int_{-\infty}^{\infty} |G_{xy}(f)| \cos \vartheta df \right]^2 + \left[\int_{-\infty}^{\infty} |G_{xy}(f)| \sin \vartheta df \right]^2}{\int_{-\infty}^{\infty} G_{xx}(f) df \int_{-\infty}^{\infty} G_{yy}(f) df} \quad (7)$$

The formula presented above is a sum of square mutual power, active and passive, normalized to a product of $x(t)$ and $y(t)$ signals power.

Analysis of the characteristics of ρ_{xy}^2 needs to the conclusion that this is the global measure of signals similarity and it can be used in diagnostics for measuring similarity of processes performed in identical configuration.

Taking normalized function of mutual correlation into consideration, the global measure of similarity of vibro-acoustic signals in given frequency generated in various time of object exploitation K_{12}^2 can be defined as [1]:

$$K_{12}^2 = \frac{\left[\int_{-\infty}^{\infty} G_{11}(f) \cdot G_{22}(f) df \right]^2}{\int_{-\infty}^{\infty} G_{11}^2(f) df \cdot \int_{-\infty}^{\infty} G_{22}^2(f) df} \quad (8)$$

where: $G_{11}(f)$, $G_{22}(f)$ – spectral density of power of vibro-acoustic signals defining technical states of an object in exploitation time Θ_1 and Θ_2 . The measure enables assessment of changes in condition of the object in its exploitation time.

Mutual measures enable comparing two states or symptoms, analyzed and standard, however they do not facilitate choosing one of the diagnostic symptoms from a large group of symptoms. One can also apply the physical probabilistic models in task of decreasing of uncertainty of reise and evolution of failure [10] or methods of automatic data classification [2],[6].

2. METHODS OF DIAGNOSTIC SYMPTOMS SENSITIVITY TO CHANGES OF TECHNICAL STATE ASSESSMENT

There are the following methods of diagnostics parameters choice presented in the literature [12], [9]:

- Maximum relative changes in diagnostic parameters method,
- Maximum variation of diagnostic parameter method,
- Maximum sensitivity of diagnostic parameter to changes in technical state method,
- Maximum information capacity of diagnostic parameter method.

Maximum relative changes in diagnostic parameters method – in this method, a diagnostic parameter which has the greatest value of k_j indicator is chosen. It takes average speed of parameters changes in time. It is calculated with the following formula:

$$k_j = \frac{b_j}{\sum_{j=1}^m b_j}$$

$$b_j = \frac{1}{K} \sum_{i=1}^K \frac{|y_j(v_{i+1}) - y_i(v_i)|}{(v_{i+1} - v_i) |y_i(v_i) - y_{j^*g}|} \quad (9)$$

where: K – the number of elements of time series in (v_l, v_b) interval.

Diagnostic parameter y^* is chosen with the following formula:

$$y^* = y_{j^*}, j^* \in 1, \dots, m \wedge k_{j^*} = \max(k_j), j = 1, \dots, m \quad (10)$$

Maximum variation of diagnostic parameter method – diagnostic parameters analyzed should presented a sufficient level of variability in machine exploitation time. The parameters with the greatest value of variability indicator g_j are chosen from the set of final results:

$$g_j = \frac{S_j}{\sum_{j=1}^m S_j} \quad (11)$$

$$S_j = \frac{1}{K} \sum_{i=1}^K \frac{|y_j(v_{i+1}) - y_j(v_i)|}{v_{i+1} - v_i} \quad (12)$$

Where: K – the number of elements of time series in (v_1, v_b) interval.

The parameter y^* is chosen with the following formula:

$$y^* = y_{j^*}, j^* \in 1, \dots, m \wedge g_{j^*} = \max(g_j), j = 1, \dots, m \quad (13)$$

Maximum sensitivity of diagnostic parameter to changes in technical state method – the idea of the method is to choose, from the set of output parameters of a configuration or an object set, a parameter that has the greatest value of a_j indicator, which includes parameters dependence on machine state:

$$a_j = \sum_{i=1}^k M(i, j); i = 1, 2, \dots, k; j = 1, \dots, m \quad (14)$$

where: $M(i, j) \in [M(i, j)]_{k \times m}$ – an element of binary diagnostic matrix of a technical object.

The parameter y^* then is chosen for the set of diagnostic parameters by choosing y_j with maximum value of a_j indicator:

$$y^* = y_{j^*}, j^* \in 1, \dots, m \wedge a_{j^*} = \max(a_j), j = 1, \dots, m \quad (15)$$

Maximum information capacity of diagnostic parameter method – based on the choice of the parameter that provides the most information on machine's technical state. The

diagnostic parameter is the more important for definition of object's technical state, the more it is connected to the object and the less it is connected to the other diagnostics parameters.

The relation discussed above is represented by the indicator of integral capacity of diagnostics parameter h_j introduced with the formula:

$$h_j = \frac{r_j^2}{1 + \sum_{i,j=1}^m |r_{i,j}|} \quad (16)$$

where: $r_j = r(W, y_j)$; $j = 1, \dots, m$ – linear correlation between variables coefficient, W – state of an object set, $r_{i,j}$ – linear correlation between y_i and y_j variables coefficient.

The parameter y^* is chosen to the set of diagnostics parameters by maximization of h_j indication with the following formula:

$$y^* = y_{j^*}, j^* \in 1, \dots, m \wedge h_{j^*} = \max(h_j), j = 1, \dots, m \quad (17)$$

Each of the methods diagnostic parameters choice presented above considers changes in parameters' values in technical state of an object analyzed function on a different level, however, they do not enable simultaneous assessment of numerous diagnostic symptoms and exploitation conditions influence on track of technical object use value. In the next chapter the example of discriminant analysis use for

forecasting changes in rolling bearings state with respect to the set of diagnostic symptoms and external enforcements given is presented.

3. DISCRIMINANT ANALYSIS

Discriminant analysis is a statistical analysis which allows to identify differences between two or more groups, analyzing several variables at the same time. Variables used for groups distinguishing are called **discriminant variables**. Practically, discriminant analysis is a general term referring to several related statistical procedures. Simplifying, the procedures can be distinguished into [5], [7], [11]:

- Descriptive procedures and inter-group differences identifying procedures. The procedures explain: if it is possible, with a set of several variables, distinguish one group from another? How well discriminant variables distinguish groups given? Which of the variables are the best in discriminating?
- Procedures of cases classification, which is definition of characteristics' values, based on observation or experience, that enable decision to which of the groups a new case should be included. It is connected with definition of one or more functions classifying the cases analyzed to the right groups.

The example of discriminant analysis to be presented is based on exploitation data concerning the group of fans introduced in the table 1. The purpose of the analysis is showing, how the use progress of rolling bearings can be predicted with the diagnostics parameters analyzed.

Table. 1. Comparison of diagnostics and exploitation parameters for the analyzed group of fans

Fan number	v(fo) [mm/s]	v(2fo) [mm/s]	T [°C]	Choking [%]	State of the rolling bearings
w1	3,6	5,2	65	5	inadmissible
w2	7,5	3	70	20	inadmissible
w3	4	4	75	25	inadmissible
w4	8,5	2,6	60	10	inadmissible
w5	4,2	3,2	84	30	inadmissible
w6	3,5	4,2	65	40	sufficient
w7	5,1	2,2	63	20	sufficient
w8	3,9	3,5	62	30	sufficient
w9	5,5	1,5	55	15	sufficient
w10	4	3,7	70	30	sufficient
w11	4,3	1,2	61	30	good
w12	2,5	0,9	74	10	good
w13	1,8	0,3	56	15	good
w14	1,5	2,6	61	20	good
w15	2	1,1	73	35	good

Symbols used in the table: v(fo) – the first harmonica of vibrations, v(2fo) – the second harmonica of vibrations, T – temperature of rolling bearing cover, Choking – percentage of flow choking.

Analysis starts with definition of **canonical discriminant function** distinguishing the groups analyzed. Any function can be used for the definition, however, the most commonly used are linear functions. The functions to be used are described with the following formula [5], [7], [11]:

$$D_{kj} = \beta_0 + \beta_1 x_{1kj} + \dots + \beta_p x_{pkj} \quad (18)$$

where: p – number of discriminant variables (in the following example $p = 4$), n – size of the sample (in the following example $n = 15$), g – number of groups (in the following example $g = 3$), D_{kj} – canonical discriminant function for k -th case in j -th group value, $k=1, \dots, n$ and $j=1, \dots, g$, x_{ikj} – value of i -th discriminant variable for k -th case in j -th group, $i=1, \dots, p$, β_i – coefficients of canonical discriminant functions defined with characteristics of the function.

The problem of β_i coefficients definition is definition is solving matrix equation given with the formula [3], [11]:

$$(\mathbf{M} - \lambda \mathbf{W})\boldsymbol{\beta} = 0 \quad (19)$$

where: \mathbf{W} – intragroup matrix of squares and mixed products, \mathbf{M} – intergroup matrix of squares and mixed products, $\boldsymbol{\beta}$ – vector of canonical discriminant functions coefficients, λ – so called matrix value.

In the table 2 there are calculated, raw and standardized values of discriminant functions coefficients. The calculations were performed with STATISTICA PL software, version 9.0.

Table 2. Coefficients of discriminant functions

	Function 1 (raw coefficients)	Function 2 (raw coefficients)	Function 1 (standardized coefficients)	Function 2 (standardized coefficients)
v(fo) [mm/s]	-0,84973	-0,07620	-1,30723	-0,117224
v(2fo) [mm/s]	-1,21239	-0,32739	-1,22125	-0,329777
T [°C]	-0,09550	0,12583	-0,73908	0,973896
Choking [%]	0,05088	-0,09304	0,51721	-0,945767
constant	11,86678	-5,09074	8,31713	0,625460
value	8,31713	0,62546	0,93006	1,000000
cumulated ratio of cleared variation	0,93006	1,00000	-1,30723	-0,117224

Canonical discriminant functions are described with the following formulas:

$$D_1 = 11,86678 - 0,84973v(\text{fo}) - 1,21239v(2\text{fo}) - 0,09550T + 0,05088\text{Choking}$$

$$D_2 = -5,09074 - 0,07620v(\text{fo}) - 0,32739v(2\text{fo}) + 0,12583 - 0,0930\text{Choking}$$

The first function is responsible for 93% of cleared variance (while the second for 7% only), which means the first function is the most important.

Raw coefficients of discriminant function can be used with the data from observation mainly for calculating function value, but they cannot be used for interpretation. One of the reasons is the fact that coordinates beginning is not equal to the

central point represented by average values of discriminant variables for all the points. To eliminate this problem standardization of coefficients is used [3], [4], [5]:

$$\hat{\beta}_i = \beta_i \sqrt{n-g} \quad \hat{\beta}_0 = -\sum_{i=1}^p \hat{\beta}_i \bar{x}_i \quad (20)$$

where: \bar{x}_i – average value of i discriminant variable,

$\hat{\beta}_i$ – standardized coefficients of canonical discriminant function, the rest as described above.

To identify how each discriminant function distinguishes the groups, the diagram presented in the figure 1 can be used.

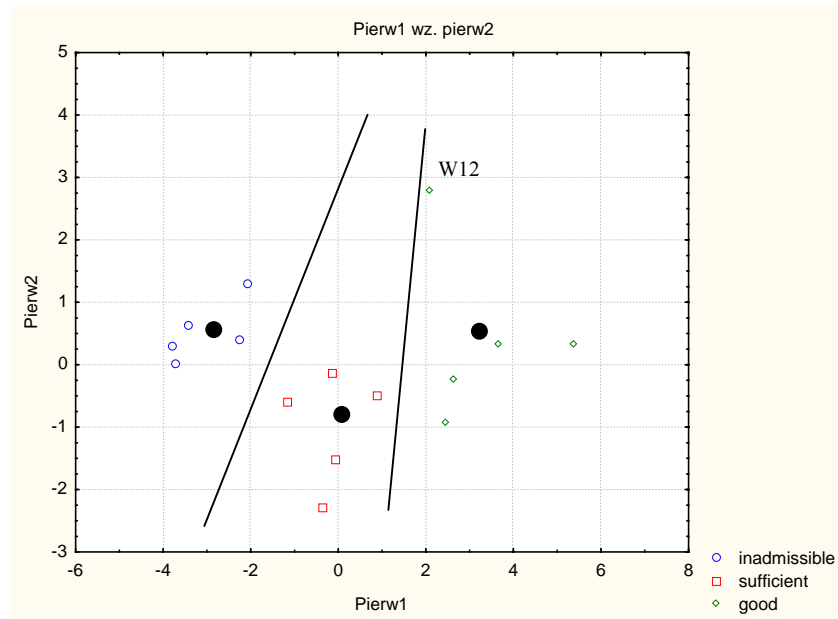


Fig. 1. The diagram of canonical values dispersion

Fig. 1 verifies the results of variation cleared. In the diagram, the fans with bearings in good, sufficient and inadmissible are distinguished with the first discriminant function (the vertical lines can be drawn to identify these groups – 93% of cleared variation). The one exception is the point identified for the fan number 12. The reason for that is the fact that despite good dynamic condition (low values of the first and the second harmonica) there is a great interaction and a load of the fan. Thus, there is a risk of changing the condition, from the “good” level to the

“sufficient” level (which means increasing the distance from “good” group centroid, marked with the black point).

Another measure in multidimensional variables space can be used – **Mahalanobis distance** [4], [7], [11]. It is a distance between each case and a group centroid. It is worth mentioning, that the smaller Mahalanobis distance, the more certain appurtenance to the group. In the figure 2, square Mahalanobis distance for the case analyzed is presented.

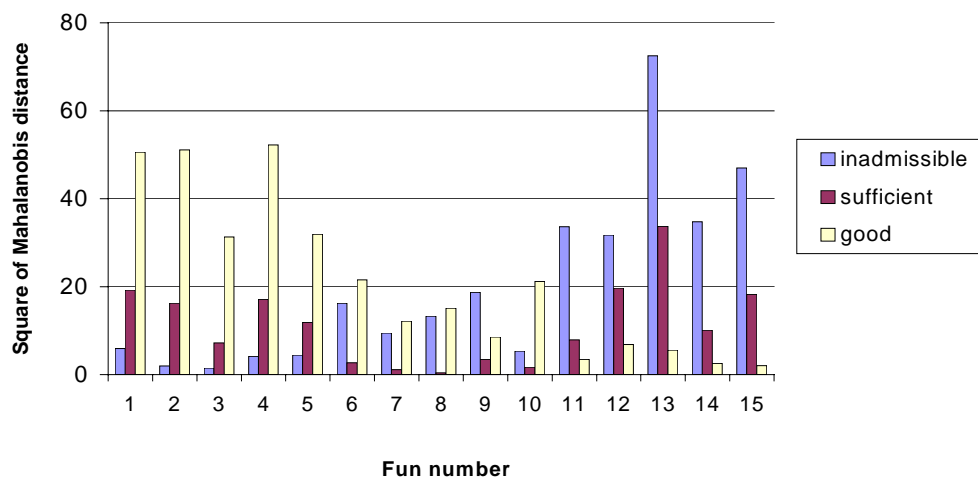


Fig. 2. Mahalanobis distance column graph

Analysis of the figure 2 leads to the conclusion, that predefined functions discriminate three groups of rolling bearings states analyzed very well. In the first five fans, condition of rolling bearings was inappropriate, and in these cases columns labeled with “inadmissible” are the smallest. The group

of five fans with rolling bearings of sufficient condition is the one in the middle, in this group the smallest values are represented by the columns labeled “sufficient”. The last group is also easy to be distinguished, columns labeled as „good” are the smallest.

4. SUMMARY

1. Application of mutual measures allows to identify and measure the difference between the signal analyzed and the standard. Mutual measures are the methods applicable for identification of signals which can be described as changing their values significantly, with respect to changes of state, exploitation time and enforcements a technical object is exposed to.
2. Signals sensitivity assessment methods should be used when choosing the best diagnostic parameter from the set of parameters given. It can be done with the following criterion: relative parameter change, maximum variance, maximum sensitivity of diagnostic parameter to technical condition changes or maximum information capacity.
3. Discriminant analysis allows to identify which variables are characteristic for diagnostic symptoms groups or for factors influencing development of considered type of machine parts use. Thus, a set of diagnostic symptoms can be used even though one of the symptoms does not identify technical condition of the object analyzed, because multidimensional analysis of the set as a whole is diagnostically useful.
4. Because of the limited size of the following chapter, the issues concerning additional methods of discriminant functions developed assessment are not included. However, the methods listed below are worth mentioning:
 - Wilks's lambda and multidimensional F statistics, both based on the level of density of points around the centroid;
 - Partial Wilks's lambda – identifying influence of a variable on group discrimination,
 - V Rao statistics, measuring groups' centroids dispersion;
 - *A posteriori* probability of identification if a case analyzed belongs to a given group.
5. The examples of diagnostics parameters presented in the chapter are not directly connected with rolling bearings condition. They introduce various states of unworthiness (including unbalancing, clutch failure, wrong smearing or assembly of rolling bearings) [6], [10], however, thanks to discriminant analysis influence of these unworthiness on rolling bearings use can be forecasted. With other words, discriminant analysis allows to identify influence of particular causes of rolling bearings failures.

REFERENCES

- [1] Cempel C. *Diagnostyka wibroakustyczna maszyn*. PWN, Warszawa 1989.
- [2] Gibiec M., Barszcz T., Bielecka M.: *Selection of clustering methods for wind turbines operational data*. Diagnostyka 4(56)/20100 p. 37-42.
- [3] Giri N. C. *Multivariate Statistical Data Analysis of Multivariate Observations*. New York, Wiley 1996.
- [4] Huberty C. J. *Applied discriminant analysis*. New York, Wiley 1967.
- [5] Klecka W.R. *Discriminant analysis*. Sage, London 1980.
- [6] Mikołajczak P. *Klasyfikacja zbiorów symptomów diagnostycznych z wykorzystaniem metody Dattoli*. Diagnostyka 4(40)/2006, p.185-190.
- [7] Morrison D. F. *Wielowymiarowa analiza statystyczna*. PWN, Warszawa 1990.
- [8] Morel J.: *Drgania maszyn i diagnostyka ich stanu technicznego*. PTDT, Warszawa 1992.
- [9] Niziński S., Michalski R.: *Diagnostyka obiektów technicznych*. ITE Radom 2002.
- [10] Radkowski S., Zawisza M. *Failure oriented diagnostic models in condition monitoring*. Diagnostyka 4(52)/2009, p. 93-97.
- [11] Staniszkis A. *Przystępny kurs statystyki z zastosowaniem STATISTICA PL*. Tom 3. Analizy wielowymiarowe. StatSof Kraków 2007.
- [12] Tylicki H.: *Optymalizacja procesu prognozowania stanu technicznego pojazdów mechanicznych*. Rozprawa nr. 86, ATR, Bydgoszcz 1998.
- [13] Żółtowski B.: *Podstawy diagnostyki maszyn*. ART, Bydgoszcz 1996.

Dr inż. **Paweł MIKOŁAJCZAK** pracuje na stanowisku adiunkta w Katedrze Budowy, Eksploatacji Pojazdów i Maszyn Wydziału Nauk Technicznych UWM w Olsztynie. Od wielu lat zajmuje się diagnostyką wibroakustyczną, systemami informatycznymi w utrzymaniu maszyn jest autorem wielu artykułów i ekspertyz z tego zakresu. Członek PTDT, redaktor „Diagnostyki”.



APPLICATION OF UML MODELLING FOR ANALYSIS OF SAFETY INTEGRITY LEVEL IN RAILWAY TRAFFIC CONTROL SYSTEMS

Mateusz MARZEC, Tadeusz UHL, Tomasz BARSZCZ

AGH University of Science and Technology, Dept. of Mechanical Engineering and Robotics
Al. Mickiewicza 30, 30-059 Kraków, Polska, e-mail: tbarszcz@agh.edu.pl

Summary

Railway traffic control systems require extremely high level of operational safety. Due to very high costs of safety failure, this field is subject to the regulation by numerous norms, which describe formal methods of safety level calculation (denoted as Safety Integrity Level – SIL). Such an analysis is tedious and time consuming, especially in case of complex systems.

The paper proposes application of UML modeling approach to perform joint analysis of the system architecture and its operation. The approach also uses the Fault Tree Analysis (FTA) and can be used to identify the weakest links in the whole system. The method allows to quickly introduce changes in system architecture or parameters and evaluate the impact on the safety. The proposed approach was successfully applied to the real case of a railway system.

Keywords: railway transport, safety integrity level, UML modeling.

ZASTOSOWANIE JĘZYKA UML DO BADANIA POZIOMU NIENARUSZALNOŚCI EZPIECZEŃSTWA SYSTEMÓW STEROWANIA RUCHEM KOLEJOWYM

Streszczenie

Systemy SRK wymagają szczególnie wysokiego poziomu bezpieczeństwa eksploatacji. Ze względu na bardzo wysokie koszty awarii, dziedzina ta jest przedmiotem podlegającym regulacjom wielu norm opisujących formalne metody obliczania poziomu bezpieczeństwa (oznaczony, jako poziom nienaruszalności bezpieczeństwa – SIL). Analiza prowadząca do wyznaczenia poziomu SIL jest trudna i czasochłonna, zwłaszcza w wypadku bardzo skomplikowanych systemów.

Niniejsza praca proponuje aplikację podejścia z wykorzystaniem modelowania UML do przeprowadzania analizy architektury systemu i jego działania. Podejście to korzysta również z analizy drzewa błędów FTA i może być użyte do identyfikacji najsłabszych elementów systemu. Metoda ta pozwala również na szybkie wprowadzanie zmian w architekturze lub parametrach systemu, oraz pozwala obliczyć ich wpływ na bezpieczeństwo. Zaproponowane rozwiązanie zostało z powodzeniem zastosowane w prawdziwym systemie kolejowym.

Słowa kluczowe: ruch kolejowy, poziom nienaruszalności bezpieczeństwa, modelowanie UML.

1. INTRODUCTION

Railway traffic control systems have to conform to very high safety standards. For classification purposes, it is practiced to use the concept of safety integrity levels (SIL), which have been described in PN-EN 61508 norm. Safety integrity levels (SIL) define device/system/subsystem failure probability for the work in continuous or on demand mode. There are four SIL discrete levels under the condition that the level 4 is characterized by the highest safety and the level 1 by the lowest safety. Advanced railway traffic control systems have to conform to the standards of SIL 4, which means 1 failure for no more than 10,000 years. In order to estimate the safety integrity level for the given railway traffic control system, it is required to

conduct a complicated reliability analysis based on modeling domain.

The basic aim of the modeling process is deduction about real railway traffic control system which reproduces control tasks [1]. Railway traffic control systems modeling is a very complicated process and both methods and tools used have been changing throughout the years. The present work utilizes the unified modeling language (UML) to describe the architecture and show the dependencies that are present in a prototype system for traffic control at the railway crossings. Created in this way models have considerably facilitated system reliability analysis with the use of fault tree analysis (FTA). Reliability analysis conducted for the described system allowed not only for estimating the safety integrity level (SIL) but also

for establishing weak components in order to increase the reliability.

2. SYSTEM MODEL

Signaling system model has been shown in the Fig. 1

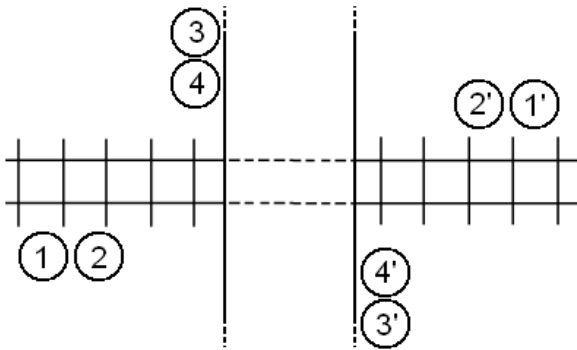


Fig.1 System model:

1, 1' – rangefinder; 2, 2' – camera; 3, 3' – LCD panel; 4, 4' - speaker

The main task of the chosen Signaling system is the improvement of safety at the railway crossings and intersections. The discussed system is a good alternative for the danger signs at the C and D category railway crossings meaning these which do not have their barriers. The main advantage of the system is its price, simplicity and the fact, that it works independently of the systems and devices of the railway traffic control system.

Functioning of the system is based on the detection of the coming to the railway crossing train and displaying the image of the coming train on the LCD panel. Additionally, there is a display of sign “STOP” and sounding of alarm.

3. SYSTEM ARCHITECTURE

The reliability analysis has to be preceded with a careful study of the system functioning and its architecture. The document that is indispensable for the architecture description is the circuit diagram. The circuit diagram shows how the electric and/or electronic elements have been joined together in the system without the reproduction of their physical location in the device. The diagram allows viewing the path of the signals within the device as well as understanding the rule on which basis the device functions. It also facilitates the device service and modifications. It includes information on types and measures of the components, often also the information on the typical voltage and electric current that are present in the circuit in the particular states of its functioning [2].

Electric circuit is very complex and includes much data that is not essential for the reliability test based on fault tree analysis. In order to simplify the

circuit diagram, the modular diagrams are applied. They are used to show only signal type, direction and flow path between particular subassemblies. Fig. 2. shows the simplified modular diagram of the system.

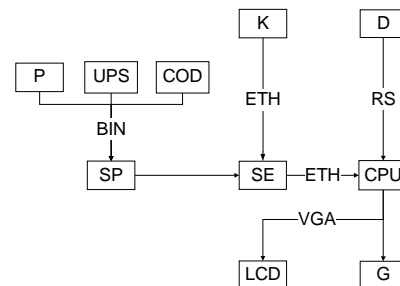


Fig. 2. System circuit diagram: K – camera, D – rangefinder, P – relay, UPS – uninterruptible power supply, COD – case open detector, SP – port server, SE – switch, CPU – computer, LCD – LCD panel, G – speaker

Modular diagrams are indispensable for the deduction about the causes for the function non-completion by particular subassemblies. The drawback of the modular diagrams is that they show only the statics of the system. In order to show dynamics of the system, the UML method has been used.

3.1. UML as a tool for the system dynamics description

In order to describe the operation part of the system, in a sense of the sequence of the conducted operations during a train ride, the UML has been used. The unified modeling language, in practice, has a form of graphical representation of the given system, consisting of logically connected diagrams [3]. Sequence diagram created using Visual Paradigm Software and shown in the Fig. 3. depicts operation of several subassemblies for their realization of the control function with highlighting of the time function. The diagram allows to determine the sequence of the communicates during certain time. UML modeling allows also determining the influence of failure of one element to the other. The drawback of the sequence diagrams is that they omit the secondary importance elements which do not take part in the flow of the main signal, such as the detector whether the case, in which the system is incorporated, is open which can have a critical influence on the reliability test. Modular diagrams and sequence diagrams complement each other and together show complete picture of the system operation describing system statics and dynamics. The discussed models constitute, together with the reliability coefficients, the input data for the reliability test with the use of FTA method.

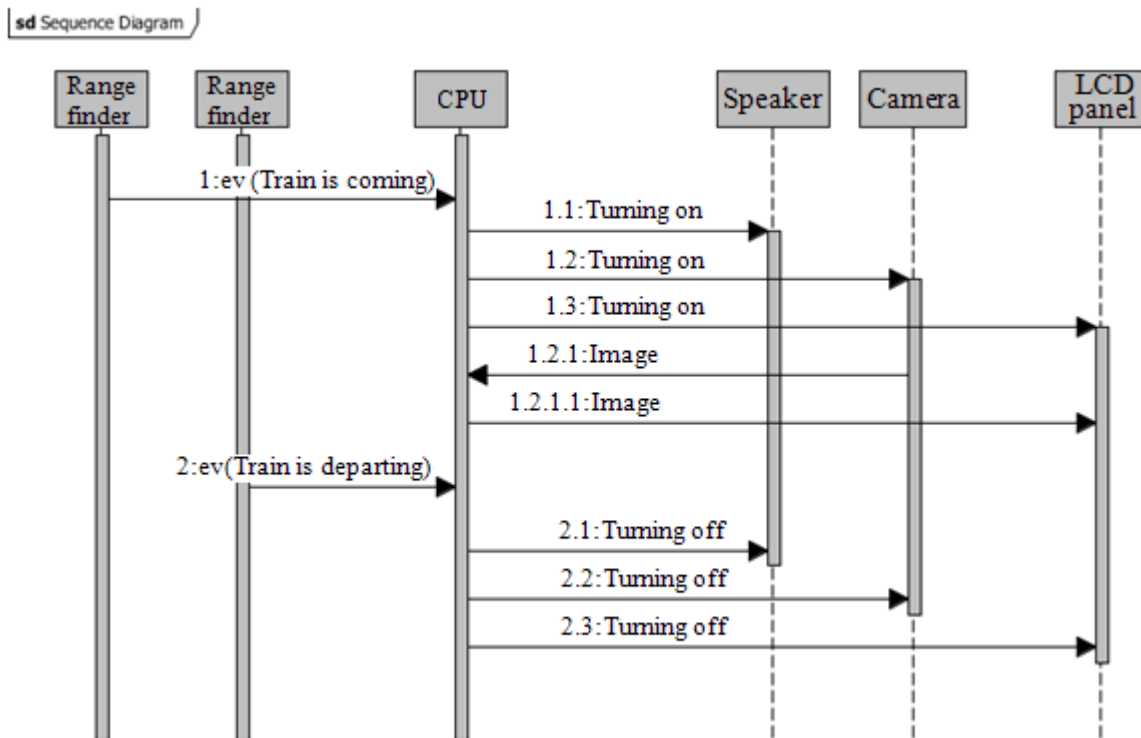


Fig. 3. Sequence Diagram

4. RELIABILITY ANALYSIS

In order to estimate the SIL of the system, the FTA method has been used. The method is based on the modular diagrams and UML sequence diagrams. Sequence diagrams allow to easily comprehend any interaction between specific components which makes the construction of fault tree (FTA) easier. The FTA is one of the most often used methods of system reliability tests. It has been discussed in the IEC1508 standard. The discussed method is a graphic representation of the logical connections with the use of AND, OR and XOR gateways between causes and basic events.

The system analysis with the use of fault tree allows not only to estimate the SIL but also to indicate all possible causes of system's failure. A part of the fault tree for the signaling system in question has been shown in the Fig. 4. Basic event being the top event is system failure, and the cause can be short circuit, unplugging or cut in the Ethernet camera cable.

The next step after the identification of the all possible failure causes is the determination, based on the UML diagrams, of what is the influence of the failure of a particular tree element on the whole system. The determination is made in order to estimate the fraction of safe failures (SFF), which in case of the particular signaling system equals to SFF=73%.

4.1. SIL determination

Subassemblies of the discussed system are widely available on the market, which considerably facilitates the SIL determination. Reliability rates of the assemblies are determined in the process of reliability analyses conducted by the producers, thanks to that subassemblies can be treated globally and assigned particular failure rate λ . In case of the lack of the information concerning reliability rate of a particular component, failure rates of the devices of the same purpose and similar structure have been used. When all the necessary reliability rates are available, they have to be assigned to the particular leaves of the tree and by the use of simple mathematical operations, in which the gateway OR is a multiplication, whereas AND is an addition, the system failure rate is determined, which amount to the level $\lambda=1,114 \times 10^{-5}$. Under the term of failure one has to understand the situations, when there is simultaneous lack of the camera image display, the STOP sign, and the alarm.

Failure rate λ is the inverse of the MTBF value (Mean Time Between Failures). MTBF value for the particular signaling system amounts to $3,742 \times 10^2$ days. One must be aware that MTBF value is not any guarantee or warranty. The fact that the system is to work for days does not mean that the system will last so many days. A big role is played by the operational conditions as well as the intensity of the usage [4].

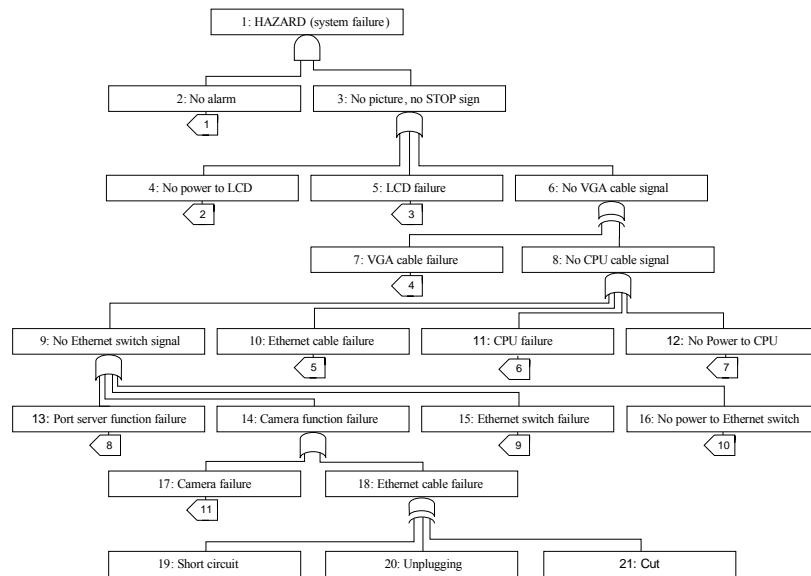


Fig. 4. Part of FTA tree for the Signaling system

System failure rate, determined on the basis of the failure rates of all modules and the possibility of adverse events, amounts to $\lambda=1,114 \times 10^{-5}$. As a consequence of having this value of the failure rate, the given system does not conform to any safety criteria and is not assigned a SIL.

4.2. Required SIL

Advanced railway traffic control systems have to conform to the safety requirements determined at SIL 4. The discussed herein system is not closely connected with railway traffic control, thus it does not have to comply to the safety standards determined at the SIL 4. In order to determine the required SIL of the system, it is necessary to use risk diagram which has been characterized in PN-EN 61508 norm. Risk diagram determines the required SIL on the basis of the consequences of the potential failure, time period, and frequency of finding oneself in the dangerous circumstances, as well as the possibility of the event avoidance and its occurrence probability. The required SIL for the system in question, determined by the use of risk diagram.

As the reliability analysis showed, the system did not meet the SIL 1 standards. In further part of the present work, there will be discussed various methods that has led to the improvement in the reliability and as a consequence the system safety requirements have been fulfilled.

5. RELIABILITY IMPROVEMENT METHODS

The system failure rate $\lambda=1,114 \times 10^{-5}$ places itself within the range , which means that it does not meets any safety criteria and cannot have a SIL assigned. The purpose of this chapter is to obtain

the SIL 1 as well as presentation of various means of the system reliability improvement.

5.1. The use of components of low failure rate

The use of components which are characterized by high reliability seems to be good way to improve the reliability of the whole system. It has to be noted, though, that the use of all components of high reliability can be uneconomical, what is more it may not improve considerably the overall system reliability. To determine, which components have considerable influence on the system reliability, there have been created graphs showing the relation between failure rates of the particular components (x-axis) and the reliability of the whole system (y-axis). Fig. 5, Fig. 6, Fig. 7, Fig. 8. Show respectively the graphs of the rangefinder, computer, ampfler and CPU power pack reliability.

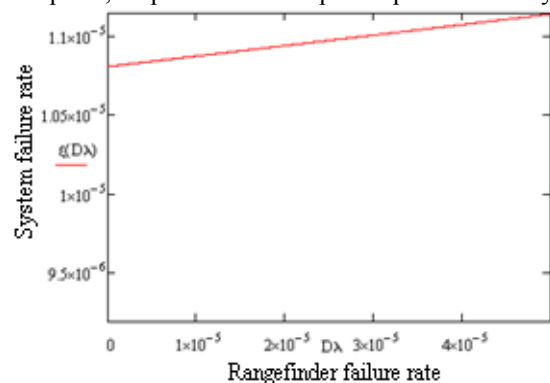


Fig. 5. Rangefinder reliability graph

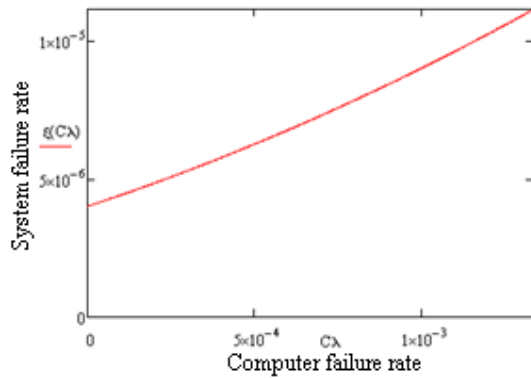


Fig. 6. Computer reliability graph

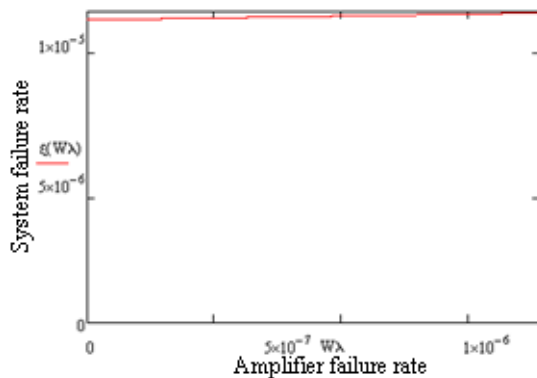


Fig. 7. Amplifier reliability graph

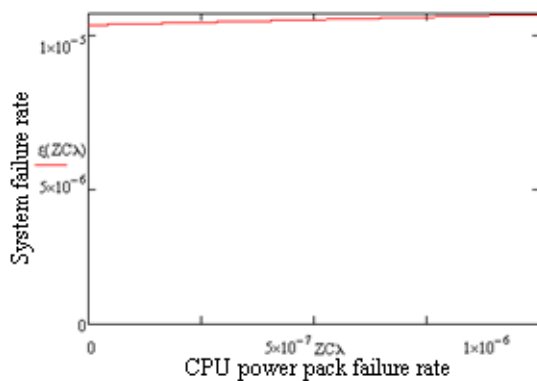


Fig. 8. CPU power pack reliability graph

Analyzing the graphs leads to conclusion that the more inclination to the perpendicular of the curve the more efficiently the reliability of the whole system can be improved by the increase in the reliability of the given component. It appears from the analysis conducted that the greatest influence on the decrease in the failure rate of the system has the computer and the rangefinder, and the smallest: the amplifier, the CPU power pack, and the accumulator. This is why the use of the amplifier, the CPU power pack, and the accumulator with very low failure rate would have no point. It could only increase the costs.

5.2. Application of the right circuit pat tern

It has been calculated on the basis of the fault tree [7] that the smallest failure rate that can be obtained for the discussed circuit pattern amounts to $\lambda=3,164 \times 10^{-6}$, thanks to which the system conforms to the safety standards of the SIL 1. To obtain greater safety, it would be necessary to prevent adverse events such as voltage surge, short circuit, unplugging. It has to be noted that the aim of the present chapter is obtaining by the systems the SIL 1. The applied uninterrupted power supply system (UPS), case open detector (COD), rely, miniature circuit breakers (MCB), and sent systematically to the central office data on the current state of the system results in the fact that the present system architecture ensures the required by the analysis SIL 1.

5.3. Application of the redundancy principles

Redundancy, in practice means the increase in number of a particular component to have greater reliability. Before planning redundancy, one has to consider the consequences of the use of additional subassemblies. In many cases the use of redundant components can have the opposite effect from what has been intended. Additionally, fully redundant system will have double price of the subassemblies.

To obtain the correct redundancy, it is necessary to conduct the analysis of the whole system. In case of the discussed system, the component which decreases the reliability to the most extent is the computer. The use of the second computer is connected with the use of additional power pack, USB hub, VGA switch and RS serial adapters.

In order to show redundancy in the modular diagram, it is necessary to introduce in brief the structure of the system reliability. Reliability structure connects functional failures of the particular components with the failure of the whole system. In classical reliability theory there are distinguished several basic reliability structures, which allows for modeling of functionalities of the analyzed objects. The discussed system has serial reliability structure, in a sense that one component failure causes the failure of the whole system. [5]. System reliability structure with the applied redundancy has been shown in the Fig. 9. The use of the second computer guarantees the safety integrity on the SIL 1, the system failure rate will then amount to $\lambda=3,164 \times 10^{-6}$.

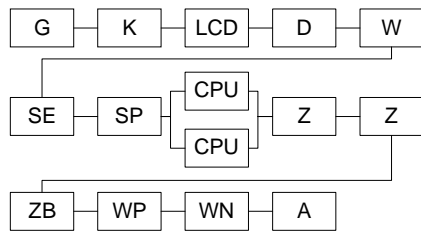


Fig. 9. Reliability structure with redundancy applied: G – speaker, K – camera, LCD – LCD panel, D – rangefinder, W – amplifier, SE – Ethernet switch, SP – port server, CPU – computer, Z – CPU power pack, ZB – buffer power pack, WP – power plug, WN – miniature circuit breaker, A – accumulator

6. SUMMARY

The reliability analysis conducted in the present work has allowed to determine the SIL of the railway system, as well as to indicate all possible causes of the system failure and the systems' weak components. Apparently, UML is a good tool to be used for the description of the system architecture as well as for the simple description of its operation. The use of UML facilitate considerably the reliability analysis with the use of FTA which allows for drawing up conclusions on the influence of the given failure on the particular subassemblies.

BIBLIOGRAPHY

- [1] Zablocki W.: *Modelowanie systemów sterowania ruchem kolejowym – struktury informacji i elementy opisu formalnego*. Prace Naukowe Politechniki Warszawskiej. Transport 2006, z. 57, s. 23-48.
- [2] Pełka A.: *Diagnozowanie urządzeń sterowania ruchem kolejowym na przykładzie napędu zwrotnicowego*. Akademia Górniczo-Hutnicza, Kraków 2009.
- [3] Chudzikiewicz A. Uhl T.: *Modelowanie procesów występujących na liniach mało obciążonych*. Prace Naukowe Politechniki Warszawskiej. Transport 2009, z. 69, s. 43-52.
- [4] Jones, James V.: *Integrated Logistics Support Handbook*.
- [5] Pietrzyk A. Piskorz Z.: *Optymalizacja serwisowania urządzeń technicznych z zastosowaniem algorytmów genetycznych*. Akademia Górniczo-Hutnicza, Kraków 2003.
- [6] Polska Norma PN EN IEC 61508.
- [7] Marzec M.: *Modelowanie systemów sterowania ruchem kolejowym*. Akademia Górniczo-Hutnicza, Kraków 2011.



Inż. **Mateusz MARZEC**
absolwent Wydziału
Inżynierii Mechanicznej
i Robotyki, Akademii
Górnico – Hutniczej w
Krakowie.



Prof. dr hab. inż. **Tadeusz UHL** jest kierownikiem Katedry Robotyki i Mechatroniki, Akademii Górniczo – Hutniczej w Krakowie. W swoich pracach zajmuje się zagadnieniami dynamiki konstrukcji, a zwłaszcza ich analizy modalnej oraz diagnostyki opartej na modelu. Jego zainteresowania obejmują także układy aktywnej redukcji drgań oraz szeroko pojętą mechatronikę.



Dr inż. **Tomasz BARSZCZ**. Pracuje jako adiunkt w Katedrze Robotyki i Mechatroniki. Zajmuje się diagnostyką maszyn oraz systemami monitoringu i diagnostyki. Jest autorem 4 książek i ponad 60 publikacji. Opracowane przez niego systemy pracują na ponad stu kilkudziesięciu instalacjach.

SINGULAR VALUES OF SYMPTOM OBSERVATION MATRIX OF A SYSTEM IN OPERATION AS INDICATORS OF SYSTEM DAMAGE

Czesław CEMPEL
Poznań University of Technology,
E-mail: czeslaw.cempel@put.poznan.pl

Summary

The last paper of the present author [19] was concerned with multidimensional condition monitoring of the machines and the application of singular value decomposition (SVD). It was shown there, the immunity of singular values against uncontrolled load change, and they are also some measures of damage intensity. Following this, a simple model of singular value evolution has been proposed here and tested by means of three cases of real diagnostics in industry. It was found that postulated linear growth of singular value is good approximation of its real behavior and the same concerns the exponential growth of singular values product. Moreover this measures are sensitive to the redundancy of observation space and can depict clearly a lifetime when real damage in a monitored system starts. These properties seem to be much wanted in condition monitoring, so further investigations are planned.

Key words: machine condition, symptom observation matrix, singular value decomposition, evolution of singular values.

WARTOŚCI SZCZEGÓLNE SYMPTOMOWEJ MACIERZY OBSERWACJI EKSPLOATOWANEGO SYSTEMU MECHANICZNEGO JAKO WSKAŹNIKI ZUŻYCIA

Ostatnia praca autora [19] pokazuje zastosowanie rozkładu wartości szczególnych symptomowej macierzy obserwacji w diagnostyce maszyn. Pokazano tam, że ewolucja wartości szczególnych rozkładu w czasie życia maszyny jest niewrażliwa na wahania obciążenia roboczego systemu. Zatem w obecnej pracy zaproponowano liniowy model ewolucji wartości szczególnych i eksponentalny model dla ich iloczynu. Porównania tych modeli z rzeczywistym przebiegiem wartości szczególnych eksploatowanych maszyn pokazują, że dla przypadku liniowego zużycia jest to dobry model, natomiast często widać skoki poziomu w ewolucji wartości szczególnej. Może to świadczyć o pojawieniu się dodatkowego uszkodzenia, bądź o przejściu zużycia do bardziej intensywnej fazy rozwoju. Planuje się, zatem przeprowadzić dalsze badania celem wyjaśnienia szczegółowego zachowania wartości szczególnych.

Słowa kluczowe: stan maszyny, symptomowa macierz obserwacji, dekompozycja SVD, ewolucja wartości szczególnych.

1. INTRODUCTION

The idea of symptom observation matrix (SOM) in multidimensional condition monitoring of machines is well established and brings several advantages, [1, 3, 15 - 19]. It is basing on $p > r$ rectangular symptom observation matrix, with (r) symptoms S_r in columns, measured along the system life θ , what gives p symptom readings in our passive diagnostic experiment [1]. This observation technique allows placing all physically different symptoms¹ measured in a phenomenal field of the machine in one SOM, and to process them in order to obtain projection of designed **observation space** to the **fault space** of machine, which we are looking for. Of course, at the beginning we usually observe more symptoms (*columns of SOM*),

than there is expected number of essential faults² in a machine.

The preprocessing of SOM may be different (*see for example* [17]), but for condition monitoring it was found that normalization and extraction of symptom initial value is the best solution, bringing all symptoms to their dimensionless and most sensitive form. Then, the application of SVD to the dimensionless form of SOM gives needed projection of observation space (*symptoms*) to the fault space - described by the generalized fault symptoms and singular values. The resultant three matrices of SVD decomposition allow calculating the two

¹ Symptom, measurable quantity covariable (*or assumed to be*) with the system condition

² Essential fault can lead to machine breakdown or terminal damage, if not interrupted by machine renewal.

diagnostically important matrices. The first is SD matrix, which give us generalized fault symptoms SD_i , and in theory they are independent each other. From this matrix we can calculate so called total damage (generalized) symptom, as the sum of all SD_i generalized fault symptoms. This is mainly in order to calculate the symptom limit value S_l , or to make the forecast of the **total damage** symptom. The second AL matrix, allows us to assess the contribution of primary measured symptoms S_r to a newly formed generalized fault symptoms SD_i . In this way we can just say which of primary measured symptom is redundant, giving no substantial information contribution to the given SD_i , and as such can be rejected from further calculations and/or future measurements.

But should we use the lifetime evolution of generalized fault symptoms SD_i as the only measure of evolving faults in a machine? From the SVD decomposition we suppose that singular values σ_i may have some diagnostic meaning. They can be interpreted as the generalized fault intensities, describing the advancement of the given kind of damage in a wearing machine. And also, they can be calculated after each new observation of symptom vector, allowing in this way the step by step tracing of this measure of evolving fault [19]. We will try to show this new possibility of inference using singular value decomposition (SVD) technique, in the way as it was shown in our earlier papers. In these papers some new measures based on singular values has been defined, namely modified Frobenius norm of SOM, being a sum of all nonzero singular values - SV, and so called volume of fault space – being the product of all nonzero SV. It will be interesting to know how the evolution of these measures can be modeled mathematically, and how they do behave theoretically and in practical circumstances of machine condition monitoring. It was found in this way that the approximate model of individual singular value and Frobenius modified measure may have the linear growth, while the volume measure is exponential function of the system lifetime. The present paper shows these properties of singular values and indicates their possible applicability in a diagnostic inference.

2. SYMPTOM OBSERVATION MATRIX (SOM) PROCESSING AND GENERALIZED FAULT EVOLUTION

It was described earlier, our information on machine condition evolution is contained in $p \times r$ SOM, where r columns (primary symptoms) and p rows of successive readings of each symptom are located. Usually they are made at equidistant system lifetime moments $\theta_n, n=1,2,\dots,p$. In pre-processing operations, the columns of SOM are centered and normalized to the three point average of initial readings of every symptom. This is in order to make the SOM dimensionless, and to diminish starting

disturbances of symptoms (averaging). This allows also to present the evolution range of every symptom from zero up to few times of its initial symptom value S_{0r} , (measured in the vicinity of $\theta = 0$). Also it was found in some earlier paper of the author, that the addition of linear growing system life symptom (LS) in the first column of SOM, give us new information concerning the intensity of use of the investigated machine.

After such preprocessing we obtain the dimensionless SOM in the form;

$$SOM = O_{pr} = [S'_{nm}] \quad S'_{nm} = \frac{S_{nm}}{S_{0m}} - 1, \quad (1)$$

This additional symptom can not have to small values or to large values, because in this way it will, or will not, influence our calculation and final result. If machine observation starts from its good condition, than usually symptoms starts also from small values, and at the end of life we have maximal symptom values. Hence one way of scaling life symptom LS may include multiplying by the average of last readings of all observed primary symptoms. Let the counting of symptom readings in SOM will be $i = 1:n$, and for r symptoms one can write;

$$LS = (r)^{-1} \cdot \sum_1^r S_{nm} \cdot (i/n), \quad i = 1:n, \quad (1a)$$

where S_{nm} means the last readings of symptom number m .

Now, adding LS symptom as a first column to the old SOM (1) we have a new appended SOM_L, which includes explicit machine life information to our diagnostic calculations and decision. Having this, we can apply the Singular Value Decomposition (SVD) [10], [12],[9], to our dimensionless SOM (1), to obtain singular components (vectors) and singular values (numbers) of SOM, in the form

$$O_{pr} = U_{pp} \cdot \Sigma_{pr} \cdot V_{rr}^T, \quad (T - \text{matrix transposition}), \quad (2)$$

where; U_{pp} is p dimensional orthonormal matrix of left hand side singular vectors, V_{rr} is r dimensional orthonormal matrix of right hand side singular vectors, and the diagonal matrix of singular values ($s. v.$), Σ_{pr} is defined as below

$$\Sigma_{pr} = \text{diag}(\sigma_1, \dots, \sigma_l),$$

$$\text{whit nonzero s.v. : } \sigma_1 > \sigma_2 > \dots > \sigma_u > 0, \quad (3)$$

$$\text{and zero s. v. ; } \sigma_{u+1} = \dots = \sigma_l = 0; \quad l = \max(p, r), \\ u \leq \min(p, r), \quad u < r < p.$$

Going back to SVD itself it is worthwhile to say, that every non square matrix has such decomposition, and it may be interpreted also as the product of three matrices [12], namely

$$O_{pr} = (\text{Hanger}) \times (\text{Stretcher}) \times (\text{Aligner}^T) \quad (4)$$

This is a very metaphorical description of SVD matrix transformation, but it seems to be a useful analogy for the inference and decision making in condition monitoring. The diagnostic interpretation of formulae (4) can be obtained very easily. Namely, using its left hand side part, we are stretching our SOM over the life (*observations*) dimension, obtaining the matrix of **generalized symptoms SD** as the columns of the matrix. And using the right hand side part of (4) we are stretching SOM over the observed (*primary*) symptoms dimension in the form of matrix **AL**, assessing in this way the contribution of each primary symptom to the generalized fault symptom $SD_i, i=1, \dots, u$. Hence

$$SD = O_{pr} \cdot V_{rr} = U_{pp} \cdot \sum pr, \quad \text{and}; \quad (5)$$

$$AL = U_{pp}^T \cdot O_{pr} = \sum pr \cdot V_{rr}^T$$

We will calculate the above matrices and use them for better interpretation of monitoring results (**SD**) and optimization of the dimension of the observation space (**AL**).

As the rows of SOM matrix are formed along the machine lifetime, so the columns of **SD** matrix have the same discrete argument of life time θ , and we can write their fault space interpretation as below;

$$SD_t(\theta) \propto F_t(\theta), \quad t=1,2,\dots, \text{Norm}(SD_t) \equiv ||SD_t|| = \sigma_t, \quad t = 1, \dots, u \quad (6)$$

For the assessment of total machine damage we can calculate the sum of all generalized symptoms

$$\text{SumSD}_i(\theta) = \sum_{i=1}^z SD_i(\theta) = \sum_{i=1}^z \sigma_i(\theta) \cdot \mathbf{u}_i(\theta) \propto \mathbf{F}(\theta) \quad (7)$$

where; \mathbf{u}_i is a column of U_{pp} matrix.

This concept of diagnostic inference, for individual fault $F_t(\theta)$, (6), and total fault damage $\mathbf{F}(\theta)$ (7) has been proven in several papers [1, 3, 11], [13-19], and we will use it here in further consideration.

The above results, based on generalized fault symptoms, have been obtained only from the first matrix **SD** of (5). And the second matrix **AL** gives us the relative measure of information contribution to each generalized symptom, as given by particular primary symptom measured during the SOM gathering. This is one way of assessment of the primary symptom redundancy, but we need some other global indicators of rejection of the redundant symptom. In our previous papers we have used modified Frobenius norm of SOM and the generalized

volume of the fault space created by SOM. What is important in such an approach, these two measures are based on singular values of SOM, which in turn can be treated as the faults advancement measure (*see (6-7)*). Hence we have;

$$\mathbf{Frob1} = \sum \sigma_i; \quad \text{and}; \quad \mathbf{Voll} = \prod \sigma_i, \quad i = 1, \dots, u \quad (8)$$

Looking for the way of value creation method of the above, one can infer that if some primary symptom will be really redundant (*small* σ_i) its rejection should give a small change to; *Frob1* measure, and in contrary it should increase much the fault space volume; *Voll*. We will notice also how it behaves with real examples of symptom rejection and addition in SOM of diagnosed machines latter on.

Such way of diagnostic inference described in (8) has been used in last papers of present author. However there is question now; why do not treat these two measures (8) as evolving along system lifetime θ , together with the evolution of all generalized faults in a machine? So instead of (8) we can write down as below

$$\mathbf{Frob1}(\theta) = \sum \sigma_i(\theta); \quad \text{and}; \quad \mathbf{Voll}(\theta) = \prod \sigma_i(\theta), \quad i = \dots, u. \quad (9)$$

And of course the system lifetime will be the discrete variable in the above, the same as moment of symptom readings $\theta_n, n=1, \dots, m$, in our primary SOM. We will see below what evolutionary property have newly defined measures (9), and how much this can help in tracing the fault evolution (*development*) and reduction of observation redundancy in the real cases of machine diagnostics.

3. THE SIMPLIFIED THEORY OF SYSTEM DAMAGE AND SINGULAR VALUES EVOLUTION

Trying to build simple theory of singular value possible behavior, let us assume that our system in operation, machine or it element, has a constant working load, what assures the low level of external disturbances in symptom observation. Of course the constant working load is a source of constant wear of machine elements, giving a constant rise of each symptom value. In such case we can assume in a first approach, that our primary symptoms have also almost linear changes, as below.

$$S_j(\theta) = S_{j_0} + \theta (b_{j_0} + \varepsilon b_j(\theta)), \quad \varepsilon \ll 1, \quad j = 1, \dots, r; \quad \theta = \theta_1, \theta_2, \dots, \theta_p. \quad (10)$$

where S_{j_0} and b_{j_0} are the initial value and the slope of symptom number j , and ε is small number allowing the deflection of symptom from a linear law of behavior during consecutive

symptom readings $\theta_1, \theta_2, \dots, \theta_p$, and forming symptom observation matrix - SOM.

The decomposition of SOM give us the generalized fault symptoms $SD_t(\theta)$ and singular values $\sigma_t(\theta)$, $t = 1, \dots, u$, and we may assume also their similar almost linear behavior. This may be written as below.

$$SD_t(\theta) = SD_{t_0} + \theta (c_{j_0} + \varepsilon c_j(\theta)), \theta = \theta_m, m = 1, \dots, p, (11)$$

$$\sigma_t(\theta) = \sigma_{t_0} + \theta (a_{t_0} + \varepsilon a_t(\theta)), t = 1, \dots, u,$$

where u is the rank of SOM being usually the number of symptoms (*columns*) in SOM, and $c_j(\theta)$, $a_t(\theta)$, $b_j(\theta)$ are set to zero in a first approach to modeling their evolution.

The initial values of generalized fault symptom SD_{t_0} and singular value σ_{t_0} depends on the way of SOM pre-processing. In case where each primary symptom (10) is normalized and centred to the initial value, they become zero; $\sigma_{t_0} = 0$, and our decomposition results (11) starts their evolution from **zero value**. There is also the difference in SOM decomposition presentation along the life coordinate and the symptom dimension. In both cases the initial value is zero for θ_t , but later on the lifetime evolution generalized symptoms and singular values differ.

Let us see also how our measures of information content in SOM (9) will fit into our model (11) taken in a first approximation.

$$Frob1(\theta) = \sum \sigma_r(\theta) \approx \theta \cdot \sum a_{t_0}, t = 1, \dots, u. (12)$$

and;

$$Vol1(\theta) = \prod \sigma_r(\theta) \approx \theta^u \cdot \prod a_{t_0} \approx \begin{cases} \theta, & t = 1, \dots, m \\ \neq \theta, & t = m+1, \dots, u \end{cases}$$

As it is seen in a first approximation, both information content measures grows with system lifetime θ , and first **Frob1** grows linearly, while the second **Vol1**

exponentially. Hence in reality of condition monitoring they must be non decreasing functions of lifetime, i.e. will grow with increased number of symptom readings, or the rows of the SOM.

The course of all generalized symptoms $SD_t(\theta)$ have nonzero values during the next life increments but singular values $\sigma_r(\theta)$ starts sequentially, the second life increment θ_m , $m=1$ gives nonzero $\sigma_r(\theta)$, for $t=1$ only, and each subsequent lifetime increment switches on the next nonzero singular value, up to the readings number $r+1$, (r being the number of symptoms), when all singular values have already nonzero values. We will see that this property is important for **s.v** product measure, when looking for processing results at the next point of the paper.

4. THE EVOLUTION OF SINGULAR VALUE OF SYSTEMS IN OPERATION -EXAMPLES

Starting our illustrative and validating examples let us take SOM of small ball bearing at durability testing stand under constant load during the whole test. Here the peak and rms amplitudes of acceleration and velocity of the bearing outer ring has been measured, together with acoustic emission energy, the temperature, and the stand driving power. Altogether the SOM has 7 symptoms and appended lifetime in the first column. During the SOM preprocessing the symptom normalization and centering to the initial value has been applied. Special Matlab® program **svdoptsvev.m** has been compiled from the author previous programs, and the processing result one can see in the figure below.

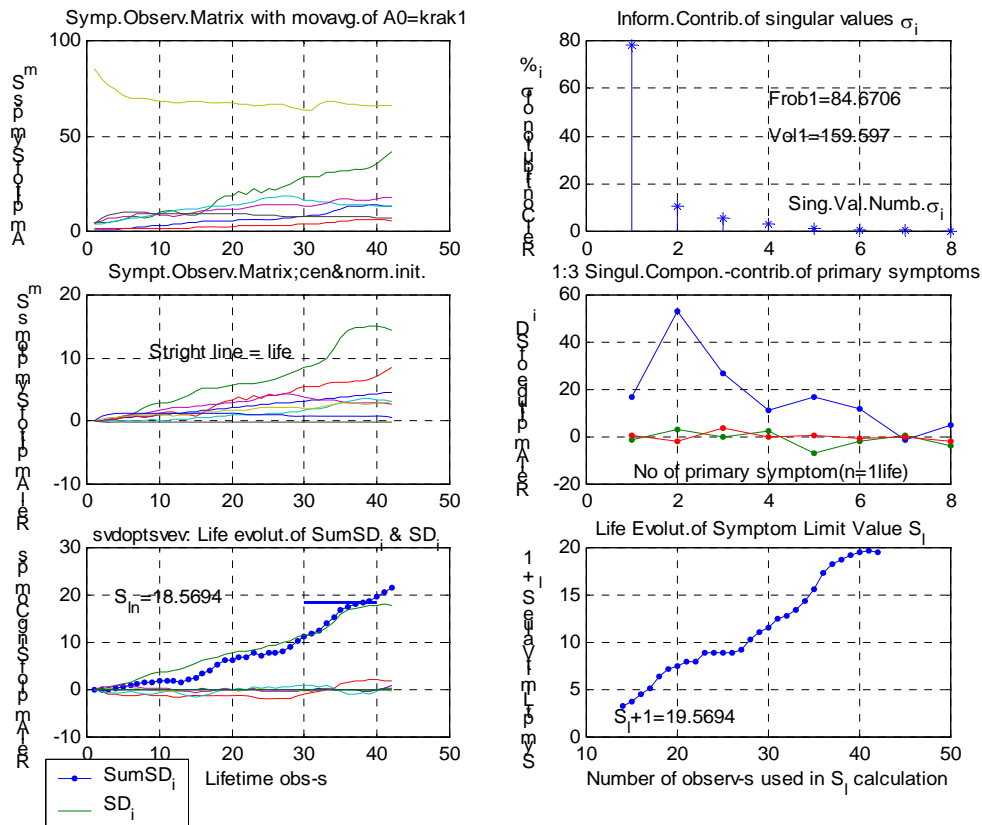


Fig. 1. Small ball bearing at durability testing stand and diagnostic decomposition of its SOM, as a sequence of pictures

The picture upper left presents graphically SOM as it was received and registered. As one can notice, one of the symptoms, the driving power of test stand is falling down, reciprocally to the deteriorating bearing condition. The other symptoms create the bunch of similar symptom life curves, much better seen after normalization and centering (*picture middle left*), where the straight line of bearing lifetime is also visible. We can notice that centering and normalization is right preprocessing method, allowing comparing the real diagnostic value and sensitivity of primary measured symptoms.

The generalized fault symptoms obtained after SVD one can see in the picture bottom left, where two life curves are distinguishable only. These are, the total

damage symptom **SumSD_i** and the generalized symptom of fault No 1 i.e. **SD_i**. This means we have one type of damage in the bearing, what is confirmed from the picture upper right, where the succession of SOM singular values (*s.v.*), σ_i is presented in descending order. There is also the assessment of information content of primary measured symptoms in the picture middle right, where one can see the low information contribution of last three primary symptoms, this means they maybe redundant. The last picture, the bottom right presents the step by step calculation of symptom limit value, needed in every diagnostic case, but not necessarily in our case.

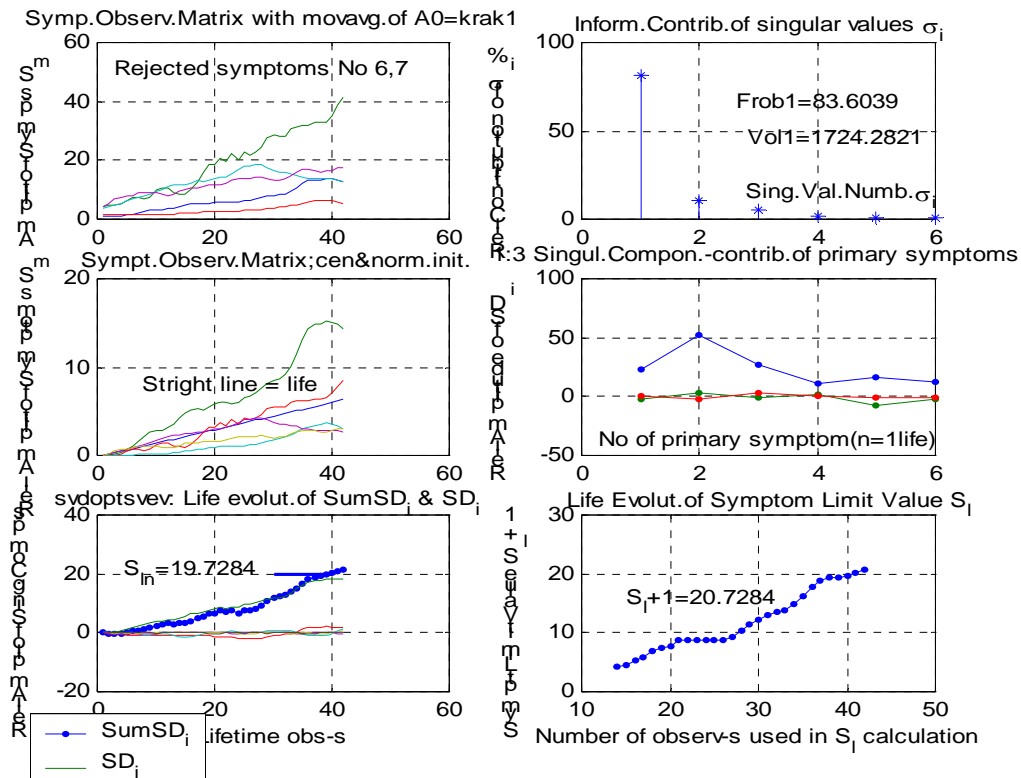


Fig. 2. SOM of the same bearing krak1 processed after rejection of 2 redundant symptoms

The presented software allows also the rejecting of some redundant symptoms from initial SOM, and the next Fig. 2 shows the result of such rejection of symptoms No 6 and 7, presented in the same mode of six pictures. One can say they are similar, but much smoother, and have different values of *Frob1* and *Vol1* information measures calculated from singular values of SOM. Hence it will of much interest to see the evolution of these measures and respective singular values as well.

The lifetime evolution of these quantities is shown in two pictures; Fig. 3 for the original SOM, and Fig. 4 for SOM with rejected symptom No 6, and 7. The left picture of each figure presents the evolution of individual singular values and sum of them, as the

total damage symptom. We can notice that our simple theory with linear and exponential grows of these quantities (12) is here approximately true in both figures, i.e. for original SOM and for abbreviated SOM, after the rejection of two symptoms. The right hand side pictures of Fig. 3 and Fig. 4 shows us that the product of singular values is continuously growing exponential function, and is much more sensitive to detect wear changes of ball bearing when the redundancy of SOM has been reduced, (Fig. 4), where bearing deterioration is noticeable starting from 0.2 of dimensionless life of bearing.

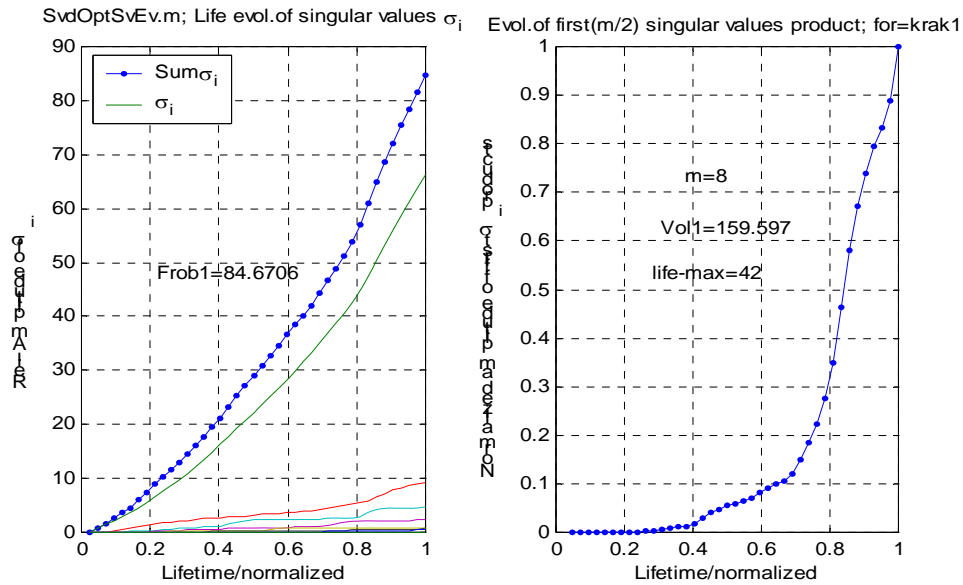


Fig.3. The lifetime evolution of singular values; their sum and product as the illustration of constant speed damage of the ball bearing krak1

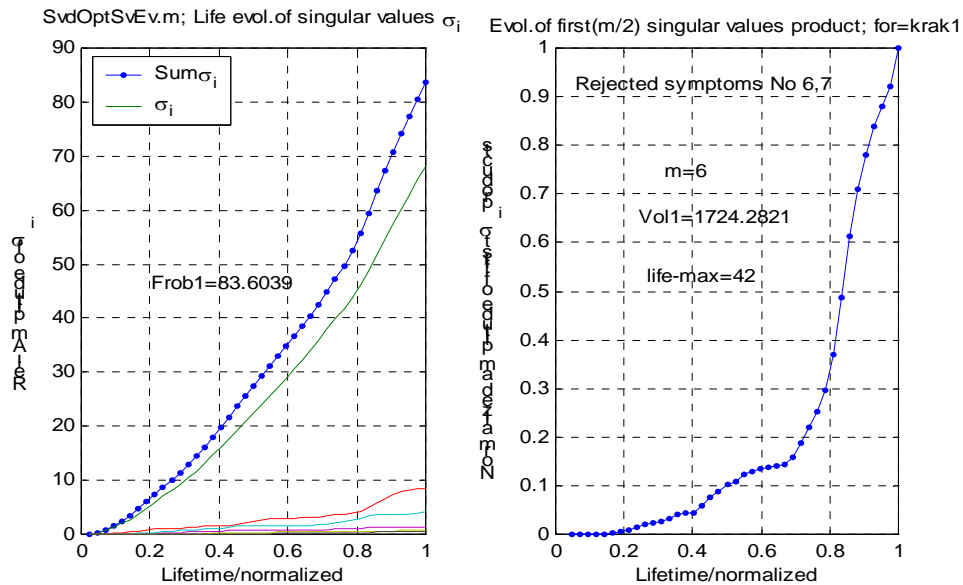


Fig.4. The lifetime evolution of singular values of ball bearing krak1, after rejection of two redundant symptoms

We can confirm again that the reduction of SOM redundancy causes small decrease of **Frob1** measure, but dramatic increase of the volume of generalized fault space **Vol1** is taking place. In conclusion one can say that **Frob1** is the good measure of overall system condition, and **Vol1** is sensitive to drop of the redundancy in SOM.

It will be of much interest to investigate the behavior of this measure at normal operating condition of the machine, not as it was just before, where ball bearing had the **constant** working load. Hence we present below two troublesome cases of real life diagnostics; ventilation fan in copper mines where the load control of the fan is impossible (Fig. 5), and the coal mill fan working with modulated load in very noisy surroundings (Fig. 9).

Fig. 5 presents the tragedy of uncontrolled load, where even after SVD decomposition; no one knows

how to infer on fan condition. Here five vibrational symptoms have been monitored over 30 week's lifetime. But after the rejection of one load sensitive symptom (No 4), the situation was much more cleared and almost diagnosable, (see Fig. 6).

Looking now for the evolution of singular values (Fig. 7 and 8) we do not see any trouble with uncontrolled oscillating load, even with load sensitive symptom (Fig. 7). One can see almost linear grows of Frobenius SOM measure **Frob1**, and damage sensitive measure of **Vol1**, which starts rapidly exponentially, grows at **0.6** of dimensionless machine lifetime.

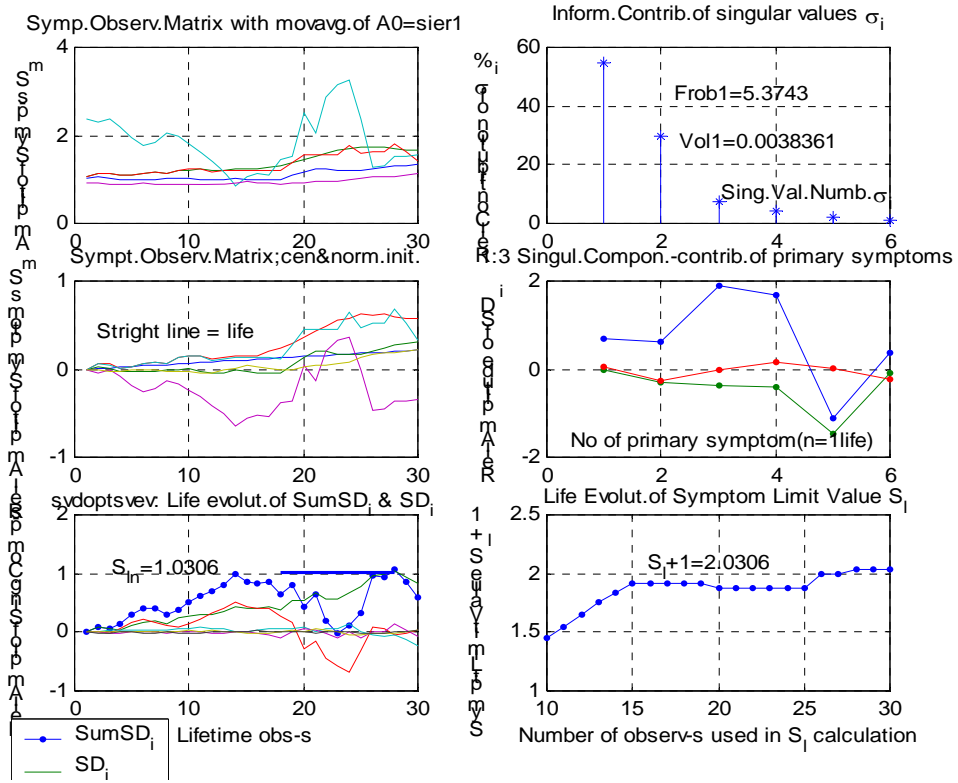


Fig. 5. Ventilation fan in one Polish copper mine with uncontrolled load, and its SOM decomposition

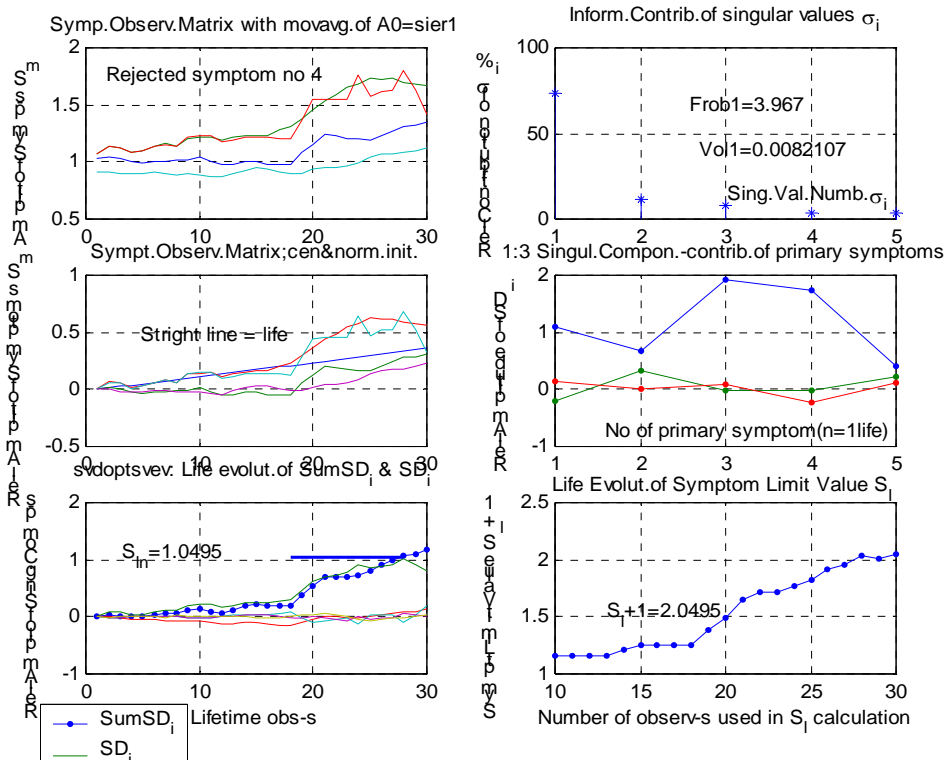


Fig. 6. SOM of the same fan as in fig.5 but without symptom no 4

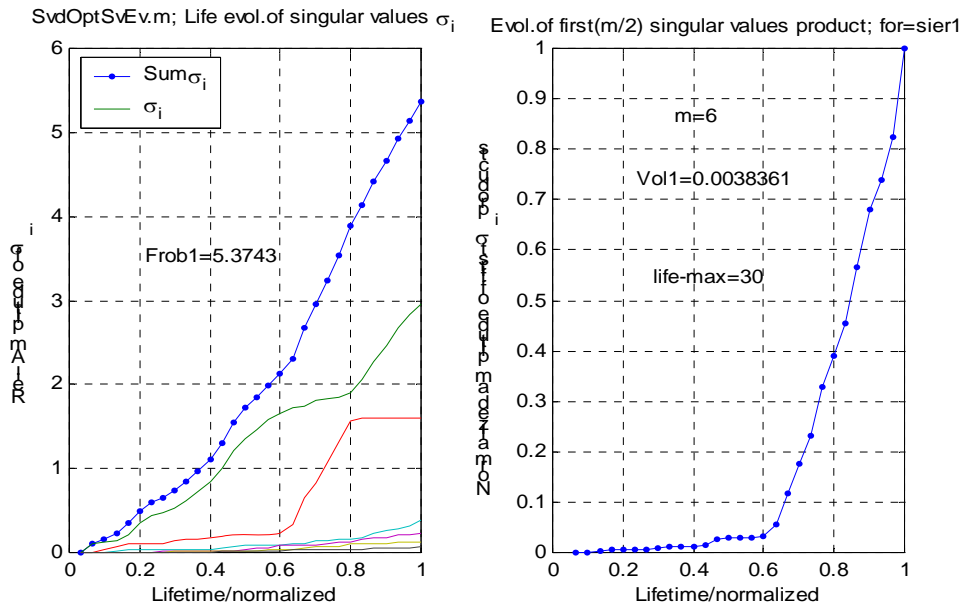


Fig. 7. The evolution of singular values for the ventilation fan with SOM presented in Fig. 5

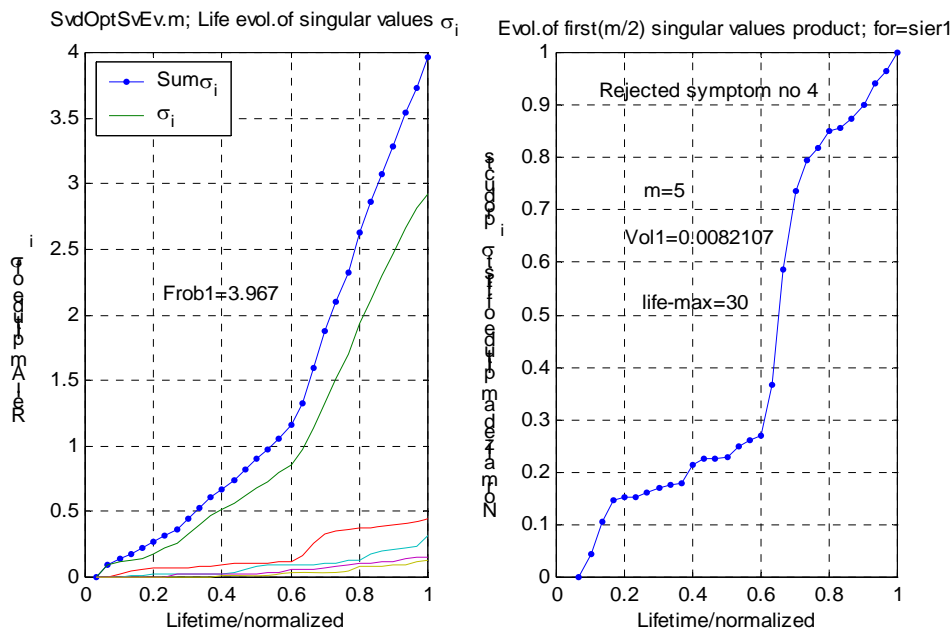


Fig. 8. Ventilation fan as before but with rejected one symptom

But when we reject the load sensitive symptom (*no 4, Fig. 8*), the course of both measure is improving much, especially *Vol1*, which shows system degradation starting much earlier, exactly at **0.2** of machine dimensionless lifetime, having damage acceleration point at 0.6 lifetime as before.

Let us apply now the same methodology to the special case of ball bearing testing with specially modulated load, as shown in Fig. 9. One can see here that such load modulation is visible in every stage of signal decomposition (*left pictures*); after normalization and centering, and after SVD decomposition as well. However the symptom limit vale S_1 is determined easily, what can be seen in the

picture bottom right of Fig. 9. And now the important question is, what will be the life behavior of singular vales and their derivative measures; *Frob1*, *Vol1* in this case? This can be seen in detail in Fig.10, where one can notice some small modulation imposed on the steady growth of all life dependent curves. This concerns only to the singular values and their sum, but not on the product of singular values, and such behavior is independent of redundancy reduction. However, after the rejection of three redundant symptoms, the course of *Vol1* curve is much more life sensitive, as it was reported before (*see Fig. 11*).

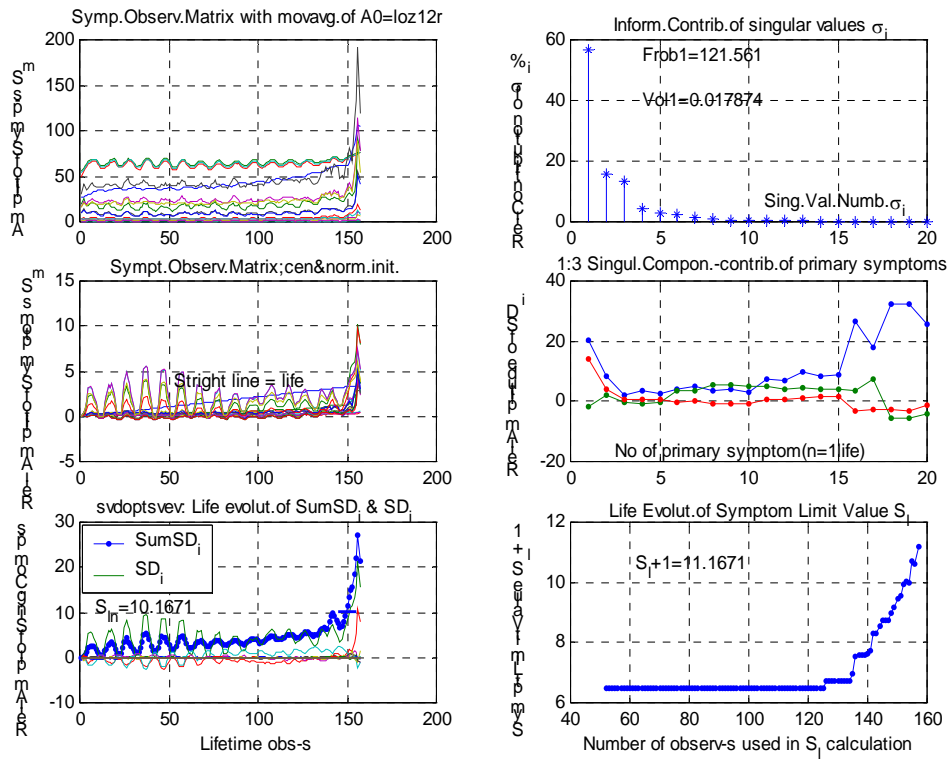


Fig. 9. The decomposition of SOM of a ball bearing at the durability testing stand with an modulated load

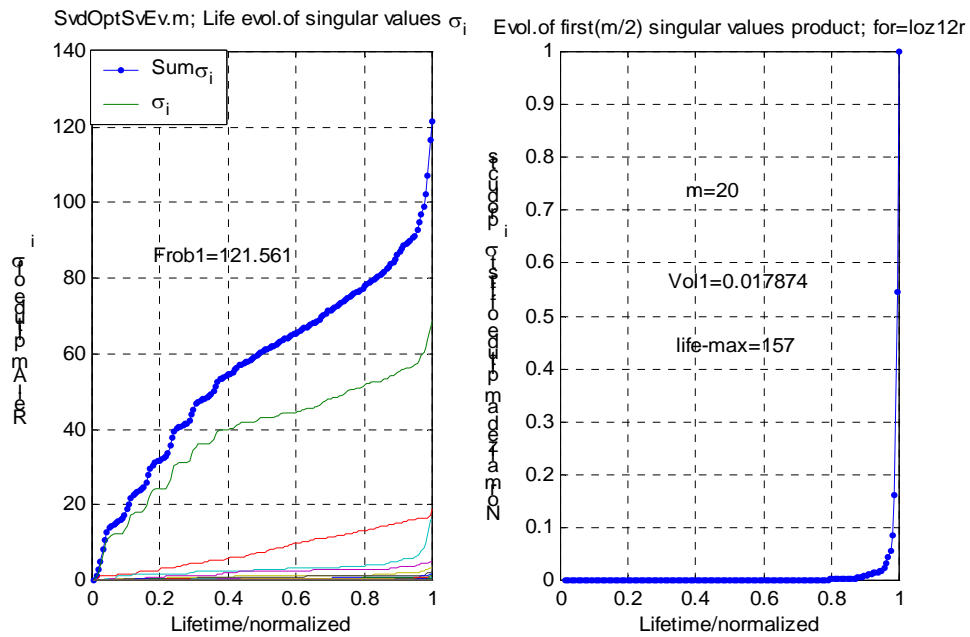


Fig. 10. The evolution of singular values and their derivative measures for the case of Fig. 9

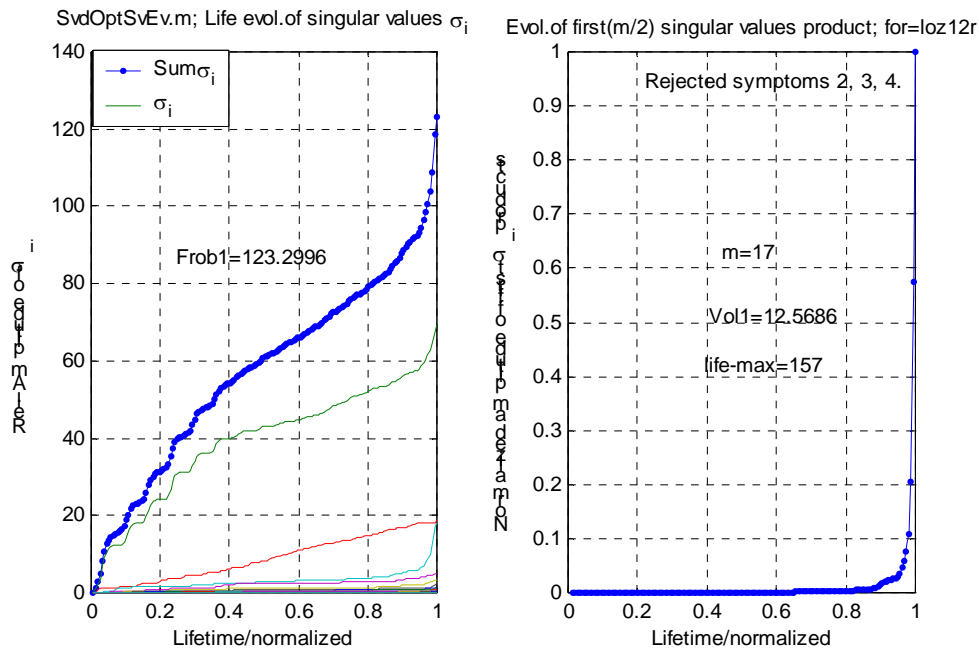


Fig.11. The same as in Fig. 10, but with rejected three redundant symptoms

When comparing the course of total damage symptom of the machine (curve with dots in Fig. 9 picture bottom left) with total damage symptoms obtained as modified Frobenius measure (Fig. 10 and 11) one can note that ongoing breakdown of the machine is much more visible when looking for the new measure *Frob1*.

It seems to the author that enough conclusive evidences have been presented above, concerning some new unknown property of singular values, when SVD is applied to SOM of system in operation. This is particularly well seen when singular values and their derivatives are presented along system lifetime. This conclusion needs more rethinking and condition monitoring verification, but up to now the presented results seems to be sound. In future investigations one should verify if the linear growths property (12) is connected with system damage or with the number of rows in a SOM matrix. This seems to be essential for a further diagnostic application of newly detected properties of singular vales.

5. CONCLUSIONS

In a recent papers [11, 13 -18] of the present author, the problem of diagnostic decision in case of load sensitive machines has been considered. And the last paper [19] brings some new useful property of SOM singular values; namely their immunity against machine load change. It s very important property, hence following this, a simple model of singular values evolution has been proposed and validated by means of several diagnostic cases; first with constant load and with unstable machine load latter on. It was found that proposed linear growth model of individual singular value fits well to the real cases of machinery diagnostic, the same as exponential model for the product measure of singular values *Vol1*. It was also found, that this measure is sensitive to the redundancy

in observation space and can depict well the beginning of the damage in monitored system.

Acknowledgment:

This paper was partially financed by research grant No 1751/B/T02/2009/37, given by Polish Ministry of Science and Higher Education.

6. REFERENCES

- [1] Cempel C., (1999), *Innovative developments in systems condition monitoring*, Keynote Lecture, Proceedings of DAMAS'99, Dublin, Key Engineering Materials, Vols. 167-168, Trans Tech. Public., Switzerland, 1999, pp172-188.
- [2] Cempel C., Natke H. G., Yao J. P. T., (2000), *Symptom Reliability and Hazard for Systems Condition Monitoring*, Mechanical Systems and Signal Processing, Vol. 14, No 3, 2000, pp 495-505.
- [3] Cempel C., Tabaszewski M., (2005), *Multidimensional vibration condition monitoring of non-stationary systems in operation*, Mechanical Systems and Signal Processing, 2007, 21 (3), pp. 1233-1241).
- [4] Korbicz J., et al, (eds.), (2004), *Fault Diagnosis – Models, Artificial Intelligence, Applications*, Springer Verlag, Berlin - Heidelberg, 2004, p828.
- [5] Tumer I. Y., Huff E. M., (2002), *Principal component analysis of tri-axial vibration data from helicopter transmission*, 56th Meeting of the Society of Machine Failure Prevention Technology, 2002.
- [6] Jasiński M. (2004), *Empirical models in gearbox diagnostics* (in Polish), PhD Thesis, Warsaw University of Technology, Warsaw, December 2004.

- [7] Cempel C., (1991), *Vibroacoustic Condition Monitoring*, Ellis Horwood Press, New York, 1991, p212.
- [8] Cempel C., (1987), *Simple condition forecasting techniques in vibroacoustical diagnostics*, Mechanical Systems and Signal Processing, 1987, pp 75 – 82.
- [9] Kielbasinski A., Schwetlik H., *Numeric Linear Algebra*, WNT Press Warsaw, 1992, p502.
- [10] Golub G. H., VanLoan Ch. F., *Matrix Computation*, III-rd edit, J Hopkins Univ. Press, Baltimore, 1996, p694.
- [11] Cempel C., Tabaszewski M., (2007), *Multidimensional condition monitoring of the machines in non-stationary operation*, Mechanical Systems and Signal Processing, Vol. 21, 2007, pp 1233-1247.
- [12] Will T., (2005), *Hanger matrix, two-thirds theorem*, Internet; <http://www.uwlax.edu/faculty/will/svd/svd/index.html>, June 2005; (see also: *SVD ingredients*, Mathematica, April 2004).
- [13] Cempel C., *Optimization of Symptom Observation Matrix in Vibration Condition Monitoring*, Proceeding of ICRMS09, Chengdu-China, July 2009, pp 944-960.
- [14] Tabaszewski M., (2006), *Forecasting of residual life of the fan mill by means of neural nets* (in Polish), *Diagnostyka*, Vol. 3, (39), 2006, pp 149-156.
- [15] Cempel C., Tabaszewski M., (2007), *Application of grey system theory in multidimensional machine condition monitoring* (in Polish), *Diagnostyka*, No 2, (47) 2007, pp11-18.
- [16] Cempel C., Double singular value decomposition (SVD) of symptom observation matrix in machine condition monitoring, *Diagnostyka*, No 1(53), 2010, pp3-12.
- [17] Cempel C., Decomposition of Symptom Observation Matrix of some Population of Applications as the Help in the Decision Process of Reviewers Board, (in Polish), *Ergonomia, Technika i Technologia - Zarządzanie*, M. Fertch (edit.), Poznań University of Technology Press, Poznań 2009, pp245-253.
- [18] Cempel C., Tabaszewski M., *Singular Spectrum Analysis as a smoothing method of machine load variability*, *Diagnostyka*, No 4(56), 2010, p3-8.
- [19] Cempel C., *The evolution of generalized fault symptoms and fault intensities as indicators of observation redundancy and coming system breakdown*, Mechanical Systems and Signal Processing, 25 (2011), p3116-3124.

DESCRIPTION OF VARYING OPERATIONAL CONDITIONS IN WIND TURBINES

Dariusz BRODA, Tomasz BARSZCZ

Department of Robotics and Mechatronics, AGH University of Science and Technology,
Al. Mickiewicza 30, 30-059 Cracow, email: dariuszp.broda@gmail.com

Summary

Vibrations of wind turbines strongly depends on the wind. For the purpose of wind turbines condition monitoring it is very important to understand the nature of the wind, especially its time variability. The paper investigates fundamental statistics of the wind and vibrations for four wind turbines in two wind farms. Seasonal and diurnal variations are presented and discussed. For both vibration and wind speed seasonal trends are clearly visible, particularly for mean values, but also for standard deviation. Variability of vibration and wind are compared using mean/std ratio. The results can be helpful to determine operational states of wind turbines. It can also help achieve comparable results of technical state assessment for different machines located in different locations.

Keywords: wind turbine, operational states variability, wind variability, vibration, monitoring.

OPIS ZMIENNOŚCI WARUNKÓW OPERACYJNYCH TURBIN WIATROWYCH

Streszczenie

Wibracje w turbinach wiatrowych zależą w znacznym stopniu od wiatru. Zrozumienie natury wiatru jako zjawiska, szczególnie jego zmienności, jest istotne dla skutecznej diagnostyki turbin wiatrowych. Artykuł opisuje podstawowe dane statystyczne prędkości wiatru oraz wibracji dla czterech turbin wiatrowych z dwóch różnych farm. Opisane są zmiany sezonowe i dzienne. Trendy sezonowe są widoczne zarówno w przypadku prędkości wiatru jak i poziomu wibracji, szczególnie w przypadku wartości średnich, ale także, do pewnego stopnia, dla odchyleń standardowych. Zmienności wibracji i prędkości wiatru są porównane przy pomocy współczynnika mean/std. Wyniki będą pomocne przy ustalaniu stanów operacyjnych turbin, a także przy ocenie stanu technicznego dla turbin zlokalizowanych w różnych lokacjach.

Słowa kluczowe: turbina wiatrowa, zmienność warunków operacyjnych, zmienność wiatru, wibracje, monitoring.

1. INTRODUCTION

Wind turbines are one of the most fastest growing branch of renewable energy sources. Wind energy resources in Poland are medium, but still not fully utilized [1].

According to the report prepared by Ministerstwo Gospodarki [2], until the year 2015 wind energy should become the major source of renewable energy. In 2030 wind farms capacity should reach 7867 MW in comparison to 976 MW in 2010. Those numbers prove, that wind turbines are considered as very important source of energy and great number of them might be expected to be built in the following years.

Wind turbine is a device that converts the kinetic energy stored in the air stream (wind) into the mechanical energy, which is afterwards converted into the electric power. Wind turbine machinery can be roughly divided into the mechanical (mechanical drive train) and electrical

subsystems [3]. The first system consist mainly of generator (synchronous or asynchronous) sometimes followed by a frequency converter. Mechanical components are blades, bearing, blade pitch mechanism, gearbox and yaw system. Gearless systems are also available, e.g. by Enercon [4]. In such a designs, low speed generator followed by the inverter is used. The solution that tries to combine advantages of both types of drive trains has been presented by AREVA in MULTIBRID M5000 offshore plant, where single stage planetary gearbox is integrated with the generator [3, 5]. Both systems (mechanical and electrical) are controlled by the control unit.

In wind turbines two different methods of controlling the output power are commonly used [6]:

- Pitch control, where blades of the main rotor are able to change the pitch. This mechanism is also used as an additional braking mechanism.

- Stall control, where the blades have fixed pitch and in stronger winds part of energy causes the stall, which in turn causes the power to decrease.

The more popular method nowadays is the pitch control, where the speed constantly changes in order to maintain the highest possible efficiency. This cause smearing of lines in the vibration spectra, what brings the necessity of order tracking [6]. In stall controlled turbines the speed is much more stable over relatively long periods of time, and thus the smearing can be observed to a lesser extent [6].

The wind, which is basically movement of air masses in the atmosphere, is mainly caused by a heating of the earth surface by the sun, particularly by differences in solar energy absorption by different terrain types. The other two reasons of wind occurrence are Coriolis forces and air particles momentum. Wind is also affected by a surface friction, and the terrain shape [3]. Such a many factors that influence the behavior of the wind cause it to be a complicated and hardly predictable phenomenon. To predict wind on a given location, we have to take into consideration its global distribution, local low and high pressure areas and local terrain shape [3]. Variability of the wind is one of the most important arguments against wind energy utilization. It is thus especially important to possess as complete knowledge about this phenomenon as possible.

Wind speed is usually presented by two parameters – mean annual wind speed and wind speed frequency distribution. In order to characterize the wind speed in a given location, measurements taken over decades are necessary [3].

Wind speed variability is determined by two factors – latitude of the site and surrounding distribution of land and water. Wind speed has random and periodic components. The first one are mainly the wind speed turbulences, although mean wind speed changes randomly from year to year [3]. Periodic component are diurnal and seasonal wind speed changes. From the economical point of view the mean annual wind speed is the most significant information, although shorter changes are interested from the point of view of machinery diagnostics.

In the rotating machinery diagnostic, one of the measured quantities is level of vibrations, which are dependent, among others, on rotational speed of the shaft and power transmitted through the shaft. In wind turbine both load and shaft speed are directly related to the wind speed (are also dependent on the control type, i.e. stall or pitch). Thus the level of vibrations should be dependent on the wind speed. On the figure 1 the relation between vibration level measured on the component of drive train and wind speed is shown. Measurements of vibrations performed at different wind speeds might cause

false evaluation of machinery state. In order to avoid such a situation, conditions in which vibrations are measured should be chosen carefully, and such an operating point evaluation is not possible without proper knowledge about operational conditions variability.

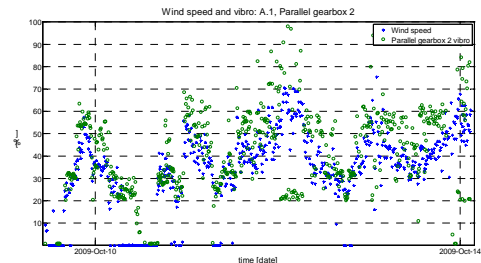


Fig. 1 Wind speed and vibrations on parallel gearbox of turbine A.1

The article is focused on the diagnostics of mechanical faults of rotating machinery (bearings, shaft, gearing). At first state of the art in wind turbine condition monitoring and wind variability are presented. The section is focused on different ways of wind variability assessment, mainly in the Europe but also in United States and Turkey. In the next section the statistical analysis of data from 4 wind turbines is presented, and on that basis seasonal trends are sought. Statistical analysis concerns both wind and driver-train vibration analysis. Examples of diurnal trend are also presented.

2. STATE OF THE ART

Some general information about wind turbine diagnostic can be found in [7 - 9]. Barszcz in [7] presents selection of diagnostic algorithms for wind turbines drive – train components. Problem of conditions variability is mentioned, along with its basic solution – order tracking. Thorough survey of condition monitoring (CMS) and fault detection (FDS) systems is presented in [8]. Beside vibration analysis also oil analysis, thermography, strain and acoustic (and more) are described. CMS and FDS of subsystems (rotor, pitch mechanism, gearboxes and bearings, electrical systems) are also reviewed.

Echavarria in [9] uses the German “250 MW Wind” test program database to investigate reliability wind turbines major components through several years. Report takes into consideration different turbines sizes (rated output power) and technology.

Example of new idea for wind turbine condition monitoring has been presented by Yang et. al in [10]. Faults are detected on the basis of generator output power and rotational speed, using continuous – wavelet – transform – based adaptive filters. Method is tested by detection mechanical unbalance and electrical asymmetry.

Wind variability is a complex topic and numerous publications bring the subject up. According to Hau [3] the most important for wind energy production are annual changes of mean wind speed, although diurnal, seasonal and even shorter changes occur. Exemplary data of annual variability are given in [3] (300kW wind turbine, north sea coast, years 1967 – 1997), which shows, that for most years power fluctuations from mean were less than 10%, although in some years they rise up to 15%. Description of annual changes can be found in works of Pryor [11] for Europe and Klink [12] for Minnesota.

Pryor in [11] focused on *historical variability of annual wind indices in Europe to provide a context for possible future scenarios, as well as possible tools for use in developing prognoses*. The analysis of inter – annual changes is conducted for Scandinavian and Baltic countries and also for whole continent. Inter - annual variability investigations and predictions are based on HadCM3 model. Klink [12] has investigated annual changes of wind speed on seven different sites in Minnesota. Beside the fact that mean annual wind speed have decreased in period from 1960s to mid 1990s, in each site different trends can be observed. The methods used in papers are described in the separate paragraph.

However, the current investigations are rather focused on seasonal, diurnal and hourly or even shorter changes. Holttinen in [13] presents data gathered from wind speed measurement in Nordic countries, along with comprehensive analysis of wind power variations. Several separate topics are in the field of his interest.

General conclusion states that *the hourly variations of large-scale wind power stay 91% - 94% of the time within +5% of installed capacity in one country, and for the whole of the Nordic area 98% of the time*. Those data concern whole region, for single turbine/farm variability is higher. For single exemplary site (in Finland) standard deviation has been higher than mean value of wind power production (28.2% to 25.9%), while for the whole Nordic region this ratio was equal to 14.5% to 25.1%. In Europe standard deviations to mean ratio is 0.5 – 0.8 for 200km radius circle and 0.3 for >2000 km. The same conclusion might be drawn from correlation analysis – which is 0.7 for WT in distances less than 100km and below 0.5 for distances 200-500 km. For distributed geographically wind farms *the total production never reaches total installed capacity and hardly ever totally calm*.

Next subject brought up in [13] are trends in wind speed. Frequency distribution for single countries and whole Norway are given for each season, with conclusion that winter months are responsible for 110% to 150% of annual energy production. According to Hau [7] the diurnal trends can be rarely observed in Europe. Holttinen in [13]

states, that such a pattern occurs when influence of sun dominates on weather front influence. Such a trend might be observed rather in the summer (in the Northern Europe). The more significant diurnal trend is observed in the southern part of Nordic area.

Another component of wind characteristics according to [13] are duration of calms, low winds and peaks, autocorrelation of wind power according to time lag (at 12h such a lag correlation becomes weak) and magnitude of variations for different time scales. For exemplary 103 MW wind farm those variations are: 4-7% of capacity in second, 10-14% in minute, 50-60% in an hour.

Apt [14] shows the turbine output in the form of power spectral density for both 1 sec and 1 hour samples. Data in [14] have been gathered from 4 wind farms for period of 4 years (2001 – 2004). *The measured output power is found to follow a Kolmogorov spectrum over more than four orders of magnitude, from 30 s to 2.6 days*. In [14] periodograms are used to present the PSD of output power, although no windowing or segments overlapping are used because no noticeable improvement in variant has been observed. *At frequencies between $2 \cdot 10^{-6}$ and $4 \cdot 10^{-2}$ the double logarithm plot of the spectrum is linear. At frequencies above $5 \cdot 10^{-2}$ the physical and electrical inertia of turbines appear to act as low pass filters*. Peaks in spectrum might be observed due to turbine blade passing. In [14] it is concluded that *Since wind is an intermittent resource, it must be matched with fill-in power sources from storage or generation if the power output of wind farms on a grid are correlated*.

Wan in [15] presents results of project undertaken by National Renewable Energy Laboratory to record long-term, high – resolution (1Hz) wind power output data from large wind power plants in various regions. Data have been gathered from 7 wind farms, the smallest 35 MW but most more than 100 MW capacity, with greatest distance between farms 1590 km (shortest 40 km). In the report coefficient of variance (COV, std/average) is frequently used to characterize the wind resource.

According to the data presented in [15] output power is less variable than wind speed. Wind power COV is generally higher than wind COV, although in some months they are almost equal.

The diurnal trends (the most strong in August, in winter almost not at all) and seasonal are mentioned in article. In the article the subject of aggregating wind turbines is also brought up (correlation between groups of turbines). *The range of 15-second correlation coefficients suggests that output powers from even nearby wind turbines are not related in short time frames. On the other hand, corr. Coeff. From 12-hour intervals are almost all close to 1*. [15]

Conclusions of [15]:

1. Short – term fluctuations of wind power plant are small – 0.1% for second data series, 1% for minute and 3% - 7% for hourly. No trends can be found in second – to – second fluctuations.
2. Output fluctuations are influenced mainly by the size of the wind power plants, more than by differences in turbine types and plant locations.
3. More wind plants connected to the system means output less volatile, although step changes in MW or kW will be even higher and calms are still possible.
4. Caution should be kept when simply scaling up wind power available from wind speed data from smaller wind power plant or single anemometer.

Petersen in [16] writes about the discipline known as wind power meteorology. According to the data presented in the article, in Northern Europe wind speed changes up to 30% from one decade to another might be expected and interannual variability up to 13%. Some laws and formulas concerning wind speed near surface are given (e.g. geostrophic drag law). Turbulence can be modeled by Kaimal spectra (atmosphere) and von Karman (rather wind channels).

Sinden in [17] investigate long-term wind patterns and their relationship to electricity demand in UK.

Giebel et. Al. [18] gives review of current methods of wind power prediction for single turbines, wind farms and whole regions, from few minutes up to a few days ahead. Ramp and variability forecasting are also in the scope of interest of researchers. Ramp forecasting has been first taken into consideration in 2006 in pilot project of the Alberta Electric System Operator, and variability *is only recently that it has come into the sight of researchers.*

Akpinar and Akpinar [19] and Celik [20] performed analysis of wind power in Turkey. Akpinar focuses on seasonal variations on 5 sites, using data gathered for 5 years. Celik studied data for year 1996 on one site, hourly values. Both papers used Weibull and Rayleigh distribution mainly. In [20] the first distribution is found to be more accurate (correlation coefficient 0.88). According to [19] ‘*c*’ parameter of Weibull distribution is near the mean wind speed.

What is interesting for the purpose of this article are also statistical tools used to wind variability description in presented papers.

Pryor in [11] used only Min, Max, Mean and std values to investigate inter – annual variability, while Klink in [12] uses also percentiles and Weibull shape parameter and percentiles to characterize the Wind speed in Minnesota. Weibull distribution and Rayleigh distribution (which is the simpler version of Weibull) have been also used in [19] and [20] as main wind speed characteristic.

In [13] wind power production in Nordic countries is presented by: mean, median, std, std/mean, range, min and max. The data were gathered for 3 years (2000 – 2002). Wind power production is also presented in the form of frequency distribution. Another characteristics are calms, low wind and peaks, correlation between different farms (with different distances between them) and autocorrelation of wind speed (up to 12h time lag).

In [14] the output power of WTs have been investigated with PSD - periodograms (with eight segments, no overlapping and no windowing).

In [16] author focuses mainly on std/average coefficient in presented data and step changes – presented separately as positive and negative changes.

3. DESCRIPTION OF METHODOLOGY AND DATA

The dataset consist of wind speed, output power and vibrations measured by wind turbine monitoring system, which stores one value every 15 minutes. Data from 4 turbines, 3 placed in windpark A and 1 in windpark B, are presented. Measurements from A cover the period from 01.07.2009 to 24.08.2010, and from B from 01.09.2009 to 26.07.2010 (additionally with data from may 2009).

Data have not been collected during repairs and maintenance actions, what results in overall number of measurement points (single collected values) as presented in table 1. In case of A.3 the overall number of samples is higher than number of 15 minutes long periods. Such a situation is caused by sampling rate, which is not exactly equal to 15 minutes but vary significantly, so average sample is shorter than 15 minutes. It should be also noted that number of samples vary on different turbines and in different seasons. The influence of periods when turbine does not work is briefly presented in the next chapter.

Table 1 Number of samples for each turbine

	no. of 15 minutes periods	A.1	A.2	A.3
01.07.2009 to 24.08.2010	40320	34428	36846	41748
July, August, September	10058	12916	9178	11900
October, November, December	10058	7204	8919	10502
January, February, March	10058	5741	9218	9661
April, May, June	10058	8567	9531	9685

Dataset has been investigated using statistical tools – mean value, standard deviation and max value (min value in every case was equal to 0) and frequency distribution of the wind speed. Data are presented in table 4.1 and exemplary frequency distribution is presented on figure 4.3.

4. STATISTICAL DATA ANALYSIS

The statistical analysis of data are presented in the table 1. In Autumn and Winter the highest mean wind speed might be observed for A turbines, while in B only in the autumn the wind speed is considerably higher. The differences in mean wind speed between single turbines in A are relatively high. Situation is not so clear in case of standard deviation of wind speed. For both A.1 and A.2 (as well as for B) highest standard deviation occurs in winter and autumn, while for A.3 occurs in winter and spring. Some explanation of those facts might be found by inspection of wind speed plot for each turbines. Comparing figure 4.1 (A.3) with figure 4.2 (A.2) it can be seen, that on the latter January and march are months of the highest variance, while on A.3 May variance is very high additionally. However, in May the measurements on A.3 have been performed only for several days, and in those days wind speed seems to vary considerably. Probably if more data for May would be available, the variance will not be so high in this month and in whole spring. This example shows the necessity of comparison of measurement for more than 1 year what let to avoid such an anomalies.

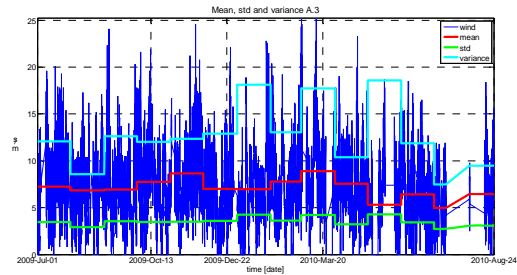


Fig. 4.1 Wind speed for A.3

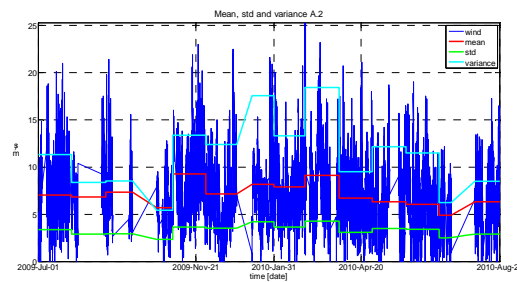


Fig. 4.2 Wind speed for A.2

Similar trend can be observed also in case of vibration measurement. In table 4.1 statistical analysis is presented – for A.1 and A.3 vibration measured on parallel gearbox is presented, for A.2 and B vibrations presented have been measured on generator. For A.1 and A.3 level of vibration is similar, while vibrations of A.2 generator are generally higher. The seasonal trend is even higher than in case of wind – for every turbine mean value of vibrations is higher in autumn and winter than in spring and summer. Situation is not so clear if vibrations standard deviation is taken into consideration.

Table 4.1 – statistical analysis

Season		Wind Turbine wind speed [m/s] / vibrations [g]			
		A.1 Parallel 1	A.2 Generator 1	A.3 Parallel 1	B Generator 1
Winter	Prob*	6	6	5	7
	Max	24,9 / 0,699	25,3 / 1,164	25,2 / 0,425	24,5 / 0,690
	Mean	7,82 / 0,189	8,39 / 0,408	7,76 / 0,166	6,46 / 0,239
	Std	3,91 / 0,168	4,07 / 0,263	4,12 / 0,110	3,89 / 0,135
	Mean / std	2,00 / 1,123	2,06 / 1,55	1,88 / 1,51	2,25 / 1,77
Spring	Prob*	6	6 / 8**	7	6
	Max	24,7 / 0,694	21,1 / 1,203	23,3 / 0,372	25,1 / 0,681
	Mean	6,47 / 0,144	6,38 / 0,269	6,560 / 0,139	6,46 / 0,152
	Std	3,33 / 0,129	3,33 / 0,291	3,74 / 0,093	3,53 / 0,122
	Mean / std	1,95 / 1,087	1,92 / 0,93	1,75 / 1,48	1,83 / 1,25
Summer	Prob*	7	6 / 8	7	6
	Max	23,2 / 0,699	21,4 / 1,132	24,1 / 0,415	24,4 / 0,685
	Mean	6,24 / 0,130	6,58 / 0,362	6,804 / 0,148	6,21 / 0,136
	Std	3,60 / 0,110	3,11 / 0,248	3,29 / 0,095	3,54 / 0,115
	Mean / std	1,73 / 1,185	2,12 / 1,46	2,07 / 1,56	1,76 / 1,18
Autumn	Prob*	7	7	7	6 / 8
	Max	23,6 / 0,693	23,0 / 1,231	24,6 / 0,416	25,4 / 0,696
	Mean	7,82 / 0,184	7,83 / 0,468	7,76 / 0,174	8,89 / 0,168
	Std	3,73 / 0,149	3,67 / 0,307	3,60 / 0,103	3,88 / 0,095
	Mean / std	2,10 / 1,241	2,13 / 1,53	2,16 / 1,69	2,29 / 1,77

* The wind speed value which probability of occurrence is the highest in given season

** There are two peaks

In order to compare variability of wind speed and vibrations amplitude, mean to std ratio has been calculated. The ratio is generally lower for vibrations, what means, that vibrations variability is even higher than variability of wind speed. In A turbines very weak seasonal effect can be observed, while in B ratio is considerably higher in autumn and winter.

On the figures 4.3a and 4.3b the exemplary histograms – for A.2 turbine in winter and spring, is shown. Histogram of summer is similar to histogram in spring, the same tendency can be observed in case of winter and autumn. The common feature of all histograms is higher probability of calms and low winds occurrence in summer and spring, as well as higher winds in autumn and winter.

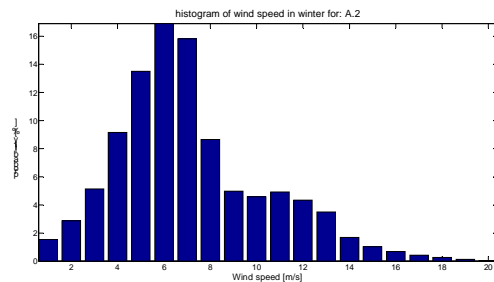


Fig. 4.3a Histogram of wind speed for A.2- winter

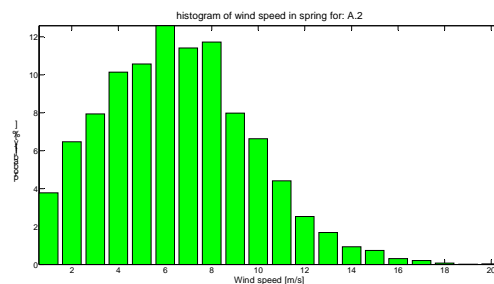


Fig. 4.3b Histogram of wind speed for A.2- spring

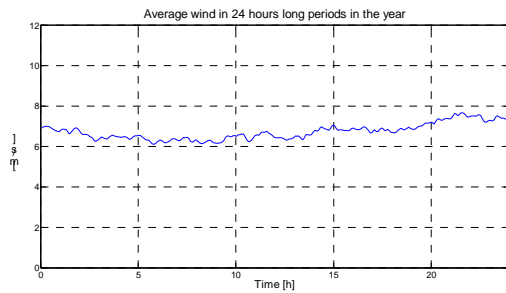


Fig. 4.4a Diurnal trend whole year A.3

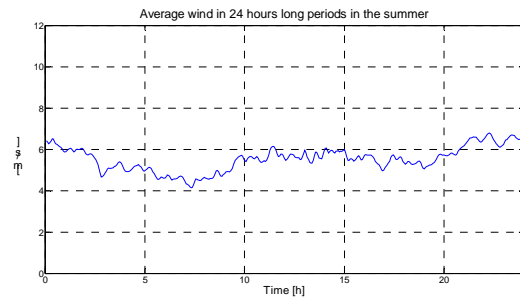


Fig.4.4b Diurnal trend May - September A.3

Diurnal trends have been sought in the data. Weak trends have been observed for turbines A.1 and A.2. The exemplary trend is shown in figures 4.4a and 4.4b (for A.3). In the summer and spring months (4.4a) the diurnal trend is more distinct, with two periods of higher wind – more visible in the night and less visible in the afternoon, but overall wind speed is smaller than in winter and fall months.

5. CONCLUSIONS

In the article the statistical analysis of variability of operational conditions is shown. Data consider both wind speed and vibration measured on drive-train of 4 wind turbines from 2 wind farms. It is clearly visible in the data, that mean wind speed is generally higher in the winter and autumn. The same trend, although not so distinct, might be observed in case of standard deviation of wind speed. For all turbines mean/std ratio is higher for wind speed than for vibration, so the latter variability is even higher than in case of wind speed. Probability distribution of wind speed is more steep in winter in autumn than in spring and summer, although in spring summer diurnal trend is much more distinct.

BIBLIOGRAPHY

[1] H.Lorenc: *Czy wiatr w Polsce można wykorzystać jako alternatywne źródło energii*, http://www.geoland.pl/dodatki/energia_lvi/mapa_energiawiatru.html

[2] Prognoza zapotrzebowania na Paliwa i Energię do roku 2030, Załącznik 2. *Do Polityki energetycznej Polski do 2030 roku*, Ministerstwo Gospodarki, Warszawa, 10 listopada 2009.

[3] E. Hau: *Wind Turbines, Fundamentals, Technologies, Application, Economics*, 2nd edition, Springer, Berlin 2006.

[4] <http://www.enercon.de/en-en/767.htm>

[5] <http://www.avea-wind.com/1/M5000/konzept/>

[6] J. Urbanek, T. Barszcz, N. Sawalhi, R.B. Randall: *Comparison of amplitude-based and phase – based methods for speed tracking in application to wind turbines*, Metrology and

Measurement Systems, vol. XVIII (2011), no. 2, pp. 00 – 00.

[7] T. Barszcz: *Application of diagnostic algorithms for wind turbines*, *Diagnostyka*, 2(50) / 2009.

[8] Z. Hameed et al.: *Condition monitoring and fault detection of wind turbines and related algorithms: A review*, *Renewable & Sustainable Energy Reviews*, 13 (2009).

[9] E. Echavarria et al.: *Reliability of Wind Turbine Technology Through Time*, *Journal of Solar Energy Engineering*, August 2008, vol. 130.

[10] W. Yang et al., *Cost – Effective Condition Monitoring for Wind Turbines*, *IEEE Transactions on Industrial Electronics*, vol. 57, no. 1, January 2011.

[11] S.C. Pryor et al.: *Annual Variability of Wind Indices across Europe* *Wind Energy*, vol. 9, issue 1-2, January – April 2006.

[12] K. Klink: *Trends and Interannual Variability of Wind Speed Distribution in Minnesota*, *Journal of Climate*, vol. 15, November 2002.

[13] H. Holtinen: *Hourly Wind Power Variations in the Nordic Countries*, *Wind Energy*, vol. 8, issue 2, April/June 2005.

[14] J. Apt: *The spectrum of power from wind turbines*, *Journal of Power Sources*, vol. 169, issue 2, June 2007.

[15] Y. H. Wan: *Wind Power Plant Behaviors: Analyses of Long – Term Wind Power Data*, Technical Report, National Renewable Energy Laboratory, September 2004.

[16] E. Petersen et al.: *Power Meteorology, Part I: Climate and Turbulence*, *Wind Energy*, vol. 1, 1998.

[17] G. Sinden: *Characteristics of the UK wind resource: Long – term patterns and relationship to electricity demand*, *Energy Policy*, vol. 35, issue 1, January 2007.

[18] G. Giebel et al.: *The State-Of-The-Art in Short-Term Prediction of Wind Power, A Literature Overview, 2nd Edition*, Specific Targeted Research Project, contract no. 038692, “Advanced Tools for the Management of Electricity Grids with Large – Scale Wind Generation”, January 2011.

- [19] E. Akpınar, S. Akpınar: *An assessment on seasonal analysis of wind energy characteristics and wind turbine characteristics*, Energy Conversion and Management, vol. 46, issues 11 – 12, July 2005
- [20] A. N. Celik: *A statistical analysis of wind power density based on the Weibull and Rayleigh models at the southern region of Turkey*, Renewable Energy, vol. 29, issue 4, April 2004



Dr hab. inż. **Tomasz BARSZCZ** pracuje w Katedrze Robotyki i Mechatroniki AGH. Zajmuje się diagnostyką maszyn oraz systemami monitoringu i diagnostyki. Jest autorem 4 książek i ponad 100 publikacji. Opracowane przez niego systemy pracują na stu kilkudziesięciu instalacjach.



Mgr inż. **Dariusz BRODA** jest doktorantem na Katedrze Robotyki i Mechatroniki AGH. Zajmuje się diagnostyką maszyn oraz modelowaniem układów wieloczołowych.

APPLICATION OF THE LOCAL MESHING PLANE IN DETECTING ASSEMBLY AND MANUFACTURING ERRORS OF GEARS

Jędrzej MAĆZAK

Warsaw University of Technology, Institute of Vehicles
Narbutta 84, 02-524 Warszawa, Poland, e-mail: jma@mechatronika.net.pl

Summary

In the paper application of the local meshing plane concept is discussed and applied for overall gear quality assessment. Knowing the kinematic properties of the machine (i.e. gear teeth numbers) it is possible to modify the gearbox vibroacoustic signal in such a manner that its fragments will be linked to different rotating parts. This allows for presentation of a raw or processed gearbox signal in a form of three dimensional map on the plane "pinion teeth x gear teeth" called local meshing plane. Meshing plane in Cartesian coordinates allows for precise location and assessment of gear faults in terms of meshing quality of consecutive teeth pairs. Although the method was applied to simulated signals generated by a gearbox model, similar results were obtained for the measurement signals recorded during the back-to-back test stand experiment.

Described method could be used for assessing the manufacturing quality of gears, the assembly quality as well as for the fatigue gear failure evaluation during normal exploitation.

Keywords: gears, gearbox diagnosis, local meshing plane analysis, nonstationary signals, fault diagnosis, gearbox modelling.

WYKORZYSTANIE LOKALNEJ PŁASZCZYZNY PRZYPORU W WYKRYWANIU BŁĘDÓW WYKONANIA I MONTAŻU PRZEKŁADNI ZĘBATYCH

Streszczenie

W artykule przedstawiono możliwość wykorzystania lokalnej płaszczyzny przyporu do oceny jakości pracy przekładni zębatej. Znając własności kinematyczne przekładni (tj. liczby zębów kół) możliwe jest takie przekształcenie sygnału wibroakustycznego emitowanego przez przekładnię, że poszczególne jego fragmenty będą związane z kinematyką wirujących wałów. Pozwala to na przedstawienie oryginalnego lub przetworzonego sygnału w formie trójwymiarowej mapy na płaszczyźnie „zęby zębnika x zęby koła” nazywanej lokalną płaszczyzną przyporu. Płaszczyzna przyporu, we współrzędnych kartezjańskich pozwala na lokalizację i ocenę uszkodzeń przekładni poprzez ocenę jakości poszczególnych przyporów wszystkich par zębatych. Metodę zaprezentowano na przykładzie sygnałów generowanych przez model symulacyjny przekładni zębatej oraz zweryfikowano na stanowisku mocy krążącej.

Opisana metoda może być używana zarówno do oceny jakości wykonania i montażu jak też do wykrywania uszkodzeń zmęczeniowych przekładni zębatych.

Słowa kluczowe: przekładnie zębate, diagnostyka przekładni, lokalna płaszczyzna przyporu, sygnały niestacjonarne, diagnostyka uszkodzeń, modelowanie przekładni zębatych.

INTRODUCTION

Methods of manufacturing quality acceptance of toothed gears are usually limited to the gear geometry measurement (radial runout tolerance, allowable pitch variation, profile tolerance, tooth alignment tolerance etc.) or quasi static composite action tests, a method of inspection in which the work gear is rolled in tight single or double flank contact with a master gear or paired gear [1]. Additionally gearcase geometry measurements are performed to assure compliance with assumed

shafts' position tolerances. As a rule, after gear assembly, sound measurements are made to check if the completed gearbox fit the ISO/AGMA norm limits. This kind of measurement is also commonly used for overall gear quality assessment.

As for now there are no other methods that will allow manufacturer to evaluate the gear quality under normal work. Vibroacoustic methods commonly used for detecting gear faults [2], [3] are usually focused on bearing and teeth faults and are not suitable for this purpose. The proposed method, simple in setup equipment and signal analysis, could

fill this gap. In its simplest form it requires only acceleration and trigger signals to be recorded simultaneously. It allows assessing meshing quality of particular teeth pairs in completed gearbox during normal gear exploitation and selection of the worst pinion – gear tooth contact in terms of dynamic overload, the factor that is critical for determining the durability of gear. It is therefore possible to detect and localise manufacturing and assembly errors such as pinion/gear shaft misalignment, misalignment of bearing mountings, pitch error, variable distance error, etc.) and investigate growth of these effects during exploitation.

1. CONCEPT OF THE LOCAL MESHING PLANE

Focusing on the single stage gearbox with z_1 teeth on the pinion and z_2 teeth on the gear wheels we could observe $z_1 \times z_2$ different mesh cycles. The cycle repeats every z_1 revolutions of the gear (and z_2 revolutions of the pinion shafts as well) [4]. Assuming averaged gearbox geometry and rotational frequencies (e.g. 25 Hz for pinion shaft) each teeth pair usually enters contact in no less than 1 or 2 seconds. Commonly used methods of vibroacoustic signal analysis are usually averaging time signals [5]. This process results in losing detailed information about mesh cycles of the particular teeth pairs, data that could be used for assessment of the teeth meshing quality. This leads us to the idea of the observation of the gearbox signal in Cartesian coordinates $z_1 \times z_2$ on the so called local meshing plane [6].

Creation of the Cartesian local plane $z_1 \times z_2$ from the gearbox vibroacoustic (VA) signal requires simultaneous recording of the trigger signal that contains synchronisation impulses every one pinion or gear shaft revolution. Only one shaft trigger signal is required, however for proper initial shaft positioning (i.e. selection of the arbitrary beginning of both shafts' revolution) observation of trigger signals from both shafts is essential. The algorithm for creating local meshing plane from the VA signal is as follows:

- Signal resampling in such a way that every revolution must contain the same number of time samples thus eliminating fluctuations in rotational frequency.
- As the results will be presented on a pinion/gear teeth matrix, number of time samples for each revolution should be divisible by the number of teeth on the trigger shaft.
- Division of the resampled signal into sections of the same length K (in number of time samples) corresponding to the arbitrary times of entering pinion-tooth contact (time equivalence of transverse radial pitch starting with a trigger). This corresponds to period T of one shaft

revolution divided by the number of teeth on this shaft gear:

$$T = \frac{1}{f_o z} \quad (1)$$

where f_o is a shaft rotating frequency and z is the number of teeth on this shaft gear.

Signal sections corresponding to the contacts of consecutive teeth pair (i, j) could then be averaged in time domain to eliminate randomness and load fluctuations in the signal. Resulting matrix could be presented in coordinates $z_1 \times z_2$ generating three dimensional local meshing plane (Fig. 1). This operation could be repeated for consecutive time records allowing for comparison and observations of changes in trends of these fragments of signal.

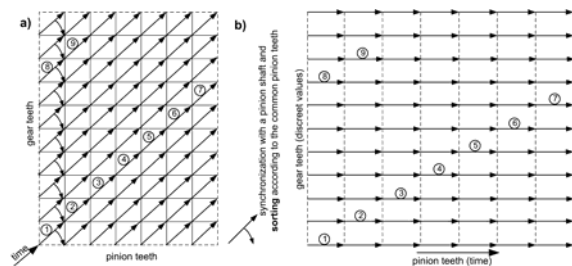


Fig. 1. Construction of local plane for tooth meshing pairs synchronized with a pinion shaft [6]

2. MODEL OF THE GEARBOX

For the purpose of evaluation of the possibility of using local meshing plane method for gearbox quality assessment a model which relied on the method of apparent interference was used [7]. The simplified diagram of the 14 degrees of freedom model is presented on Fig. 2. In the model the mating of toothed wheels is realized by means of a complex flexible element representing meshing. It is assumed that both the gear and the pinion have the possibility of making, without any sliding, an additional rotation in relation to the motion resulting from the revolution of their base circles. Thus the principle of the constant transmission ratio is not maintained enabling analysis of the modulation effects which occur during the toothed gear's operation. This requires modelling of the forces working between the mating teeth to define the relationship between the angular velocities of both toothed wheels. The result of such a wheels motion is the apparent interference (i.e. mutual penetration) of meshing which should be interpreted as the scope of deflection of the teeth in the gear. This interference can be determined by taking into account the meshing geometry and is being compensated by the flexible deformation of teeth.

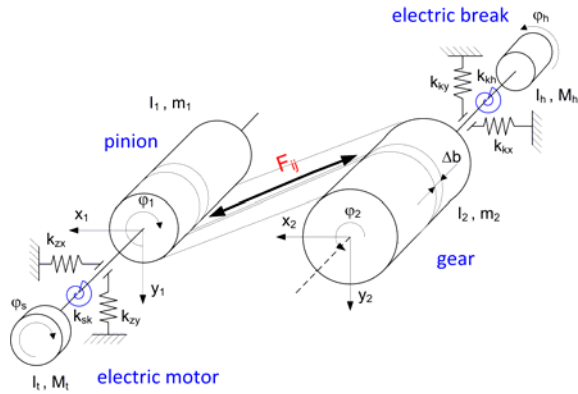


Fig. 2. Diagram of the gearbox model [7]

While calculating the interference of the teeth and the meshing force, a series of factors which influence the geometry of meshing were taken into account:

- variable distance between gear axes resulting from shaft runout or flexible shaft deformation,
- variable radii of addendum circles as well as variable radii of the rounding of tooth tips,
- instantaneous error of standard contact angle,
- pitch errors, variable meshing stiffness along the path of contact etc.

The teeth stiffness and the changes of its value for the entire path of contact were defined by way of a three-dimensional model of a toothed wheel developed with the use of FEM. Although the model allows for helical gear simulations for the results presented in this paper spur gears were selected ($z_1=27, z_2=35, m=4, Load=850 \text{ Nm}$). High load parameters were selected to allow comparison of the results with back-to-back tester experiments [8].

3. LOCAL MESHING PLANE ANALYSIS OF THE SIMULATED MANUFACTURING ERRORS

A series of simulations were run to evaluate the influence of the manufacturing errors on the gearbox behaviour. The modelled meshing force was selected for this purpose as it is closest to the source of the gear vibrations and is not altered by the signal propagation path, bearings and case stiffness etc. Simulations were run without any other than clearly stated introduced manufacturing errors. All results were pre-processed according to the local plane algorithm described above. In the following analysis squared envelope of the meshing force were used and presented in $z_1 \times z_2$ coordinates as it emphasizes small changes in the signal.

2.1. Simulation of Pitch Errors of gear teeth

Different types of accumulated pitch errors as presented on Fig. 3 were introduced to both gears.

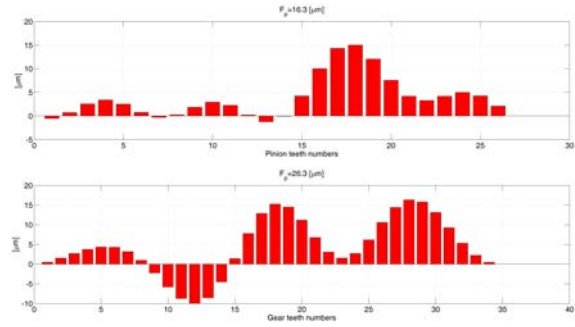


Fig. 3. Simulated accumulated pitch errors of pinion and gear teeth

Additionally some simulations were run with additionally emphasised pitch error introduced on a single pinion and gear teeth. Typical meshing force waveform and it's envelope for one pinion revolution was shown on Fig. 4.

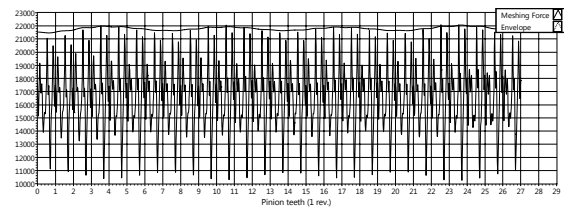


Fig. 4. Meshing force waveform for one pinion revolution

On Fig. 5 maximum values of the squared envelope of meshing force for contacts of all teeth pairs combinations with pitch errors applied as from Fig. 3 were presented in Cartesian “pinion teeth x gear teeth” meshing plane coordinates. Visible are meshing force variations caused by the different pitch errors of pinion and gear teeth and thus the meshing quality in terms of best/worst contact pair of teeth could be determined. If the measured acceleration signal of a gear case would be used instead of simulated meshing force, changes in the accelerations similar to the changes shown on Fig. 5 would be observed reflecting dynamic overload and also allowing for meshing quality assessment.

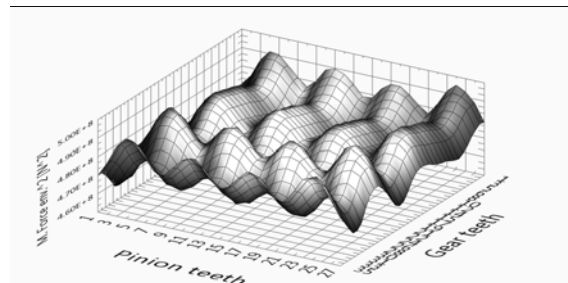


Fig. 5. Local plane analysis of the squared envelope of the meshing force for gears with pitch errors

Local plane analysis allows for easy selection of particular badly machined teeth or teeth under fatigue degradation. This kind of errors could be

introduced into the simulation model as an additional pitch error on one teeth (machining error) or reduced stiffness of the teeth. Fig. 6 presents the simulation results for gears with accumulated pitch errors discussed above but with additionally introduced emphasised pitch errors on single pinion and single gear tooth. These imperfections are introducing periodic deformations into the signal visible on the signal spectrum as a modulations of the meshing frequency with rotational frequencies of both shafts. Observation on the local plane allows for more detailed analysis and selection of the teeth that differ from all others. They are visible as areas of increased amplitudes across one dimension – pinion or gear tooth.

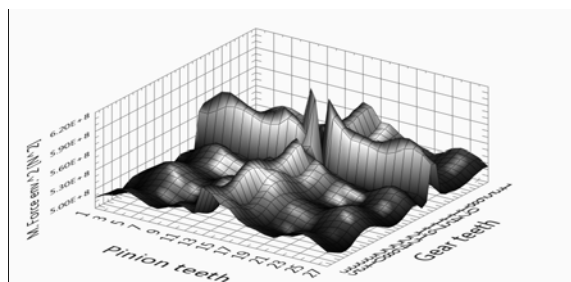


Fig. 6. Local plane analysis of the squared envelope of the meshing force for gears with additional pitch errors on single pinion and gear teeth

Observation of the maximum values of the signal on the Fig. 6 reveals the same pitch error caused structure as on Fig. 5 but with an addition of characteristic cross pattern caused by contacts of badly manufactured single pinion and gear teeth. In case of the contact of these teeth (centre of diagram) additional excessive signal deformations are visible resulting in additional gear vibrations – additional dynamic overload. This is a typical pattern that will be observed anytime when two deformed teeth will match each other.

2.1. Simulation of Runout Error (F_r) of gear teeth

Runout error defines the runout of the pitch circle. This error, in radial position of the teeth, is most often measured by indicating the position of a pin or ball inserted in each tooth space around the gear. It introduces periodic changes in the signal resulting from the modifications of the shape of the involute, mainly modifications of the radii of the beginning of teeth profiles. As it is impossible to directly model runout error it was alternatively introduced to the model as an error of the base circle.

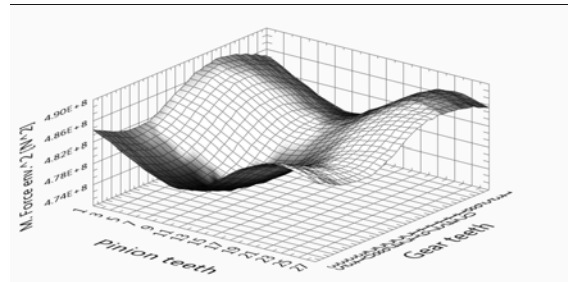


Fig. 7. Local plane analysis of the squared envelope of the meshing force for gears with sinusoidal base circle errors

On the local plane this kind of error with period of shaft rotation on both shafts is visible as a “hat shaped” surface. Results presented on Fig. 7 were obtained assuming sinusoidal base circle errors of less than $40 \mu\text{m}$ on both gears. The exact shape depends also of the phase shift of the signal caused by the trigger position (see Fig. 8).

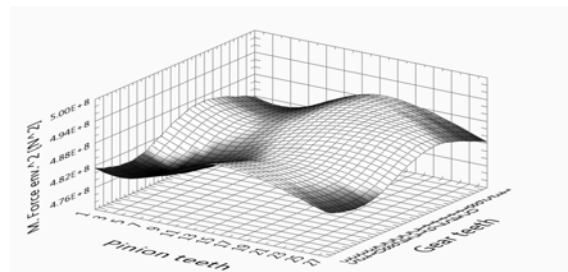


Fig. 8. Local plane analysis of the squared envelope of the meshing force for gears with cosinusoidal base circle errors

3. VERIFICATION OF THE METHOD ON THE GEAR TEST STAND

Application of the local meshing plane method for the control diagnostic of gears was verified on a back-to-back test stand. Test stand was equipped with strain gauges applied to the pinion shaft. Telemetric module allows for recording load changes in this shaft during normal operation. Observation of the load variations on the local plane (Fig. 9) reveals small periodic load changes that could be linked to the gear mounting errors that exists due to the eccentricities and looseness in the gear mounting keyways.

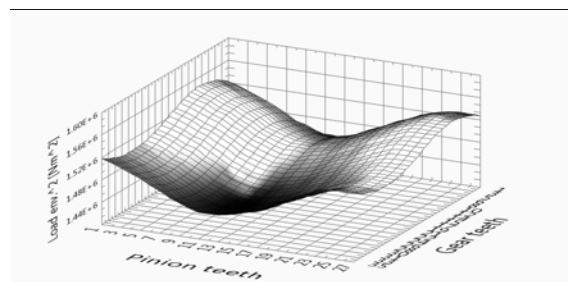


Fig. 9. Local plane analysis of the squared envelope of the pinion shaft load (experiment)

Observation of the gearbox acceleration on the local plane (Fig. 10) for the same gear set reveals increased acceleration level for pinion teeth 14-19 indicating their slightly increased pitch errors.

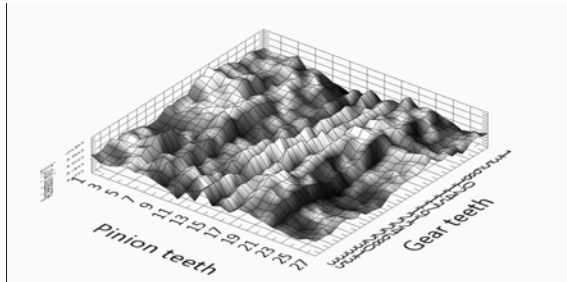


Fig. 10. Local plane analysis of the squared envelope of gearbox accelerations (experiment)

Fig. 11 shows the local plane acceleration signal analysis performed on the same test stand but equipped with different gear set. There is an increased signal level visible for several consecutive pinion teeth (9-13) indicating their manufacturing errors. Some variations of the signal with period of one gear revolution are also visible. This could be linked to the eccentricity of mounting gear wheel.

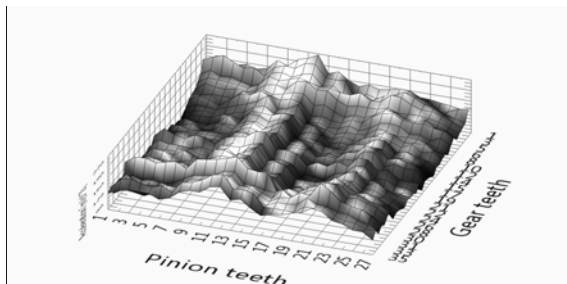


Fig. 11. Local plane analysis of the squared envelope of gearbox accelerations (experiment)

4. SUMMARY

Creation of the local meshing plane should be treated as a type of signal pre-processing. Local meshing plane is simply a new domain of presenting bare or processed signal or even its parameters. Data could be displayed as an easy interpretable three dimensional maps. Each chunk of the signal on this plane has its own physical interpretation as an image of the particular teeth pair contact. It could be averaged over consecutive contacts of the same pair and stored for future trend comparison. Any signal post-processing could then be applied for this time data. In the paper maximal values of squared envelope of the signal were used for this purpose.

Usage of the gear mathematical model allowed for easy introduction of precisely known gear imperfections and observations of the changes in the signals they are producing. As an example of manufacturing errors pitch and runout errors were selected although comparable results will be

obtained when analysing other manufacturing errors that are periodic with period related to the shafts revolution (eg. eccentricity, shaft misalignment etc.).

The described method of the local plane can be a useful complement of currently used methods of machinery quality acceptance procedures. Proposed method is noninvasive and requires relatively simple equipment. It allows to investigate an assembled gear working in its natural conditions. It is possible to detect manufacturing and assembly errors (such as: pinion/gear shaft misalignment, misalignment of bearing mountings, pitch error, variable distance error etc.) and investigate growth of these errors during exploitation. Observation on a local "pinion teeth x gear teeth" plane allows observation of tooth contact during normal work and selection the worst pinion – gear tooth contact in terms of dynamic overload, the factor that is critical for determining the durability of gear.

Additionally local plane allows for detecting fatigue damages that occur to the gears during the exploitation [9].

REFERENCES

- [1] AGMA ANSI/AGMA 2000-A88 - *Gear Classification and Inspection Handbook: Tolerances and Measuring Methods for Unassembled by American Gear Manufacturers Association (AGMA)*. .
- [2] J. Zakrajsek, *A review of transmission diagnostics research at NASA Lewis Research Center*, Lewis Research Center, Cleveland, Ontario, NASA Technical Memorandum 106746, Dec. 1994.
- [3] M. Jasiński and S. Radkowski, *Nonlinearity and Intermodulation Phenomena Tracking as a Method for Detecting Early Stages of Gear Failures*, The Archives of Transport, vol. XXII, no. 4, pp. 447-462, 2010.
- [4] R. Filonik, J. Maćzak, and S. Radkowski, *Apparent interference method as a way of modeling the meshing process disturbances*, Machine Dynamics Problems, vol. 19, pp. 95-108, 1998.
- [5] M. Jasinski, *Use of bispectral measures in the failure stage evolution development*, Acta Acustica united with Acustica, vol. 96, no. 1, pp. 80-81, 2010.
- [6] J. Maćzak, *Local meshing plane as a source of diagnostic information for monitoring the evolution of gear faults*, Engineering Asset Lifecycle Management, vol. 19, D. Kiritsis, C. Emmanouilidis, A. Koronios, and J. Mathew, Eds. London: Springer London, 2010, pp. 661-670.
- [7] R. Filonik, J. Maćzak, and S. Radkowski, *Simulation and modelling of low - energy tooth failure in a helical gearbox*, Machine Dynamics Problems, vol. 26, no. 2/3, pp. 89-104, 2002.

- [8] J. Mączak and M. Zawisza, *Miary zmęczeniowego uszkodzenia kół zębatych*, Diagnostyka, vol. 34, pp. 121-126, 2005.
- [9] A. Jabłoński and T. Barszcz, *Instantaneous Tooth Cyclic Power (ITCP) – a tool for diagnosis of planetary gearbox*, presented at the Structure Health Monitoring Conference, Kraków, Poland, 2011.



Jędrzej MĄCZAK, PhD, is an assistant professor at the Institute of Vehicles of the Warsaw University of Technology. His scientific interests are distributed diagnostic systems, machine diagnostics, mathematical modelling of power units and methods of

analysis of vibroacoustic signals.

MONITORING OF INSTANTANEOUS ANGULAR SPEED OF THE CRANKSHAFT FOR CONTROL OF THE SHIP ENGINE PERFORMANCE CHANGES

Adam CHARCHALIS, Mirosław DERESZEWSKI

Gdynia Maritime University, Mechanical Faculty
Akademia Morska w Gdyni, Wydział Mechaniczny
ul. Morska 83, 81-225 Gdynia, Tel.:+48 81 6901398, e-mail: achar@am.gdynia.pl

Summary

The paper presents an idea to utilize crankshaft's angular speed variation and its derivative for monitoring of trouble of diesel engine combustion quality. Measurement of instantaneous angular speed, long term recording and archive of values is enable by modern programmable logic controllers. Measurement of IAS (Instantaneous Angular Speed) is done using optical sensor and toothed disc. Advantage of this method is simple installation and constant signal. Collected data can be processed on board, basing on MS Excel formulas. Observation of changes of instantaneous speed and acceleration can not replace Main Effective Pressure measurement or vibration monitoring, but tool for early warning. When a signal of deteriorating of engine performance is obtain, more accurate diagnostic can be implemented. Expected final result will be elimination of engine's cycle's irregularity. Proposed method is at early stage of investigation and further steps to prove its utility and to develop concluding rules are to be conducted. In the paper are presented preliminary analysis of some bunches of data collected from two bulk carriers, operating in similar conditions.

Keywords: diagnostics, marine diesel engine, instantaneous angular speed.

MONITOROWANIE CHWILOWEJ PRĘDKOŚCI KĄTOWEJ WAŁU KORBOWEGO W CELU KONTROLI ZMIAN JAKOŚCI PRACY SILNIKA OKRĘTOWEGO

Streszczenie

W artykule przedstawiono ideę wykorzystania funkcji zmian prędkości kątowej wału korbowego oraz jej pochodnej do monitorowania zakłóceń równomierności pracy cylindrów. Pomiar prędkości chwilowej, zapis i archiwizacja wartości jest możliwa dzięki zastosowaniu sterownika programowalnego. Zalety powyższej metody to łatwość instalacji systemu oraz uzyskiwanie bieżącego sygnału. Zebrane dane mogą być obrabiane na statku, w oparciu o formuły zapisane w programie MS Excel. Obserwacja zmian chwilowej prędkości i przyspieszenia kątowego nie zastąpi typowych pomiarów takich jak pomiar ciśnienia indykowanego lub monitoring drgań, jest jednak doskonałym narzędziem do wczesnego informowania i ostrzegania. Przedstawiona metoda jest na wczesnym etapie badań i wymaga dalszych analiz w celu wykazania jej użyteczności diagnostycznej oraz określenia reguł wnioskowania. W artykule przedstawiono wstępne analizy pakietów danych pochodzących z dwóch masowców operujących w podobnych warunkach.

Słowa kluczowe: diagnostyka, silnik okrętowy, chwilowa prędkość kątowa wału.

1. INTRODUCTION

Internal combustion piston engines, due to its work principles create periodical forces with variable directions and values. It is a source of torsion stress and resonance torsion vibrations affecting crankshaft and periodically variable mechanical loads affecting main and journal bearings.

For every main engine, its barred revolutionary speeds are known and procedures how to increase and decrease load avoiding danger values are presented in manuals, or automatically executed by automatic control systems. Prohibited revolutionary

speed is related to main harmonics, and must be avoided due to risk of crankshaft damage. One has to take under consideration, that during low speed passages (canals, fairways and harbor maneuvering) engine works on partly load, and due to higher probability of invalid combustion, creates additional stress and subsequently higher than calculated magnitudes of torsion vibrations [4].

The most often reason of slide bearings damages is material fatigue, caused by periodically variable forces in function of combustion pressure and revolutionary speed. Probability of crack occurring is strictly related to forces irregularity, caused by

improper combustion or changeable load (periodically partly submerged screw propeller). Improper combustion is a reason of additional dynamic load of bearings what cause in primary phase small cracks and finally lost of sliding layer [4]. The conclusion from above facts is that constant control of combustion and proper fuel pumps regulation can be crucial for extension of engines' lifetime.

Mentioned above stress creating factors, can caused in long term exploitation periods, shaft's bearings and couplings material fatigue, and finally be a reason of serious damages, creating not only economical losses but also risk of setting ship in distress situation.

Even most modern vessels are not very often equipped with systems dedicated to constant monitoring of engine performance [1, 4]. The most effective method of combustion control which is measurement of in-cylinder pressure can not be executed permanently because of temperature immensity of gauges. What more, standard routine is engine's indication when is on nominal load. During maneuvers or passing canals, machine crew is focused on steaming safety and is not performing measurements. Taking above into consideration, one has to come into conclusion that any system giving on-line information about quality of combustion or instantaneous rotational speed changes would be very useful engine control aid.

2. OBJECT OF ANALYSIS AND METHOD OF MEASUREMENT

As objects of analysis, has been selected two sister bulk carriers, propelled by two stroke marine diesel engines the same type. For further considerations vessels are identified as "object 1" and "object 2".

Both vessels were performing its duty under similar condition, and were encompassed by the same maintenance and exploitation routines. The bulk carrier propulsion arrangement composes of a 5 cylinders, two-stroke main engine, straight connected with a FPP (fixed pitch propeller) driven by intermediate and propeller shaft; all couplings are stiff, flange type.

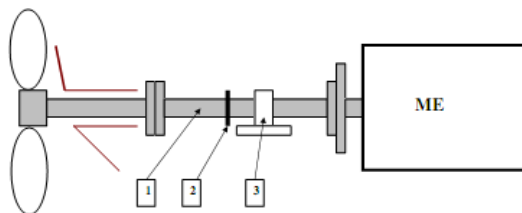


Fig. 1. Layout of ships propulsion with toothed rings mounted at intermediate shaft

1 – intermediate shaft; 2- measurement toothed rings; 3 – shaft bearing; ME – main engine

Due to straight connection, one can assume that the speed values measured at the intermediate shaft reflect pistons forces action.

The engine's parameter taken as its condition identifier is instantaneous angular speed of the crankshaft. This parameter is pointed by many authors as representative and adequate value for combustion quality evaluation [2, 7, and 9].

All data measurement and collecting has been carried out using torque meter ETNP-8 and ETNP-10, produced by enterprise ENAMOR Ltd. The torque meter is mounted at intermediate shaft and measure instantaneous angle of shaft torsion and instantaneous angular speed. Measured values are given in the form of numbers of laser beam impulses emitted with constant frequency, received by photodiode when a slot is crossing laser beam and blind signal when tooth is cutting the beam. Example of measuring discs mounted at the shaft is presented in Phot. 1.



Phot. 1. Toothed rings and laser sensor ETNP-8 mounted at intermediate shaft

All data has been collected during vessels' exploitation and cover a period of three years. The aim of analysis is to proof utility of constant measurement of angular speed variation and further comparison with a corresponding waveforms template for preliminary engine diagnostics. As a base condition status, shall be measurement registered during sea trials of new vessel or after periodical repair, confirmed by accurate internal combustion pressure indication. When engine technical condition is declared as proper, recorded angular speed waveform can be treated as a template. Any deviation from a status determined as a basic, shall be a signal to improve combustion uniformity, on the way of fuel pumps regulation and subsequently checked by using electronic indicators. Even proposed method cannot replace the indicator graphs, the advantage of on-line information and early warning seems to be obvious.

3. MEASUREMENTS RESULTS

First step of measurements is recording and analysis of quality of manufacturing of toothed rings.

Having rings mounted around the shaft, one has to start engine's turning using turning gear. Record of one revolution without impact of combustion forces gives an picture of every tooth in a form of "impulses map". This step of measurement gives us an information about deviations of tooth size from a mean value. All differences are due to machine processing inaccuracy and construction of rings. Records of turning of the engine shall be also an object of observation as is assumed that can carry an information about increasing of friction in pairs the cylinder liner – piston and journal – bearing. At Fig.2 is presented the record of engine turning by turning gear. Maximum magnitude of deviation reaches 0,0008 rev/min what is around 0,5% of mean speed value (big engines turning gear action is very slow: 0,16 -0,17 rev/min)

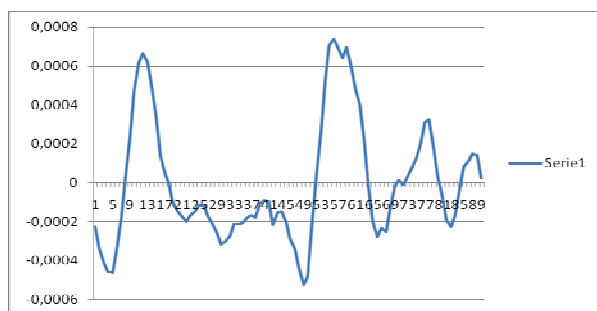


Fig.2. Example of measurement of IAS during turning by turning gear. Deviation from mean speed (rev/min) in domain of samples of 1 revolution

The second step is measuring and recording Instantaneous Angular Speed (IAS) of the shaft, when the engine is working under typical load profiles, during sea trials. Collected data will be a basement for further comparisons.

Instantaneous angular speed was recorded on board of both objects under different loads of main engines. Measurements were performed for two most common rotational speeds zones occurring during exploitation, low speed in range 29-39 r/min and sea passage speed in range 79- 84 r/min.

As a value representing angular speed variations, deviation from one revolution's mean speed is taken. Mean speed is calculated on the basis of 5 subsequent revolutions.

In order to eliminate random disturbances and obtain wave-form's smoothing, progressive approximations with approximation object in a form of polynomial exponent 3. (Sawitzky – Golay filter). was implemented. This method is most proper for analysis of an angular speed and acceleration changes due to its usefulness for non - periodic functions treatment [1]. The chart in Fig. 2. presents a comparison of the angular speed raw record wave-form and its wave-form after the third step of smoothing using the approximation by moving polynomial of exponent 3.

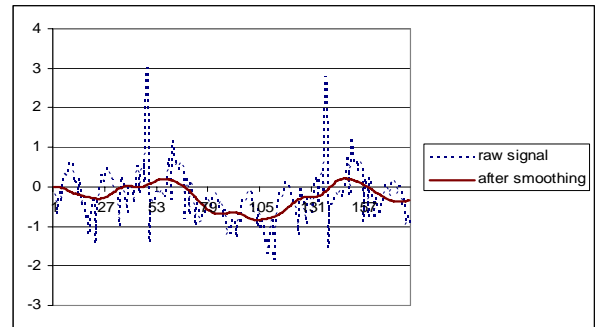


Fig. 3. Recorded angular speed waveform (dotted line) and the same after third step of smoothing

In order to obtain an information concerning dynamics of instantaneous angular speed variations derivative of function of speed deviations is calculated. Waveforms obtained in this way are a subject of comparison and analysis. All charts present sampling of one revolution of the crankshaft.

4. COMPARISON OF LOW SPEED DERIVATIVE WAVEFORMS

At figures 4 and 5 are presented recorded waveforms of angular speed of the shafts of *object 1.* and *object 2.*, when engines were running with low speed. That situation occurs during maneuvering or canal passages. Very clear 5 regular peaks, corresponding with periodical forces created by five cylinders can be observed. Picture of *object 1* is similar to the picture of *object 2.* Magnitudes of *object 1.* are included between values of -2 to 1,5. and are higher than *object 2.* The more regular waveform of *object 2* is due to better combustion at higher rotational speed. Both pictures gives information that in all cylinders combustion process is proper.

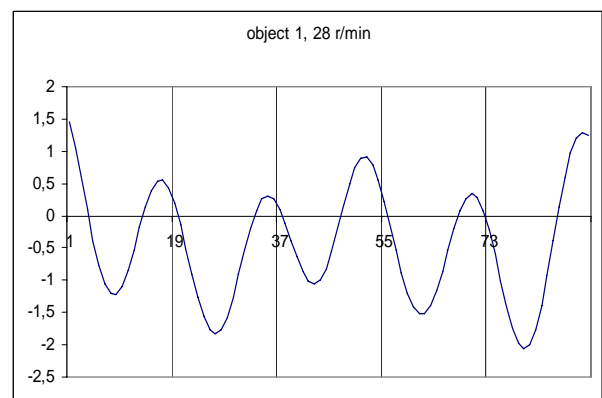


Fig. 4. Recorded waveform of angular speed deviations around mean value (rev/min), object 1, running with 28 r/min. Domain of sampling of 1 rev. (90 samples)

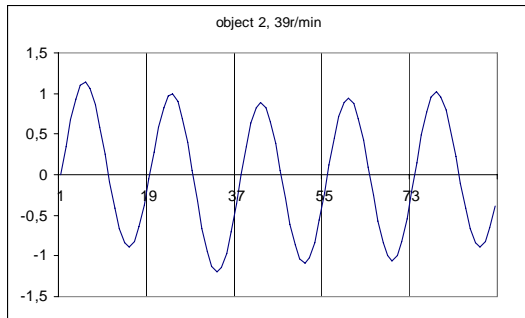


Fig. 5. Recorded angular speed deviations waveform (rev/min), object 2, running with 39 r/min. Domain of sampling of 1 rev. (90 samples)

Increasing of engine load and rotational speed will effect with less symmetric peaks pattern and decreasing of magnitudes, what means more regular instantaneous speed. Example of speed increasing impact at acceleration waveform is presented in Fig.6.

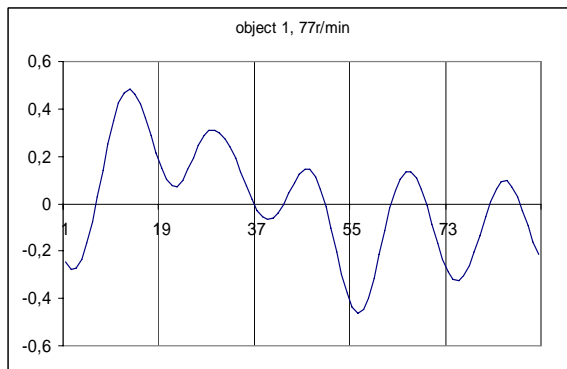


Fig. 6. Recorded angular speed deviation from the mean value waveform, object 1, running with 77 r/min/ Domain of sampling of 1 rev. (90 samples)

5. COMPARISON OF SPEED DERIVATIVE WAVEFORMS OF ENGINE UNDER NOMINAL LOAD

Under nominal load, forces of rotating engine masses and strong impact of a screw propeller action masks signals coming from pistons forces, thus acceleration waveform is more irregular and peaks in zones corresponding with subsequent strokes are not observed. Nevertheless, as long as engine is sustaining combustion characteristic, the run of acceleration function keeps constant form. Every change either improving or decreasing combustion quality will change the waveform and become diagnostic signal. In Fig. 7, the comparison of waveforms and the impact of maintenance action carried out in 2009 is presented.

Taking *object 2* for analysis, one has to notice, that in the period between year 2007 and 2010, the form of waveform of angular acceleration did not changed significantly (see Fig.8).

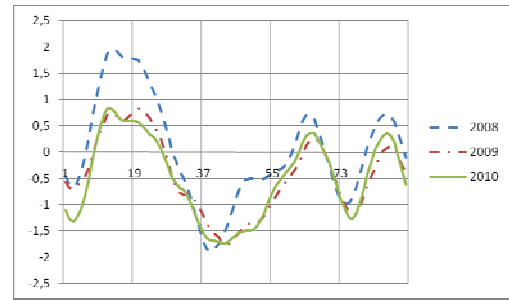


Fig.7. Comparison of recorded angular speed derivation waveform, object 1, running with 82 r/min. records from years 2008/2009/2010. Domain of sampling of 1 rev. (90 samples)

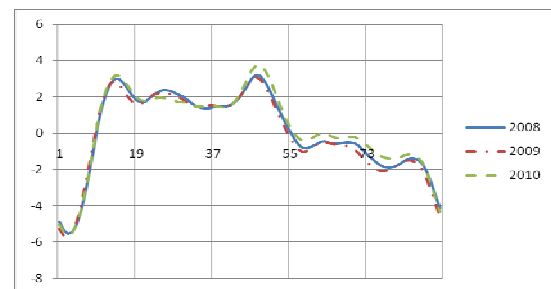


Fig. 8. Comparison of recorded angular speed derivation waveform, object 2, running with 84 r/min. records from years 2008/2009//2010. Domain of sampling of 1 rev. (90 samples)

From the other hand, is visible that maximum magnitude observed for *object 2* is much higher than maximum observed for *object 1*. (Fig. 9) but only in the zone of one cylinder stroke.

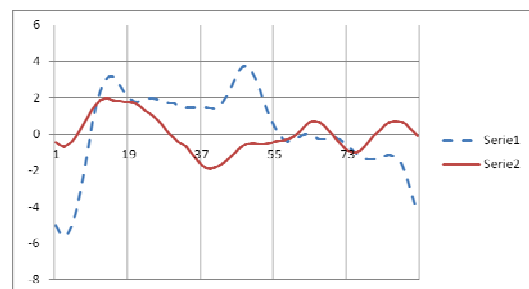


Fig. 9. Comparison of recorded angular speed derivation waveform, object 2 (dotted line) and object 1, running with 84 r/min. Domain of sampling of 1 rev. (90 samples)

Taking above under consideration, one could came into conclusion, that mean effective pressure (MEP) in one cylinder have higher value than in other four. As the results of MEP indication are available, comparison of angular speed and MEP pattern is possible. Fig. 10 presents angular speed oscillation and Fig. 11 presents MEP deviations from mean value. The correspondence between two

pictures can be observed, both functions taking negative and positive values in the same zones.

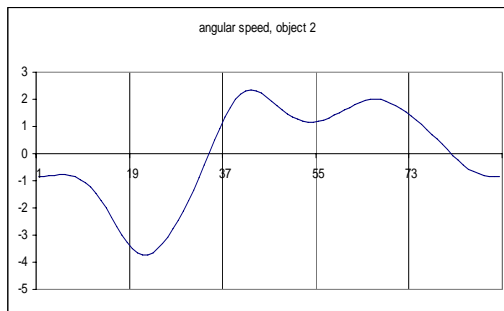


Fig. 10. Recorded angular speed waveform, object 2, running with 84 r/min

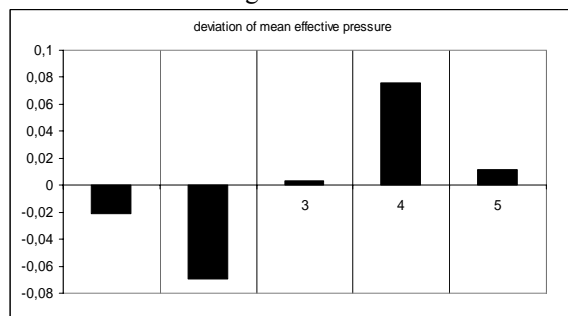


Fig. 11. Graph of deviation from mean value (MPa) of mean effective pressure, object 2, running with 84 r/min

4. CONCLUSION

Results of experiment presented in this paper, let assume that using photo optical speed indicator based on toothed rings mounted at a shaft is very useful diagnostic signal source. Analysis of measurements carried out using the torque meter ETNP enable to detect irregularity of engine work, and to show the tendency of changes. One has to realize that irregularity detection is very important, because any imbalance of combustion forces creates additional vibrations, and finally additional zones of barred rotational speed. Results of presented analysis are a justification of further development of the method of instantaneous angular speed (IAS) measurement based at a toothed ring and an optical sensor. Angular acceleration signal, after smoothing, is assumed as one most contributing and reflecting combustion process disturbances. The further investigations have to be focused on determination of relation between deviations of angular acceleration and Mean Effective Pressure pattern. It is obvious that proposed method can be acknowledged only in the way of long term analysis and requires bigger than two, population of object encompassed by investigation program.

REFERENCES

- [1] Dereszewski M., Charchalis A., Polanowski S.: *Analysis of diagnostic utility of instantaneous angular speed of a sea going vessel propulsion shaft*. Journal of KONES, vol. 18, No 1, 2011.
- [2] Polanowski, S.: *Studium metod analizy wykresów indykatorowych w aspekcie diagnostyki silników okrętowych*. Zeszyty Naukowe AMW, Nr 169 A (2007).
- [3] Merkisz J., Jakubczak M.: *System monitoringu silnika tłokowego z wykorzystaniem sensora optycznego*. Journal of KONES, 1999.
- [4] Piotrowski I., Witkowski K.: *Okrętowe silniki spalinowe*. TRADEMAR, Gdynia 2003
- [5] Krzyżanowski J., Witkowski K.: *Possibility of using visualisation to present running point of marine diesel engine*. Journal of KONES 2010.
- [6] Geveci M., Osburn A.W., Franchek M.A.: *An investigation of crankshaft oscillations for cylinder health diagnostics*. Mechanical Systems and Signal Processing 19 (2005).
- [7] Jianguo Yang, Lijun Pu, Zhihua Wang, Yichen Zhon, Xiping Yan.: *Fault detection in a diesel engine by analyzing the instantaneous angular speed*. Mechanical Systems and Signal Processing 15(3) (2001).
- [8] Bonnier J. S., Tromp C.A.J., Klein Woud J.: *Decoding torsional vibration recordings for cylinder process monitoring*. CIMAC vol.3 1998.
- [9] Margaronis I. E.: *The torsional vibration of marine diesel engines under fault operation of its cylinder*. Forsh Ingenieurw., 1992, No 1-2.
- [10] Citron S.J., O'Higgins J.E., Chen L.Y.: *Cylinder-by-Cylinder Engine Pressure and Pressure Torque Waveform Determination Utilizing Speed Fluctuation*. SAE Paper No 890486.



Adam CHARCHALIS, born in 1944 in Przemyśl. In 1968 he accomplished engineering course in Polish Navy University and subsequently followed master studies in Gdansk University of Technology, in Faculty of Shipbuilding. Finally graduated to Msc. Eng. in 1971. In years 1968 - 1971 was appointed as a chief engineer on board a mine sweeper ORP „Krogulec”. Since 1971 had been working in Polish Navy Academy. In 1979 was appointed in substitution as a Commander of Institute of Ships Construction and Propulsion. From 1990 to 2003 was performing the duty of Institute Commander. From 1994 to 2003 was appointed as a Dean of Mechanical -Electrical Faculty of Polish Navy Academy. Since 1999 has been a professor in Maritime Academy in Gdynia where is a Dean of Mechanical Faculty since 2008. Promoted to Phd. of Engineering in 1978, professor since 1994. Zone of

scientific interest is Marine Propulsion, Marine Power Plants, Gas Turbine Propulsion and Diagnostics of Marine Mechanisms.. Author of 3 monographs, 8 handbooks and more than 250 articles.



Mirosław DERESZEWSKI, born in 1961 in Puck. In 1987 had accomplished studies in Polish Navy University and was promoted to Msc. Eng degree. In years from 1987 to 2002 was appointed at various Navy positions, from chief engineer on board a corvette up to squadron deputy commander.

In years 2002 – 2005 was performing a duty in NATO Headquarters as Maritime Infrastructure Officer. From 2005 to 2007 was Logistics Section Officer in Polish navy Headquarters. From 2007 to 2010 was employed by company ENAMOR Ltd in Gdynia as Research and Development Engineer. From beginning of 2011 has been appointed in Maritime University in Gdynia as an assistant in Mechanical Faculty, Chair of Marine Power Plants. Area of scientific interest is Marine Diesel Engines, Gas turbines and Diagnostics of Marine Propulsion.

AGENT APPROACH IN MACHINE DIAGNOSIS

Maciej KLEMM, Maciej TABASZEWSKI

Poznan University of Technology, Poland
ul. Piotrowo 3, 60-965 Poznan, Poland

fax. +48 61 665 2307, email: klemm.maciej@gmail.com, maciej.tabaszewski@put.poznan.pl

Summary

The paper presents a new approach to software development of diagnostic machines. The proposed system is a collection of many independent applications called agents which gain the diagnostic information, process it and inform the user of the system of the occurrence of significant events concerning the operation of the object. This allows a comprehensively support of the operation process by detecting the current condition and forecast a failure. An important feature of the proposed system is the speed, ability to learn through the use of artificial intelligence and openness that allows for any development of the system by adding more new items pursuing new activities or the same action on a different basis (increasing the reliability of inference).

Keywords: condition monitoring, agent system, multisymptom diagnostic, artificial intelligence, data mining.

PODEJŚCIE AGENTOWE W DIAGNOSTYCE MASZYN

Streszczenie

W pracy przedstawiono nowe podejście do tworzenia oprogramowania diagnostycznego maszyn. Zaproponowany system jest zbiorem wielu niezależnych aplikacji nazwanych agentami, które pozyskują informację diagnostyczną, przetwarzają ją i informują użytkownika systemu o wystąpieniu istotnych zdarzeń dotyczących eksploatacji obiektu. Pozwala to kompleksowo wspomagać proces eksploatacji poprzez wykrywanie aktualnego stanu i prognozę do awarii. Istotną cechą zaproponowanego systemu jest szybkość działania, zdolność uczenia się poprzez zastosowanie metod sztucznej inteligencji oraz otwartość pozwalająca na dowolny rozwój systemu poprzez dodawanie kolejnych nowych elementów realizujących nowe działania lub te same działania w oparciu o inne zasady (zwiększanie niezawodności wnioskowania).

Słowa kluczowe: diagnostyka, system agentowy, diagnostyka wielosymptomowa, sztuczna inteligencja, eksploracja danych.

1. INTRODUCTION

Modern machines are characterized by ever greater complexity and requirements for higher reliability. In order to cover the costs associated with maintenance of machines, developed countries need to spend billions of dollars annually [1]. For industrial power plants, refineries, oil-producing and gas plants which perform an important function in the economy an interruption of technological process or a failure of critical equipment can be extremely costly. For example, when designing important objects in the gas industry essential for the functioning of the country an additional construction performing as a reserve in case of unexpected failure (additional gas distribution station, additional compressor station, etc.) is assumed. Despite the additional reserve, inadequately maintained production equipment depletes regularly financial revenue of the company

and can cause a very expensive failure. Extending the life of machines and maintaining optimum working conditions through proper maintenance practices is a very important investment to avoid significant costs arising from major accidents. The key to a successful prevention-based monitoring system is the accurate determination of limit values for measured parameters or the construction of learner induction system based on a set of rules. However, mere identification of the current condition is insufficient in case of important objects. Modern surveillance systems should be further equipped with the tools of identification of damage and prognosis of the residual time for its failure. It allows the planning and organization of the repair work resulting in reduced downtime and reduced costs often associated with the unjustified replacement of many items that are in good condition as is often the case with the traditional approach based on a preventive system. In order

to accomplish the above tasks, particularly for machines with complex structure where use of traditional diagnostic tools is insufficient, it is reasonable to introduce multisymptom diagnostic machines, artificial intelligence and data mining while maintaining high speed operation of the system (preferably a parallel data processing).

2. AGENT APPROACH IN MACHINE DIAGNOSIS

Since the beginning of the 90s technological solutions based on intelligent software agents are said to be the next revolution in computing. This concerns not only the way they communicate with the computer, but also software development methodologies [2]. An agent can be defined as a unit operating in an environment capable of communicating with the environment including other agents of the system (communication), monitoring their environment (perception), and autonomous decision-making (autonomy) in order to achieve the goals set during the design or operation. Examples of application of agent systems can be found in [3, 4, 5, 6, 7, 8]. Agent software is usually installed on one computer which communicates with another agent via the Internet in order to exchange information and derive a common, optimal decision. A diagnostic system based on the agent approach has been recommended as a result of the work conducted by the authors of this paper. The system is a new solution using the independence and specialization of agents to solve specific diagnostic tasks. The resulting system is a collection of many independent programs working parallelly that acquire the diagnostic information, process it and inform the user of the occurrence of significant events concerning the operation of the plant. This solution makes the system open and flexible. During the operation, substitution of any agent can be made which facilitates the maintenance of the computer without interfering with other agents. In addition, a new agent can be introduced into the system, increasing its capabilities without stopping the data collection and conversion process. The only condition here is adapting the agents or their new versions to the accepted form of databases and knowledge bases. A characteristic feature of the agent approach is the adaptation and learning ability. In particular, the presence of the latter characteristic is desirable for the effective operation of the diagnostic system. In such a system new information must be worked out automatically which helps to improve the system and alerts the user about any problems. Of course this requires interaction with the operation of the system because it is necessary to enter some necessary data related to the confirmation of certain defects or confirmation of the earned value limits, etc. Interacting with the service staff allows the use of heuristic knowledge based on years of experience

gained by maintenance services. In order to complete the diagnostic tasks it is necessary to apply artificial intelligence methods and some statistics methods. An important characteristic of agents is independent decisions based on changes in the environment in which they operate.

The initiative of the most important agents in the suggested diagnosis system, among other things brings to:

- developing new symptoms on the basis of the existing data,
- developing their limits,
- assessing the "quality" of the symptom in relation to its usefulness for further tasks,
- selecting the optimal classifier for the purpose of determining the machine condition on the basis of many symptoms,
- optimizing the selection of forecasting model.

3. SCHEME OF AGENT SYSTEM

Figure 1 shows the schematic diagram of the agent system.

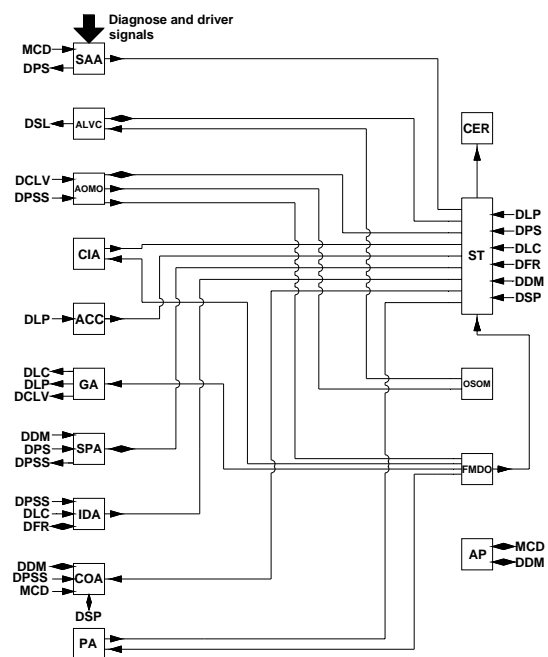


Fig. 1. Simplified diagram of the agent system

Diagnostic agents:

- SAA** – signal acquisition agent,
- ALVC** – agent of limit value calculation,
- AOMO** – agent of observation matrix optimization,
- CIA** – current inference agent,
- ACC** – agent of condition class,
- GA** – genesis agent with the review of current results,
- SPA** – signal processing agent,
- IDA** – identify the damage agent,
- COA** – change observation agent,
- PA** – prognostic agent.

Databases:

MCD – measurement control database,
DPS – database of primary signals,
DSL – database of suggested limits,
DCLV – database of current limits value,
DPSS – database of primary symptoms and spectrums,
DDM – database of definition measurement,
DLC – database of learner cases,
DLP – database of learning patterns,
DFR – database of fuzzy rules,
DSP – database of spectrum patterns.

Applications and support files:

CER – current events report,
ST – synoptic table,
OSOM – optimized symptom observation matrix,
FMDO – full matrix of diagnostics observation,
AP – administrator programme.

Diagnostic agents are combined with databases and applications which serve to configure the system or to present the results. Technically the various agents were made as 32-bit Windows applications run simultaneously and working „in parallel”. The number of processors (cores) supported by the operating system determines the extent of the parallel operation. Applications are written in an object in C++ language. In many cases, applications that perform complex calculations refer to the MATLAB® engine. The MATLAB® engine then performs calculations and returns the results available to the application.

Figure 2 shows a general scheme of co-operation with the application of MATLAB® engine.

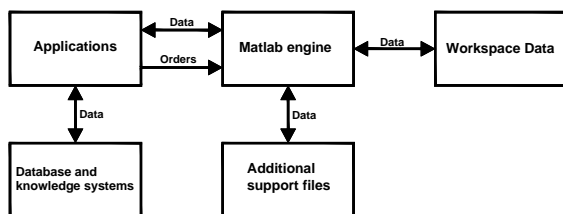


Fig. 2. General scheme of co-operation with the application of MATLAB® engine

This approach allows the implementation of even very complex algorithms. Most of the agents require no user interface so they work in the background. Specialized applications such as program administrator for configuring the system or synoptic table are responsible for the interaction with the user. Data necessary to realize the applications are read and written directly by the applications themselves. Thus, only applications have a direct contact with the database or knowledge base. Whereas, triggered scripts realized by the MATLAB® engine collect and store, if necessary, the data from and to the auxiliary

configuration files. In order to test the proper operation of algorithms, simulated data validating the predictable results were introduced. In order for the, simulated data to be close to the actual data random interferences were implemented. Additionally, some tests were carried out based on measurement data. The tests helped determine the correctness of the procedures by individual agents and the proper operation of the system as a whole.

4. DESCRIPTION OF DIAGNOSTIC AGENT

Signal Acquisition Agent (SAA) - reads signal transducers and / or diagnosed machine control system in accordance with the configuration preset in the administrator program (AP) by the user of the system. Signal acquisition takes place without the nonstationary conditions. In addition, when the machine stops, the agent's task is to stop the acquisition process to prevent erroneous results to be entered into the database. The current agent is to stop the data stream when the other agents do not keep up with its processing (queue overflow detection).

Signal Processing Agent (SPA) - Its task is to define measures of the signal point in the frequency bands given by the user and worked out by the system and to calculate the signal amplitude spectrum. The agent samples the data from the queue waiting to be processed and removes them from the queue. As soon as signal measurement values are set, they are recorded in the corresponding table also containing information about the values of operating parameters of the measurement time and measurement uncertainty. The agent sets out the following useful diagnostic measures:

- root mean square (RMS),
- peak,
- kurtosis,
- peak factor,
- clearance factor,
- impulse factor.

Change Observation Agent (COA) - The task of this agent is to identify changes in the signal and to generate new frequency bands for measurement in which the change is significant. This is done by detecting changes in the current spectral image and comparing it with the reference spectrum obtained at the earliest possible stage of machine life. The spectrum of a model is created for each combination of operating parameters thus the reference standard may occur later than at the beginning of the operations. New frequency bands are stored in an appropriate database which is interpreted by the signal processing agent (SPA). It should be noted that the newly generated frequencies are not removed from the database, even if for some reason there are no more changes of the effective value of the signal in the band

or even in case of a return to the initial baseline (recorded for the reference spectrum). In other words, once found changes-sensitive band is saved in the database.

Agent of Observation Matrix Optimization (AOMO)

- The task of the agent is to assess individual symptoms in terms of their suitability for diagnostic tasks. In addition, this agent assesses the symptom sensitivity. The Signal Processing Agent (SPA) evaluates the measurement uncertainty associated with that measure. Quality assessment of symptoms (no recognized power of the trend), the numerical value of sensitivity and measurement uncertainty are recorded in the database. In this way, none of the defined symptoms is removed from the processing queue; at the most, it will be ignored by successive agents if it is rated "insufficient".

The agent distinguishes the following types of curves of life:

- no trend (fluctuation around a constant value),
- linear trend,
- trend of an average dynamics describable with a second-degree polynomial,
- stronger trend, growing rapidly.

Another task of the agent is to include in the observation additional information about generalized symptom which by definition must carry information about the overall condition of the machine. This symptom is developed on the basis of PCA distribution [9].

Agent of Limit Value Calculation (ALVC) – Agent of limit value calculation is based on the method of symptom reliability [10, 11, 12, 13, 14, 15, 16, 17, 18, 19]. Having collected several measurements (for a given combination of operating parameters), and having taken into account suggestions as to the curve of life (in the absence of a significant limit value trend is not determined), the agent sets the empirical distribution of the symptom and chooses the best model of symptom reliability. The dependence is determined by the designated limit symptom. Information about the limit value is added to the table representing the optimized observation matrix. Independent limits value may be defined by the user. The first measurement being taken, the values are set at the level larger by 16dB than the value of the measurement. The user of the system decides if the obtained limit value is to replace the existing one (the initial value or the user-defined one).

Identify the Damage Agent (IDA) - The main goal of the agent is signal observation (additional and independent from the observation done by CIA) to detect characteristic components (combinations of components) that are associated with certain defects [20, 21]. A fuzzy classifier has been used here which conditions not only the type of damage but also classifies the contractual rate on the basis of the rules. The choice of location, width and shape

of the corresponding fuzzy sets are of paramount importance, so that the user is notified only of the essential problems, i.e. those where individual damages are fully traceable. In addition to defining the fuzzy rules, it also requires defining stage adaptation of specific sets of signals available immediately after booting a new machine or after repairs. It is the only agent in which expertise is required during the system startup. After the startup, the agent makes it possible to correct the fuzzy sets as soon as specific examples of measurements with the identified defects appear.

Current Inference Agent (CIA) - The algorithm of the agent reads the new data and compare the current value of the symptom to its limits. The task of the agent to respond to the emergence of new data in the system, to compare the obtained readings of symptom values with the limits and the technical assessment based on the results of these comparisons as well as to inform the user about the occurrence of exceedances by means of a synoptic chart.

Agent of Condition Class (ACC) - Agent of status classification is based on the classification of distance and "k nearest neighbors" method [22]. This allows to run the classifier on the relatively small number of observations learners. Based on the collected examples learners, the agent allows to distinguish between two conditions: fit and unfit. The proposed method is a supervised method which means that it requires the existence of many examples of classes of learners to describe both conditions. This undoubtedly represents a significant problem. Therefore, it is assumed that initially a major role in determining the status of the class will be played the Current Inference Agent. But with the influx of cases related to both learners: the system operation as well as archival data, or data obtained from other machines of the same type, given by the service, the classifier will be able to suggest the resulting class status for specific data (recognition), as well as to run a testing phase and define a classifier error.

Genesis Agent with the review of current results (GA)

- The current agent allows the user to enter some information about events and the identification of operating symptoms which probably correspond to the change in status. The latter possibility stems from the fact that the exclusion of an object and the statement of its unavailability may occur after the fact of failure. For example, a spindle bearing failure may be detected through the analysis of the deficiencies that arise as a result of grinding. The user must associate the information about the damage with the observation of trends in symptoms. In some cases it may be very simple (e.g. crack identification manifested with a sudden jump in symptom), but sometimes, if there is a slow upward trend, determination of transition time

into an unfit condition will be done only with some approximation.

Prognostic Agent (PA) - The task of the agent is to develop estimates of the residual time to failure based on a variety of symptoms [23]. It should be noted that the final estimate of the residual time to failure based on the number of independent measurements is not easy. This is due to the fact that each symptom may indicate a different value of the residual time. It is important to eliminate the symptoms that are not sufficiently sensitive (no reaction to wear) from the process of multisymptom forecast construction, hence the need for the selection of symptoms. The selection of an adequate predictive model is also of paramount importance. Forecasts built on outdated models will lead to significant errors. A separate forecast based on the best (of the group considered) model is developed for each symptom. In the next step generated information is used to estimate the residual time. The limit values of symptoms are determined using the Border Designation Value Agent (BDVA).

5. SUMMARY OF THE SYSTEM AS A WHOLE

The final version of multiagent diagnostic system allows the implementation of the following diagnostic tasks:

- acquisition of diagnostics signals,
- processing and analysis of diagnostic signals,
- evaluation of the symptoms,
- detecting changes in the signal and searching for sensitive frequency bands, changing significantly with the severity of the operation time,
- comparison of symptoms with the limits,
- independent classification based on multiple symptoms,
- implementation of fuzzy decision rules,
- evaluation of symptom forecasting models,
- setting limits by method of reliable symptoms,
- visualization of results,
- system configuration.

6. CONCLUSIONS

The developed system enables a comprehensive service to assist the maintenance process by detecting the current condition and forecast the time to change it. This is essential for critical machinery, the sudden failure could result in large financial losses resulting from the interruption process, or a sharp object injury, which can endanger human life and health. The proposed system is unique and although it has been tested at various levels, it is a prototype solution. A significant feature of the proposed system is its openness allowing any development of a system by adding more new items pursuing new activities,

or the same action under different rules (to increase the reliability of inference). The system was tested at different levels, from the testing algorithms used by testing the implementation of individual agents, finishing all tests based on the test stand. Made every effort to ensure that the proposed system was quite reliable. It is, however, important to realize that, as is the case with everyone, even much simpler programs, such a complex system may have some imperfections and errors undetected. Thus, as is the case in all programs, the system must be further developed and bugs must be removed as they are identified.

ACKNOWLEDGMENT

The paper was written partly due to financial support of Ministry of Science and Higher Education of Poland, grant No 1751/B/T02/2009/37 and project 4.R.09 financed by the Ministry of Science and Higher Education of Poland and coordinated by the Central Institute for Labour Protection - National Institute.

REFERENCES

- [1] W.Q. Wang, M.F. Golnaraghi and F. Ismail, *Prognosis of machine health condition using neuro-fuzzy systems*, Mechanical Systems and Signal Processing 18 (2004) 813-831.
- [2] Kamil Żarów, *Przewidywanie awarii*, Inżynieria i Utrzymanie Ruchu Zakładów Przemysłowych, czerwiec 2009.
- [3] Stranjak A., Ebden M., Rogers A., *A Multi-Agent Simulation System for Prediction and Scheduling of Aero Engine Overhaul*, Proc. of 7th Int. Conf. on Autonomous Agents and Multiagent Systems (AAMAS 2008), May, 12-16., 2008, Estoril, Portugal.
- [4] McArthur S.D.J., E. Davidson M., Hossack J.A., McDonald J.R., *Automating Power System Fault Diagnosis through Multi-Agent System Technology*, Proceedings of the 37th Hawaii International Conference on System Sciences – 2004
- [5] S. D. J. McArthur S.D.J., Davidson E.M., *Multi-Agent Systems for Diagnostic and Condition Monitoring Applications*, Internet publication: <http://www.emse.fr/~boissier/enseignement/sma06/exposes/01372751.pdf>, availability: September 2011
- [6] Rouff C.A., Hinchey M., Rash J., Truszkowski W., Gordon-Spears D., *Agent Technology from a Formal Perspective*, Springer-Verlag London Limited 2006
- [7] Chiung-Hon Leon Lee, Wen-Shang Tseng, Chin-Mu Chen, Alan Liu, Syuan-Ming Huang, Huang-Bin Huang, *Designing an Intelligent Agent for Information Appliances*, Journal of Computers Vol.18, No.1, April 2007.

-
- [8] Savarimuthu B. T. R., Purvis M., Fleurke M., *Monitoring and controlling of a multi - agent based workflow system*, Australasian Workshop on Data Mining and Web Intelligence (DMWI 2004), Dunedin. *Conferences in Research and Practice in Information Technology*, Vol. 32.
- [9] Kornacki J., Ćwik J., *Statystyczne systemy uczące się*, Warszawa, WNT 2005
- [10] Cempel C., *Pareto Law of Damage Evolution in Application to Vibration*, Condition Monitoring. *Bulletin of the Polish Academy of Sciences*, vol. 39, No 4, 1991, str. 573-588
- [11] Cempel C., *Passive Diagnostic Experiment, Symptom Reliability and Their Applications in Vibration Condition Monitoring*, *Zagadnienia eksploatacji maszyn*, Zeszyt 2-3 (82-83), 1990.
- [12] Papoulis A., *Probability, Random Variables, Stochastic Processes*, McGraw Hill, New York 1965.
- [13] Cempel C., Natke H.G., Yao J.P.T., *Symptom - Based Reliability for Critical Operating Systems*, Intern. Workshop on Damage Assessment, Pescara - Italy, May 1995.
- [14] Tomaszewski F., Cempel C., *An Attempt to Diagnose a Locomotive Combustion Engine by Utilizing Vibroacoustic Processes*. *The Archives of Transport*, No 1, 1991.
- [15] Cempel C., *Pre-Breakdown Symptom Value for Vibration Condition Monitoring*, *Bulletin of The Polish Academy of Sciences, Technical Sciences* Vol. 37, No 7-12, 1989.
- [16] Cempel C., Natke H. G., Tabaszewski M., *A Passive Diagnostic Experiment with Ergodic Properites*, *Mechanical Systems and Signal Processing*, 1997, vol. 11, s. 107 – 117.
- [17] Cempel C., *Damage Initiation and Evolution and Operating Mechanical Systems*, *Bulletin of The Polish Academy of Sciences, Technical Sciences*, 1992, vol. 40, no. 3, s. 201 – 214.
- [18] Cempel C., Natke H. G., *System Life Cycle – System Life: The Model Based Technical Diagnostics*, *A View on Holistic Modeling*, *System Research*, 1993, 10 (1), s. 53 – 62.
- [19] Cempel C., *Theory of Energy Transforming System and their Application in Diagnostics of the Operating Systems*, *Applied Mathematics and Computer Science*, 1993, vol. 3, no. 3, s. 533 – 548.
- [20] Białko M., *Sztuczna inteligencja i elementy hybrydowych systemów ekspertowych*, Koszalin, Wydawnictwo Uczelniane Politechniki Koszalińskiej 2005.
- [21] Łachwa A., *Rozmyty świat zbiorów, liczb, realizacji, faktów, reguł i decyzji*, Warszawa, Akademicka Oficyna Wydawnicza EXIT 2001.
- [22] Larose D. T., *Odkrywanie wiedzy z danych. Wprowadzenie do eksploracji danych*, Warszawa, PWN 2006.
- [23] Tabaszewski M., *Wielosymptomowa prognoza stanu i czasu do awarii z wykorzystaniem sieci neuronowych*, *Diagnostyka*, 2007, vol. 2 (42), s. 43 – 48.

TESTS OF LM2500 NAVAL GAS TURBINE WITH THE OBJECTIVE OF DETERMINING ITS OPERATING CHARACTERISTICS

Bogdan POJAWA

Polish Naval Academy, Institute of Ship Construction and Operation
ul. Śmidowicza 69, 81-103 Gdynia, pojawa@o2.pl

Summary

The article presents the results of preliminary tests concerning the determination of operating characteristics of the examined engine in steady states. The study concerned main propulsion engines of an Oliver Hazard Perry class frigate operated by the Polish Navy. The propulsion system of that frigate consists of two LM2500 marine gas turbine engines, reduction gear, shaft line and a controllable pitch propeller (CPP). The tests were conducted in the ship's engine room when the ship was at sea. Operating characteristics were determined on the basis of the measurements recorded over the entire load range of the engine, from minimum to rated load. During the tests, the load of both engines of the ship was simultaneous and balanced. In order to facilitate the comparison of the operating characteristics of the tested engines, as well as to make a reference to various weather conditions, the data obtained was reduced to standard day conditions. For the aforementioned characteristics approximation relations were determined using statistical analysis. The relations obtained may be utilized in technical diagnostics and for further studies concerning the engines examined in the present research study.

Key words: naval gas turbine, naval power unit, operating characteristic.

BADANIA OKRĘTOWEGO TURBINOWEGO SILNIKA SPALINOWEGO LM 2500 W ASPEKCIE WYZNACZENIA CHARAKTERYSTYK OBROTOWYCH

Streszczenie

W artykule przedstawiono wyniki badań dotyczących opracowania charakterystyk obrotowych obiektu badań, w stanach pracy ustalonej. Obiektem badań były silniki napędu głównego fregaty typu Oliver Hazard Perry będącej na wyposażeniu Marynarki Wojennej RP. Układ napędowy składa się z dwóch okrętowych turbinowych silników spalinowych LM 2500, przekładni redukcyjnej, linii wału oraz śruby napędowej o skoku nastawnym. Badania przeprowadzono podczas wyjścia okrętu w morze, w warunkach siłowni okrętowej. Do opracowania charakterystyk wykorzystano wyniki pomiarów zarejestrowane w zakresie obciążeń silników od minimalnego do nominalnego. Podczas badań silniki zostały poddane jednoczesnemu i równomiernemu obciążeniu. W celu umożliwienia porównywania charakterystyk badanych silników, jak również odniesienia ich do różnych warunków atmosferycznych, wyniki pomiarów na podstawie których je wyznaczono, sprowadzono do tzw. unormowanych warunków atmosferycznych. Dla przedmiotowych charakterystyk dokonano wyznaczenia zależności aproksymacyjnych z wykorzystaniem analizy statystycznej. Otrzymane zależności mogą być wykorzystywane na potrzeby diagnostyki technicznej oraz dalszych badań rozpatrywanego obiektu badań.

Słowa kluczowe: okrętowy turbinowy silnik spalinowy, okrętowy układ napędowy, charakterystyka obrotowa.

1. INTRODUCTION

In practical operation of naval power plants, including marine propulsion systems, there is a need for analyzing them and comparing various solutions as well as for evaluating their technical condition. Such analyses usually concern the aspects of economics, operation and energy. Economy of operation is in the case of a marine power plant usually of secondary importance because of the fact that the intended role of a given naval ship is to perform specific tasks. Operational

indicators of a naval power plant show its reliability, possibility of overloading main propulsion engines, ship's maneuverability, time between overhauls (TBO), etc. Energy-related indicators on the other hand, e.g. efficiency, individual fuel consumption, power and torque determine the ship's speed through the water, its range, etc. [1,2,6].

The specifics of operating naval gas turbine propulsion systems is different from operating conventional marine piston engines. This is due to differences in design and construction, the use of

different thermodynamic cycle, the implementation of a continuous transformation of internal energy and a large variation range of operating parameters, especially engine speeds. In the most general terms, a naval gas turbine consists of a gas generator and a free power turbine. The function of the gas generator, just as its name suggests, is to produce the working medium (gas) having predefined parameters whereas the task of the power turbine is to drive the load. There is no mechanical coupling between the wheels of the gas generator and those of the power turbine. The coupling between those components is of thermal gas-dynamic nature. Because of that the gas generator and the free power turbine work independently from each other. Consequently, the working mass accumulates in the flow channels between the gas generator and the free power turbine, which at too high load of the latter (accompanied by reduction of its speed) may lead to undesirable processes that may, in turn, lead to engine damage (due to compressor stall). To sum up, it is that dynamic coupling of thermo-gas-dynamic nature that has the greatest impact on the different operating specifics of naval gas turbine engines. The Polish Navy currently has two types of ships equipped with gas turbine propulsion systems. These are Tarantula missile corvettes and Olivier Hazard Perry missile frigates [3, 6].

Operation of naval gas turbines requires the knowledge of their operating parameters, which are dependent on the load resulting from the speed of the ship through water. The relationships mentioned above are illustrated by engine operating characteristics, on the basis of which areas of application of a given engine may be identified, and its performance and economical operation analyzed [1, 2, 5, 6]. With regard to naval gas turbine, those operating characteristics result from the interaction between fluid-flow machines that are the major components of the engine. They include: the compressor, the combustion chamber and the turbine. Moreover, as it has already been mentioned, the naval gas turbine contains the free power turbine, which is not mechanically coupled to the gas generator, but the connection between them is of thermo-gas-dynamic nature [3,6].

The article identifies the object of the research study and presents the test results concerning the determination of the operating characteristics in steady states of the LM2500 naval gas turbine being a component of the Oliver Hazard Perry class frigate. Preliminary tests were conducted in the ship's engine room when the ship was at sea. Operating characteristics of the engines were determined on the basis of the measurements recorded over the entire engine load range, from minimum to rated load.

2. CLASSIFICATION CHARACTERISTICS OF NAVAL GAS TURBINE

Operating characteristic can be best defined as a graphical or an analytical presentation of the relationship between the basic values which define the engine performance, as well as the working medium parameters measured in the specific engine cross-sections, and the values characterizing the working conditions of the engine mated with a specific load [3,5,6].

The engine's (gas generator's) load state, being its current performance in terms of energy, depends on the values of the energy-related parameters whose values are dependent on the position of the engine (fuel jet) control lever (ECL) and directly affecting the engine power output (gas stream of enthalpy). In the case of a dual rotor naval gas turbine, such parameter is the gas generator speed whereas in the case of a triple rotor naval gas turbine - with a separate power turbine rotor and a dual rotor gas generator - it is most commonly the speed of the high pressure rotor. The basic energy-related parameters characterizing the work of every engine are: power output, torque, rotor speed and specific fuel consumption. The values of those parameters, depending on the engine load state, may be maximum, rated, working and minimum [1, 2, 3, 5, 6, 8]. Additional parameters characterizing engine operation may also be distinguished. As far as naval gas turbines concerned, those parameters include:

- temperature and absolute pressure of the working medium in specific engine cross-sections corresponding to the nodal points of the engine's thermodynamic cycle. Temperature and absolute pressure may be static or total (impact);
- streams of air mass, fuel and exhaust gases;
- compression ratio of the compressor.

The following engine load states may be distinguished in the naval gas turbine operation:

- **steady**, in the range from minimum (informally called "idle run") to maximum power, including particular states: maximum, rated (calculated), partial (working), and minimum power;
- **unsteady** (transient), including: engine start-up and shut-off as well as acceleration and deceleration.

Consequently, operating characteristics of marine gas turbine engines can be classified as [6]:

- static:
 - rotational;
 - full-load;
 - mating engine with load;
- dynamic (transient):
 - start-up;
 - acceleration and deceleration;
- general or universal (multiparameter).

The article presents functional dependencies of rotational characteristics of the examined engine, which represent the dependence of engine operating parameters on the gas generator speed, while maintaining the free power turbine speed resulting from its mating to a load in the form of a controllable pitch propeller (CPP). Having the rotational characteristics available, it is possible to determine on their basis the full-load characteristics and the characteristics of the engine operation when mated to a given load.

3. PRELIMINARY TESTS

The objective of the preliminary tests was to measure the operating parameters of the examined engine with regard to determining functional dependencies of its rotational characteristics. The study concerned LM2500 marine gas turbine engines used as main propulsion engines of the Olivier Hazard Perry class missile frigate. The tests were conducted onboard such a frigate in service with the Polish Navy for steady load states, determined on the basis of the gas generator speed over the entire load range of the engine, from minimum to rated load. Engine was loaded in accordance with the propulsion system control program, which - depending on the preset speed of the ship - selects the optimum setting of propeller pitch and fuel flow and controls the angle of attack of six stages of Variable Stator Vanes (VSV) in the engines' axial compressor.

The parameters were measured when the load of both engines was simultaneous and balanced. The measurements were made using the portable measuring-recording system, Multichannel Recorder, type 908416161C and, additionally, the operating parameter values were read and recorded from digital displays on the main control panel in the engine control room. The measurements were made for 60 seconds at specific load settings, with the sampling rate of 2Hz, and then averaged. Measurements were preceded by the calibration of individual measuring circuits including the assessment of their uncertainties.

The propulsion system of the Olivier hazard Perry class missile frigate (Fig. 1) consists of three basic components: main propulsion engines LM2500 with automation module, the reduction gear, the shaft line and the controllable pitch propeller (CPP) [8].

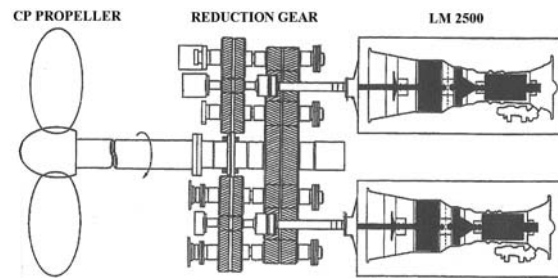


Fig. 1. Propulsion system of Oliver Hazard Perry class frigate [8]

Main propulsion engines are two LM2500 naval gas turbines manufactured by General Electric. General Electric LM2500 engine (Fig. 2) has dual-rotor design, with axial flow of the working mass. It consists of two main components: a gas generator and a free power turbine making the complete engine. The gas generator consists of a 16-stage axial flow compressor, an annular type combustor equipped with 30 injectors and a two-stage high pressure turbine. Downstream of the gas generator there is a 6-stage power turbine coupled with the gas generator in a thermo-gas-dynamic manner [8].

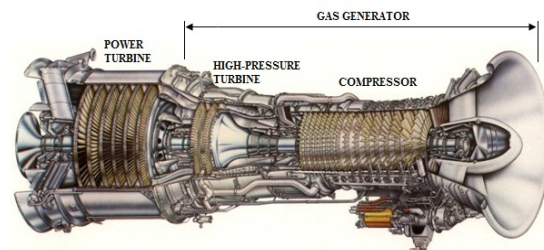


Fig. 2. Cross-section of LM2500 naval gas turbine [8]

4. RESULTS OF PRELIMINARY TESTS

The results of the measurements concerning operating parameters of the examined engine at specific ranges of steady-state operation were reduced to SI units or their multiples. Ambient pressure was taken into account when determining absolute pressures. In order to facilitate the comparison of the operating characteristics of the tested engines, as well as to make a reference to various weather conditions, the data obtained was reduced to standard weather conditions. Standard weather conditions are: barometric pressure $p_{0WZ} = 101325 Pa$, absolute temperature $T_{0WZ} = 288,15 K$ and absolute humidity $\varphi = 0$ [1,3,6].

Operating characteristics of the examined engine were determined on the basis of the measurement results. Operating characteristics present functional dependencies of between engine operating parameters and the gas generator speed, while maintaining the free power turbine speed resulting from its mating to a load being a controllable pitch propeller (CPP). Because of the simultaneous and equal load of both engines during the tests, the results of measurements recorded on

both engines were utilized in order to determine the said characteristics.

Subsequently, the characteristics obtained were analyzed to determine approximating dependencies. Statistical analysis was used to that end. Statistical analysis is the method of processing data (results of measurements performed according to an assumed program of tests) in order to find regularities in the examined phenomena and to interpret them using the methods employed in mathematical statistics. This facilitates establishing the mathematical function of the examined object, which may also constitute its mathematical model. The results obtained by means of statistical analysis are the basis for obtaining useful information concerning the examined object and for drawing conclusions from the conducted research. The most common measure of relating the obtained function of the examined object to the measurement results is the

coefficient of determination R^2 and the average approximation error $\sigma(y)$ (also known as standard deviation). In addition to the statistical analysis, a substantive analysis of the test results was also carried out. That analysis concerned particularly the validation of the mathematical model obtained for its compliance with the physical phenomena occurring within the relevant examined engine, taking into consideration both theoretical foundations and the principles of operating the engine [4, 7].

In order to approximate the rotational characteristics, least-squares method (LSM) was used, making use of polynomials. The rotational characteristics of the examined engine, together with their functional dependence, coefficient of determination R^2 and the average approximation error $\sigma(y)$, are shown in the graphs below.

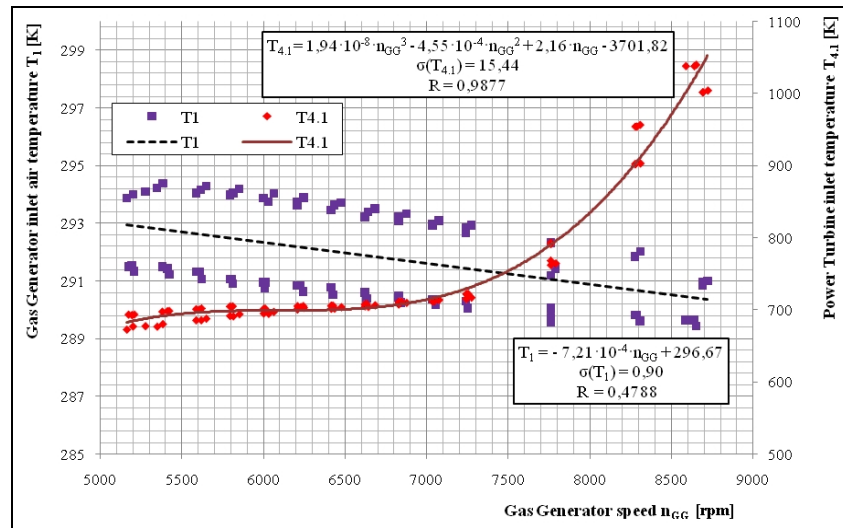


Fig. 3. Approximation function and the results of the measurements of gas generator inlet air temperature T_1 and power turbine inlet air temperature $T_{4,1}$, recorded for steady-state operation of LM2500 engine, in relation to gas generator speed n_{GG}

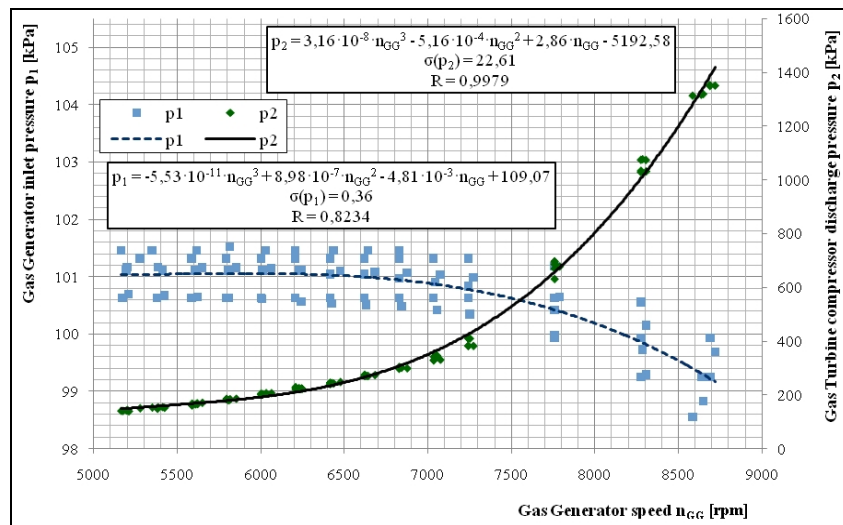


Fig. 4. Approximation function and the results of the measurements of compressor inlet air pressure p_1 and compressor discharge pressure p_2 , recorded for steady-state operation of LM-2500 engine, in relation to gas generator speed n_{GG}

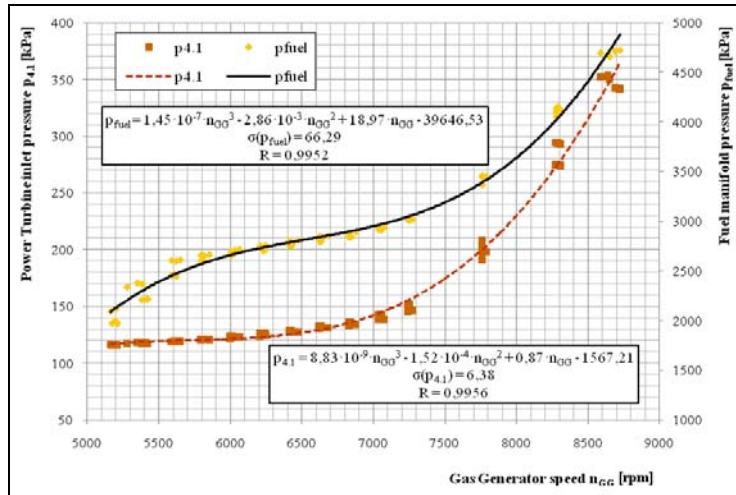


Fig. 5. Approximation function and the results of the measurements of power turbine inlet pressure $p_{4,1}$ and fuel manifold pressure p_{fuel} , recorded for steady-state operation of LM2500 engine, in relation to gas generator speed n_{GG}

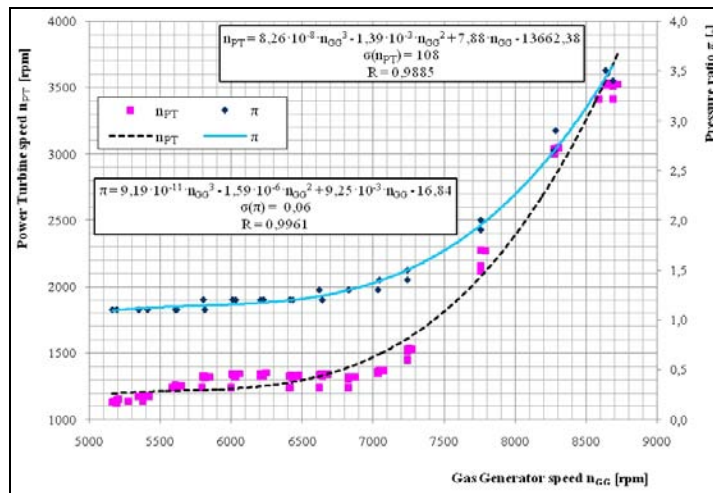


Fig. 6. Approximation function and the results of the measurements of power turbine speed n_{PT} and compression ratio of compressor π , recorded for steady-state operation of LM2500 engine, in relation to gas generator speed n_{GG}

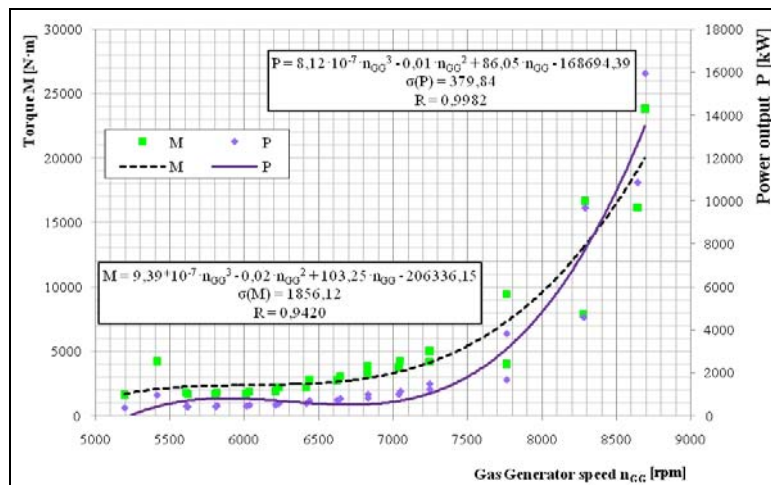


Fig. 7. Approximation function and the results of the measurements of torque M and engine power P , recorded for steady-state operation of LM2500 engine, in relation to gas generator speed n_{GG}

Analyses of the functions describing operating characteristics of the examined engine show that variation range of the studied operating parameters is in compliance with the specification given by the ship's documentation. The operating characteristic graphs point out to the nonlinear character of the relationships between operating parameters and the engine load. The non-linear character of the said relationships results from the fact that the power turbine is mated to a controllable pitch propeller (CPP). Only the characteristic of the compressor inlet temperature (CIT) is linear. It is also noticeable that the curves are linear in the range from minimum load to the load at which maximum propeller pitch angle is reached. Maximum propeller pitch angle occurs at the gas generator speed of approximately 7000 RPM. The characteristics also show that a significant increase in engine power output occurs after reaching the maximum propeller pitch angle, when the free power turbine is mated with the propeller set at its maximum steady pitch angle. Upon reaching the maximum propeller pitch angle, the engine delivers an output of approximately 1400 kW, with a maximum power output of 18500 kW.

5. SUMMARY

The possibility of determining engine operating characteristics facilitates their use in the process of diagnostics in its broad sense. Owing to that, there is a possibility of conscious operation of equipment according to its technical condition. Observing the trends present in the changes of the operating characteristics and selected diagnostic symptoms facilitates obtaining data which may be used in the decision-making process related to equipment operation in order to ensure naval combat readiness, as well as to maintenance, adjustment or replacement of engine components and, finally, to repairs. That data may also be used to design new engines or upgrade the existing models.

The determined functional dependencies of the LM2500 naval gas turbine will facilitate analytical determination of engine operating parameters on the basis of gas generator speed, for any ambient parameters. The values of engine operating parameters determined on the basis of the aforementioned dependencies are approximate but their accuracy is sufficient for engineering applications to meet the need of further research concerning this type of engine.

Knowledge and experience related to operating characteristics are also used in the process of education and training people responsible for operating of such engines, carried out at the Department of Mechanical and Electrical Engineering of the Naval Academy in Gdynia. This is particularly important because incorrect operation often leads to serious failures, which affect the combat readiness of the ship, and also

generate large and unexpected costs in the process of ship's operation.

BIBLIOGRAPHY

- [1] Charchalis A.: *Warunki przeprowadzania i weryfikacji oceny diagnostycznej na okręcie*. Diagnostyka Vol. 34, 2005
- [2] Charchalis A.: *Diagnozowanie okrętowych silników turbinowych*, AMW, Gdynia 1991.
- [2] Dzygadło Z., Łyżwiński M., Otyś J., Szczeciński S., Wiatrek R.: *Napędy lotnicze – zespoły wirnikowe silników turbinowych*, WKiŁ, Warszawa 1982.
- [3] Pieriegudow W.: *Metoda najmniejszych kwadratów i jej zastosowanie*, PWE, Warszawa 1967.
- [4] Pojawa B.: *Stanowisko laboratoryjne dwuwirnikowego silnika turbinowego*, XXVI Sympozjum Siłowni Okrętowych SYMSO 2005 Gdynia.
- [5] Pojawa B.: *Rola charakterystyk eksploatacyjnych w eksploatacji okrętowych turbinowych silników spalinowych*, Logistyka 6/2010.
- [6] Taylor J.R.: *Wstęp do analizy błęd pomiarowego*, Wydawnictwo Naukowe PWN, Warszawa 1999.
- [7] *Instrukcja obsługi układu napędowego fregaty FFG9*.



Mr **Bogdan POJAWA** DSc. Eng. – Assistant Professor at the Institute of Ship Construction and Operation, Polish Naval Academy in Gdynia. His main research interests include maintenance and diagnostics of naval propulsion units. He is a member of Polish Society of Technical Diagnostics as well

as Polish Scientific Society of Combustion Engines.

WYKORZYSTANIE TRANSFORMACJI HOUGH'A W PROJEKTOWANIU MODUŁU DECYZYJNEGO SYSTEMU PROAKTYWNEJ EKSPLOATACJI

Stanisław RADKOWSKI, Robert GUMIŃSKI

Institute of Vehicles, Warsaw University of Technology, Warsaw, Poland
 Narbutta 84, 02-524 Warsaw, Poland, fax. 022 234 81 21, ras@simr.pw.edu.pl

Streszczenie

W artykule zostało podjęte zagadnienie proaktywnej strategii eksploatacji. Zwrócono uwagę na fakt, że w wyborze sposobu zbierania informacji diagnostycznej należy uwzględnić niezawodnościowe wskaźniki ważności elementów. W planowaniu czynności obsługowych ważne jest posługiwanie się modelami rozwoju uszkodzenia umożliwiającymi aktualizację na podstawie aktualnego stanu technicznego. Zaproponowano wykorzystanie transformaty Hough'a w celu wyznaczenia kluczowych punktów rozwoju uszkodzenia na przykładzie funkcji logistycznej, która może być wykorzystana do modelowania zmian energii sygnału drganiowego w trakcie rozwoju uszkodzenia.

Słowa kluczowe: funkcja logistyczna, transformacja Hough'a.

USE OF HOUGH'S TRANSFORM FOR DESIGNING THE DECISION-MAKING MODULE OF A PROACTIVE OPERATIONS SYSTEM

Summary

The article takes up the issue of a proactive operations strategy. Attention is drawn to the fact that while selecting the method of collecting the diagnostic information one should account for the respective elements' reliability indicators from the point of view of their importance. While planning maintenance activities, it is important to use the defect development models which offer the possibility of information updating based on the current technical condition of an object. A proposal has been made to use the Hough's transform in order to determine the key points of defect development on the example of a logistic function which can be used for the purpose of modeling the energy changes in a vibration signal during defect development.

Keywords: Logistic curve, Hough transform.

1. WSTĘP

Ważnym zagadnieniem w procesie eksploatacji obiektu [8] jest problem wyboru strategii utrzymania ruchu umożliwiającej maksymalizację funkcji niezawodności systemu. Dla zapewnienia poprawności rozwiązania tego zadania niezbędnym jest uwzględnienie wpływu zarówno struktury układu na niezawodność systemu, jak i poszczególnych jego elementów. W literaturze wskazuje się w tym miejscu na możliwość wprowadzenia wskaźnika wpływu elementu na zachowanie niezawodności systemu w postaci miary ważności elementu. Najczęściej istotność elementów jest określana za pomocą wskaźników oceny strukturalnej (*SRF*), które uwzględniają ryzyko uszkodzenia zmęczeniowego (*FT*), degenerujący wpływ środowiska (*ED*) oraz ryzyko przypadkowego uszkodzenia (*AD*). Zatem wybór określonego sposobu zbierania informacji, w szczególności określenie zakresu i głębokości prowadzenia diagnozy będzie zależny od wymaganego średniego okresu do wystąpienia



Rys. 1. Schemat niezawodnościowo zorientowanej analizy sytemu stosowanej w lotnictwie [8]

uszkodzenia (*MTTF*), przewidywanych kosztów napraw i przestoju oraz związanej z tym oceny efektywności czynności obsługowo-naprawczych. Z drugiej strony niezbędnym jest ustalenie akceptowalnego ryzyka pojedynczego uszkodzenia, określenie okresu kumulacyjnego wzrostu warunkowego prawdopodobieństwa rozwoju uszkodzenia oraz oszacowania prawdopodobieństwa uszkodzeń wielokrotnych. Jednym z istotnych czynników proponowanego systemu niezawodności jest ustalenie krytycznych elementów maszyny.

Ustalenie rankingu elementów pozwala określić właściwą sekwencję inspekcji diagnostycznych dla dominujących uszkodzeń. Szczególne znaczenie w określaniu zadań diagnostycznych ma miara Vessely – Fussella, przedstawiona obok wielu miar w pracy [5].

Wykorzystanie niezawodnościowych miar ważności elementów pozwala w procesach diagnozowania uwzględniać wpływ struktury układu i możliwą sekwencję zdarzeń, jaka może towarzyszyć wystąpieniu odpowiedniego zdarzenia szczytowego. Podobnie dobór testu diagnostycznego, którego zadaniem byłoby zmniejszenie poziomu ryzyka powinien uwzględniać wpływ struktury diagnozowanego obiektu.

Podstawowym problemem w tym ujęciu pozostaje określenie prawdopodobieństwa zdarzenia inicjującego, bowiem dla innych wartości prawdopodobieństwa wystąpienia zdarzenia inicjującego za optymalną może zostać uznana inna sekwencja inspekcji diagnostycznych. W przypadku układu mechanicznego, w którym dominują procesy zużycia można oczekiwać istotnych zmian wartości wspomnianych prawdopodobieństw.

Wymaga to prowadzenia analizy wpływu sposobu i warunków użytkowania na przebieg obciążeń oraz związanych z tym uszkodzeń. Po uwzględnieniu wpływu warunków środowiskowych powstaje możliwość określenia zakresu diagnostyki i prawdopodobnego zakresu oraz harmonogramu napraw.

Kolejnym działaniem pozwalającym na lepsze zrozumienie zachodzących procesów i jednocześnie bardziej świadome podejmowanie decyzji eksploatacyjnych jest zbudowanie modelu uwzględniającego fazę rozwoju uszkodzenia. Model taki powinien dawać możliwość uwzględnienia w prowadzonej analizie dodatkowej nowo-zdobytej informacji. Dlatego tak ważne jest budowanie modelu rozwoju uszkodzenia, który to model powinien być uaktualniany wiedzą o stanie obiektu uzyskaną w drodze diagnostyki. W tak rozumianym systemie eksploatacyjnym szczególnie ważny jest dobór odpowiednich symptomów stanu i metod diagnostycznych.

Najczęstsza przestrzeń cech jest to przestrzeń Euklidesowa jedno, dwu lub wielowymiarowa, a rozkład wartości cech względem poszczególnych współrzędnych założonej przestrzeni jest przedstawiany przy pomocy funkcji. Wybór cech zależy od zadań wyznaczonych dla systemu

diagnostycznego i przyjętych strategii eksploatacji [2]. Przyjęcie proaktywnej strategii eksploatacji wiąże się z koniecznością ekstrakowania z sygnału diagnostycznego symptomów nukleacji uszkodzenia bądź niskoenergetycznych faz rozwoju [4, 6, 10].

Transformacja z jednej przestrzeni do innej określa się jako operacja przekształcenia z uwzględnieniem zmiany współrzędnych. Właściwe transformowanie jest szczególnie ważne w projektowaniu diagnostyczno – prognostycznego interfejsu: system – operator i w opracowaniu sposobu przesyłania informacji pomiędzy operatorem a decydem. Kryterium doboru transformacji może być z jednej strony redukcja nadmiaru informacji, możliwość przyłożenia odpowiedniej wagi i nadanie niezbędnego priorytetu, z drugiej możliwość rekonstrukcji sygnału na podstawie dostępnej projekcji. Stosowane sygnały umożliwią otrzymanie informacji o wewnętrznych rozkładach szeregu parametrów, charakteryzujących zmiany zachodzące w nadzorowanych obiektach.

2. WYKRYWANIE CECH Z WYKORZYSTANIEM TRANSFORMATY HOUGH'A

Szczególnie interesującym jest możliwość diagnozowania i prognozowania wartości cech sygnału w efekcie zmian jednej współrzędnej. Taką własnością charakteryzuje się transformata Radona [3] za pomocą której jednowymiarowa transformata Fouriera, może przekształcać wielowymiarową przestrzeń do postaci przekroju wielowymiarowej transformaty Fouriera, określonej względem tej samej współrzędnej.

Własność ta stała się podstawą wykorzystania transformaty Radona w tomografii komputerowej. Podobnie jest szeroko wykorzystywana w rozpoznawaniu obrazów. Jeśli w tym ostatnim przypadku podstawowym problemem jest detekcja linii prostych to odwołuje się do transformaty Hough'a (*TH*) [7], która jest szczególnym przypadkiem transformaty Radona. Przyjęło się, że obraz poddany jest preprocessingowi przy pomocy innych detektorów krawędzi [11], a następnie mapowany z wykorzystaniem *TH*.

Podstawą transformaty Hough'a jest spostrzeżenie, że linia prosta, która w układzie współrzędnych kartezjańskich (x, y) może być opisana równaniem (1):

$$y = b + ax \quad (1)$$

to w przestrzeni Hough'a o współrzędnych (r, θ) ta sama prosta może być zapisana w postaci równania parametrycznego (2):

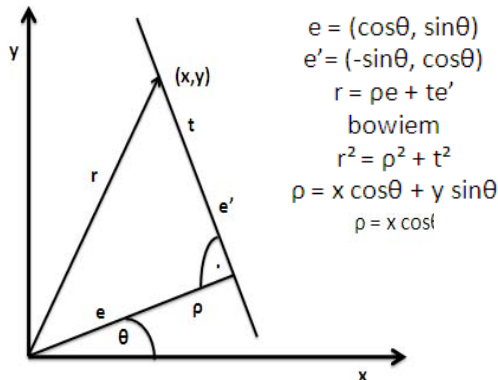
$$r = x \cos \theta + y \sin \theta. \quad (2)$$

To ostatnie równanie otrzymuje się z równania ogólnego prostej (3):

$$Ax + By + C = 0 \quad (3)$$

przez normalizację, pamiętając że wektor $[-B, A]$ jest wektorem kierunkowym prostej, natomiast odpowiednio ρ jest promieniem wodzącym, a θ jest kątem pomiędzy promieniem ρ , a współrzędną x .

Obecnie jest wiele odmian transformaty Hough'a, a zakres zastosowań w cyfrowej analizie obrazu obejmuje nie tylko detekcje prostych, ale również innych krzywych analitycznych.



Rys. 2. Ilustracja wykorzystania podstawowych zależności analitycznych w transformacji Radona i Hough'a

W efekcie zastosowania transformaty Hough'a linia prosta w układach (x, y) jest przekształcana do punktu w układzie (ρ, θ) . Inaczej, zakładając że na ekranie monitora przedstawiona jest przestrzeń Hough'a, obrazem obrotu prostej wokół punktu (x_0, y_0) będzie krzywa Hough'a, obrazy punktów leżących na jednej prostej przecinają się w punkcie (w przestrzeni Hough'a) odpowiadającym współczynnikiem prostej, do której należą punkty w przestrzeni cech sygnału, natomiast np. równoległemu przesunięciu prostej, będzie odpowiadać przesunięcie punktu na ekranie obrazującym przestrzeń Hough'a.

Ta ostatnia własność transformaty może być wykorzystana w detekcji jakościowych zmian zachodzących w zachowaniu się nadzorowanego obiektu.

3. MODELOWANIE ZMIAN ENERGII SYGNAŁU WIBROAKUSTYCZNEGO Z WYKORZYSTANIEM FUNKCJI LOGISTYCZNEJ

Z punktu widzenia proaktywnej eksploatacji podstawowym zadaniem jest diagnozowanie okresu nukleacji pęknięcia. Szerzej zagadnienie wykorzystania cech sygnału wykorzystywanego w diagnozowaniu zmęczeniowego pęknięcia u podstawy zęba w przekładniach zębatych, zostało przedstawione w [9].

Porównując względne zmiany energii występujące w przypadku propagacji pęknięcia [1], z jakościowymi zmianami energii wibroakustycznej

w artykule zaproponowano logistyczny model rozwoju pęknięcia:

$$\gamma(\varepsilon) = \frac{a}{1 + be^{-c\varepsilon}} \quad (4)$$

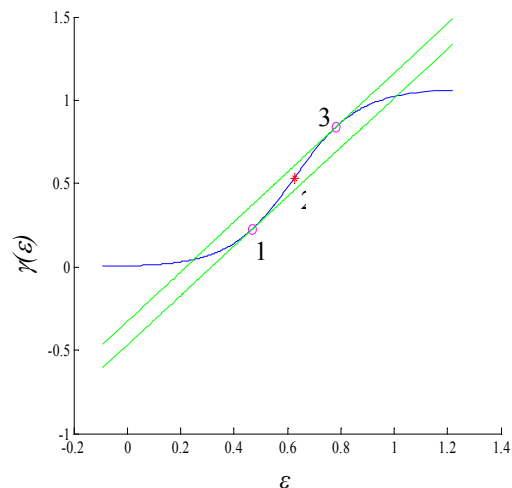
gdzie: a, b, c – parametry krzywej logistycznej, $\gamma(\varepsilon)$ – zmiana energii względnej sygnału drganiowego w funkcji rozmiaru szczeliny.

Zgodnie z przyjętą zależnością na krzywej logistycznej (Rys. 3.) można wyróżnić trzy punkty:

- 1 – punkt oznaczający przyrost prędkości względnej zmiany energii,
- 2 – punkt, w którym występuje deakceleracja przyrostu prędkości względnej zmiany energii,
- 3 – punkt, w którym rozpoznany jest okres saturacji krzywej logistycznej.

4. PRZYKŁAD

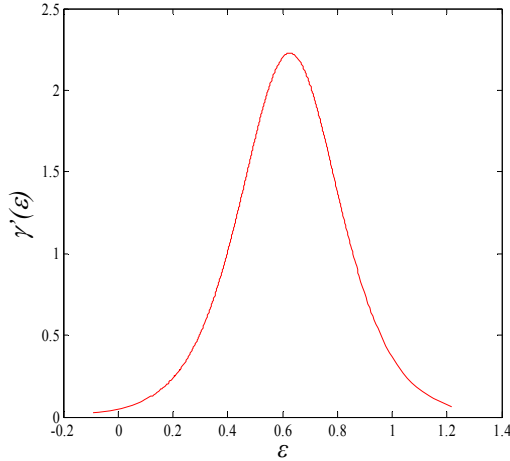
Szczególnie interesującym jest możliwość ustalenia osiągnięcia punktu 1 na podstawie obserwacji przyrostów krzywej logistycznej obserwowanej na ekranie operatora sygnału diagnostycznego. Za podstawę przyjęto wyniki analizy pochodnych krzywej logistycznej. Na rysunku 4 przedstawiono pierwszą pochodną (funkcję błędów). Drugą pochodną przedstawiono na rysunku 5. Osiąga ona swoje ekstremum w punktach 1 i 3 krzywej logistycznej. Zauważmy, że styczne do drugiej pochodnej w punktach 1 i 3 są poziome.



Rys. 3. Wykorzystanie krzywej logistycznej do ustalenia początku propagacji uszkodzenia (1) i końca fazy szybkiego rozwoju uszkodzenia (3)

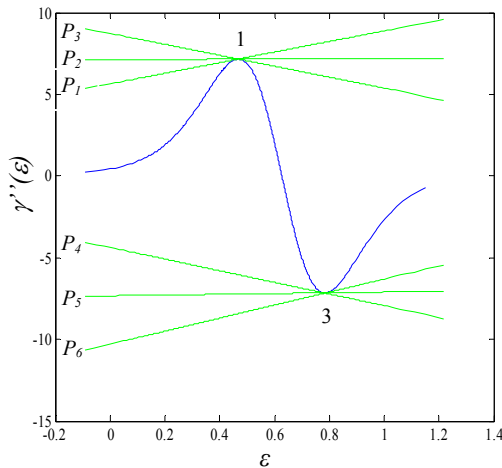
Na kolejnych wykresach (Rys. 6-8) przedstawiono wyniki transformaty Hough'a dla trzech wybranych punktów leżących na stycznych $P_1 - P_3$ do drugiej pochodnej krzywej logistycznej (każdy wykres – osobna prosta). Zgodnie z oczekiwaniem jedynie na rysunku 7 krzywe leżą

blisko siebie, a ich punkt przecięcia wypada dla kąta ok. 90° . Wyznaczenie prostych dla kąta najbliższego 90° (z wykorzystaniem płaszczyzny Hough'a) jednoznacznie definiuje punkt 1 na krzywej logistycznej. Punkt 3 krzywej logistycznej został wyznaczony analogicznie jak dla punkt 1.

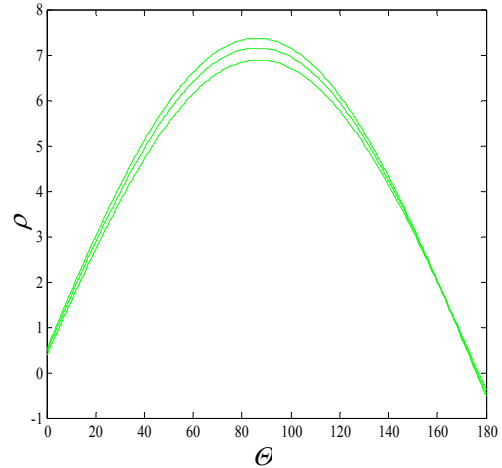


Rys. 4. Przebieg pierwszej pochodnej (funkcji błędów) funkcji logistycznej – maksimum odpowiada punktowi 2 krzywej logistycznej

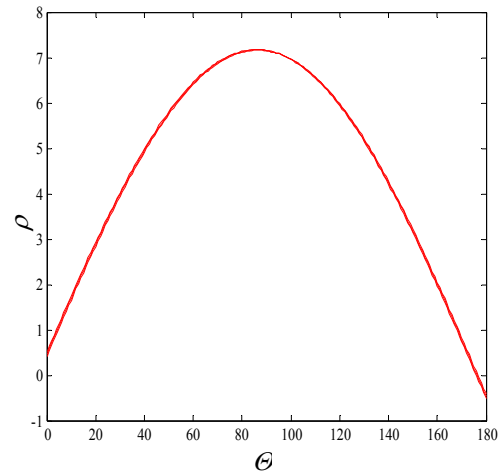
Korzystając z zależności analitycznych pomiędzy współzrzednymi w przestrzeni parametrów diagnostycznych oraz przestrzeni Hough'a [7, 11], można ustalić punkt, w którym występuje nukleacja uszkodzenia.



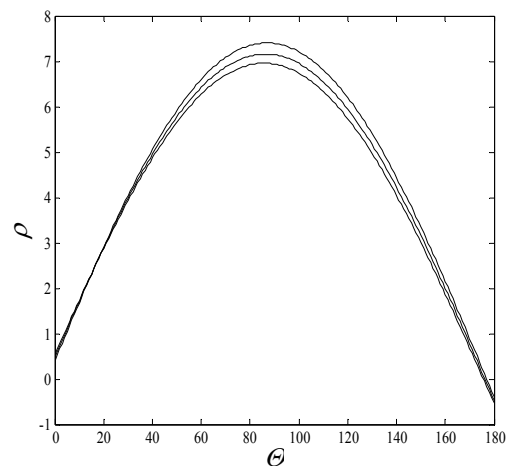
Rys. 5. Druga pochodna funkcji logistycznej – ekstrema odpowiadają punktom krzywej logistycznej: 1- (początek propagacji uszkodzenia) i 3-(koniec fazy szybkiego rozwoju uszkodzenia)



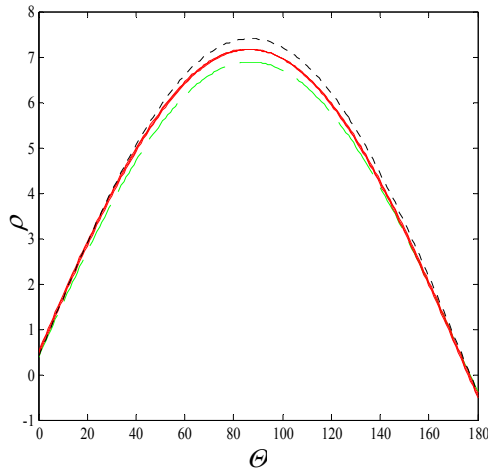
Rys. 6. Obraz trzech punktów (znajdujących się na prostej P_1 – Rys. 5) w przestrzeni Hough'a



Rys. 7. Obraz trzech punktów (znajdujących się na prostej P_2 – Rys. 5) w przestrzeni Hough'a



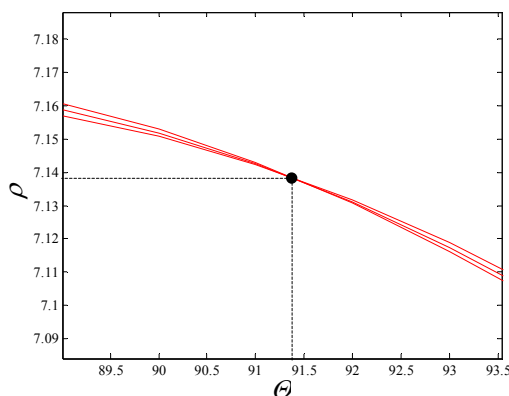
Rys. 8. Obraz trzech punktów (znajdujących się na prostej P_3 – Rys. 5) w przestrzeni Hough'a



Rys. 9. Obraz trzech punktów (znajdujących się na prostej P_2 – Rys. 5) w przestrzeni Hough'a linia ciągła i dwóch punktów nieleżących na prostej P_2

Rysunek 9 przedstawia obraz trzech punktów leżących na jednej prostej, linie przecinają się w jednym punkcie (Rys. 10). Linie: punktowa i kreskowa wyznaczają kolejne punkty przecięcia na podstawie których możemy wyznaczyć kolejne proste. Nakładając odpowiednie warunki tzn.

1. szukana prosta ma być styczna do drugiej pochodnej,
 2. szukana prosta ma być pozioma, czyli kąt Θ jest równy 90° (lub najbliższy 90°),
- wyznaczamy użyteczną w postawionym zadaniu prostą, a w konsekwencji punkty na krzywej logistycznej.



Rys. 10. Punkt przecięcia krzywych w przestrzeni Hough'a określający parametry poszukiwanej prostej

Na rysunku 7 przecięcie krzywych Hough'a wypada dla kąta bliskiego 90° . Różnica wynika z dokładności prowadzonych obliczeń, a w szczególności rozdzielczości z jaką jest wyznaczana krzywa logistyczna. Taki wynik prowadzi do wniosku, że w przypadku analizy prowadzonej na podstawie danych pomiarowych, należy on-line obrabiać wyniki i w czasie zbliżania

się do kluczowych punktów rozwoju uszkodzenia zageścić pomiary celem uzyskania dokładniejszych rezultatów.

5. WNIOSKI

Możliwość wykorzystania transformaty Hough'a stwarza szanse redukcji redundancji informacji diagnostycznych oraz odpowiedniej wizualizacji umożliwiającej przekazanie operatorowi tylko informacji o dużym priorytecie z punktu widzenia przyjętej strategii. Użycie transformaty Hough'a pozwala określić krytyczne punkty na krzywej logistycznej opisującej propagację pęknięcia zmęczeniowego przekładni zębatej.

Dostępność procedur w popularnym środowisku jakim jest MATLAB, ułatwia proces implementacji tego typu modułu decyzyjnego w autonomicznych układach diagnostyczno – prognostycznych.

LITERATURA

- [1] Arutyunyan R. A.: *The Problem of Deformation Aging and Prolonged Fracture in Material Science*, S.-Petersburg University Press, Sankt-Petersburg, 2004.
- [2] Dybała J.: *Wykrywanie wczesnych faz uszkodzeń metodami sztucznej inteligencji*, Wydawnictwo Naukowe Instytutu Technologii Eksploatacji, Warszawa-Radom, ISBN 978-83-7204-757-1, 2008.
- [3] Helgason S.: *Radon Transform*, MIT Cambridge, 1999.
- [4] Jasiński M., Radkowski S.: *Zastosowanie składowych głównych w diagnozowaniu maszyn*, Diagnostyka, Vol. 30; tom 1, 2004, str. 207-210.
- [5] Kovalenko J. N., Kuznestov N. Y., Pegg P. A., *Mathematical Theory of Reliability of Time Dependent Systems with Practical Applications*, John Willey & Sons, Nowy Jork, 1997.
- [6] Mączak J.: *Local meshing plane as a source of diagnostic information for monitoring the evolution of gear faults*, in: D. Kiritsis, C. Emmanouilidis, A. Koronios, J. Mathew (Eds.), *Engineering Asset Lifecycle Management*, Springer London, 2010. pp. 661-670.
- [7] Pawłowski M.: *Zastosowanie transformacji Hough'a do analizy dwuwymiarowych widm pits*, Materiały Elektroniczne, T-34, N3/4, 2006, str. 19-39.
- [8] Radkowski S.: *Wibroakustyczna diagnostyka uszkodzeń niskoenergetycznych*, ITE Warszawa – Radom, 2002.
- [9] Radkowski S., Gumiński R.: *Spectrum Width Factor as a Diagnostic Parameter Determining the Degree of Damage of Tooth Surface*, Diagnostyka 1(53)/2010, pp 55-60.
- [10] Radkowski S., Szczurowski K.: *Use of vibroacoustic signals for diagnosis of*

prestressed structures. Eksploatacja i Niezawodność – Maintenance and Reliability, Vol. 14, No. 1, 2012, pp. 84-91.

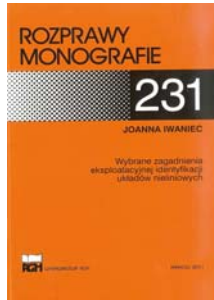
- [11] Żorski W., (2000): *Metody segmentacji obrazów oparte na transformacie Hougha*. Instytut Automatyki i Robotyki, Wydział Cybernetyki, WAT, Warszawa.



Prof. **Stanisław RADKOWSKI**, profesor Instytutu Pojazdów PW, kierownik zespołu Diagnostyki Technicznej i Analizy Ryzyka. W pracy naukowej zajmuje się diagnostyką wibroakustyczną i analizą ryzyka technicznego



Dr inż. **Robert GUMIŃSKI**, zatrudniony na stanowisku adiunkta w Instytucie Pojazdów Politechniki Warszawskiej. Zainteresowania naukowe – bezpieczeństwo systemów technicznych, ryzyko techniczne.



Joanna IWANIEC

**Wybrane zagadnienia
eksploatacyjnej identyfikacji
układów nieliniowych**

Głównym celem przeprowadzonych i zaprezentowanych w rozprawie prac badawczych była synteza metody identyfikacji modeli nieliniowych konstrukcji mechanicznych, dedykowanej do zastosowania w czasie normalnej eksploatacji obiektu.

Na podstawie przeprowadzonych badań eksperymentalnych i literaturowych stwierdzono, że ze względu na silne założenia, dotyczące znajomości wymuszenia działającego na układ oraz liniowego zachowania układu w otoczeniu punktu pracy, znacząca większość klasycznych metod identyfikacji nie może być stosowana w celu operacyjnej identyfikacji układów nieliniowych. W badaniach własności układów mechanicznych pracujących pod wpływem obciążeń eksploatacyjnych bezpośredni pomiar sił wymuszających drgania jest trudny lub niemożliwy do przeprowadzenia. Problem ten dotyczy także obiektów o bardzo dużej masie lub sztywności, których zapotrzebowanie na energię przy wzbudzeniu ruchu jest zbyt duże aby można było ją doprowadzić dysponując klasycznym sprzętem do badań dynamiki strukturalnej. Znane z literatury i stosowane w praktyce metody identyfikacji oparte o niemiernie w czasie eksperymentu wymuszenia eksploatacyjne znajdują zastosowanie jedynie w badaniach dynamiki układów liniowych. Z tego względu, przeprowadzone przez autorkę badania miały na celu dokonanie syntezy metody identyfikacji modeli nieliniowych układów mechanicznych, realizowanej podczas ich normalnej eksploatacji.

Opracowana i przedstawiona w pracy metoda operacyjnej identyfikacji układów nieliniowych polega na sekwencyjnym zastosowaniu metod sił resztkowych, zaburzeń brzegowych oraz bezpośredniej identyfikacji parametrów. Metoda nie wymaga znajomości wymuszenia działającego na układ, a ponadto, jak wykazano w pracy, może być również stosowana do celów operacyjnej identyfikacji układów liniowych. Dodatkową zaletą jest możliwość zastosowania tej samej procedury badawczej zarówno do detekcji nieliniowości jak i estymacji parametrów badanego układu. Przeprowadzone przez autorkę badania dowiodły, że metoda może być z powodzeniem stosowana dla szerokiej klasy liniowych i nieliniowych układów mechanicznych.

Zaproponowana metoda została zaimplementowana w powszechnie stosowanym środowisku programowym MATLAB, a następnie zweryfikowana na podstawie danych uzyskanych metodą symulacji odpowiedzi dynamicznej modelu konstrukcji o własnościach nieliniowych oraz danych zmierzonych na stanowiskach badawczych. Zweryfikowana metoda została zastosowana do

identyfikacji modeli rzeczywistych układów mechanicznych – układu zawieszenia samolotu oraz wybranych elementów mostu stalowego. Dokładność uzyskiwanych rezultatów w zależności od metodyki przeprowadzania eksperymentu identyfikacyjnego oraz dokładności pomiaru charakterystyk dynamicznych badanego układu oszacowano z zastosowaniem metody analizy wrażliwości.



Krzysztof MENDROK

**Inverse Problem in Structural
Health Monitoring**

Monografia "Inverse Problem in Structural Health Monitoring" składa się z dziewięciu rozdziałów.

Pierwsze rozdziały zawierają uzasadnienie podjęcia tematu, podstawowe informacje o zagadnieniu odwrotnym i układach SHM. Zdefiniowano dwa typy zagadnienia odwrotnego oraz sposoby ich rozwiązywania i regularyzacji. Dalej zawarto podstawowe informacje dotyczące układów SHM, a więc pojęcia i definicje z zakresu tej nowej dziedziny wiedzy, różnice pomiędzy układami SHM a klasyczną diagnostyką maszyn wirnikowych oraz technikami badań NDT. Pokazano też ogólną strukturę układów SHM oraz ich podstawowe zadania jak również sklasyfikowano układy SHM biorąc pod uwagę różne kryteria oceny. Kolejne dwa rozdziały zawierają przegląd literatury światowej w zakresie algorytmów wykrywania, lokalizacji i identyfikacji uszkodzeń stosowanych w układach SHM oraz identyfikacji wymuszeń na podstawie pomiaru sygnałów odpowiedzi. Skupiono się przede wszystkim na metodach opartych o niskoczęstotliwościowe sygnały drganiowe. Rozdział siódmy prezentuje wybrane prace autora w obszarze algorytmów detekcji uszkodzeń. Główną część rozdziału stanowi opis autorskiej metody wykrywania i lokalizacji uszkodzeń opartej o filtrację modalną. Pokazano tutaj kolejno: zastosowanie filtracji modalnej do wykrywania uszkodzeń, rozszerzenie algorytmu o ich lokalizację, modyfikację metody dla potrzeb maszyn wirnikowych i wreszcie zastosowanie adaptacyjnego filtra modalnego do monitoringu zaladzenia łopat morskich elektrowni wiatrowych.

Ósmy rozdział to także prezentacja badań autora z zakresu zastosowania zagadnienia odwrotnego, tym razem do identyfikacji wymuszeń działających na obiekty. Należą tutaj prace poświęcone identyfikacji wymuszeń działających w czasie lotu na elementy samolotu oraz problem identyfikacji sił kontaktu koło – szyna. A także identyfikacja nierówności torów kolejowych.

Ostatni rozdział niniejszej monografii, rozdział dziewiąty, stanowi jej podsumowanie w postaci zebranych najistotniejszych problemów tutaj poruszanych.

**Lista recenzentów artykułów opublikowanych
w czasopiśmie Diagnostyka w 2012 roku**

- prof. dr hab. inż. Jan ADAMCZYK
dr hab. inż. Tomasz BARSZCZ
prof. dr hab. inż. Walter BARTELMUS
prof. dr hab. inż. Wojciech BATKO
prof. dr hab. inż. Adam CHARCHALIS
prof. dr hab. inż. Wojciech CHOLEWA
prof. dr hab. inż. Zbigniew DĄBROWSKI
dr hab. inż. Jacek DYBAŁA
prof. dr hab. inż. Janusz GARDULSKI
prof. dr hab. inż. Jerzy GIRTLER
dr hab. inż. Andrzej GRZĄDZIELA, prof. AMW
dr inż. Robert GUMIŃSKI
dr inż. Marcin JASIŃSKI
prof. dr hab. inż. Jan KICIŃSKI
prof. dr hab. inż. Yewhen KCHARCHENKO
dr inż. Tomasz KORBIEL
dr hab. inż. Piotr KRZYWORZEKA, prof. AGH
prof. dr hab. inż. Henryk MADEJ
dr inż. Jędrzej MAĆZAK
prof. dr hab. inż. Stanisław NIZIŃSKI
dr hab. inż. Andrzej PIĘTAK, prof. UWM
prof. dr hab. inż. Stanisław RADKOWSKI
dr inż. Krzysztof SZCZUROWSKI
prof. dr hab. inż. Wiesław TRĄMPCZYŃSKI
prof. dr hab. inż. Tadeusz UHL
dr inż. Jacek URBANEK
dr inż. Mirosław WITOŚ
prof. dr hab. inż. Andrzej WILK
dr hab. inż. Radosław ZIMROZ
prof. dr hab. inż. Bogdan ŻÓLTOWSKI

Obszar zainteresowania czasopisma to:

- ogólna teoria diagnostyki technicznej
- eksperymentalne badania diagnostyczne procesów i obiektów technicznych;
- modele analityczne, symptomowe, symulacyjne obiektów technicznych;
- algorytmy, metody i urządzenia diagnozowania, prognozowania i genezowania stanów obiektów technicznych;
- metody detekcji, lokalizacji i identyfikacji uszkodzeń obiektów technicznych;
- sztuczna inteligencja w diagnostyce: sieci neuronowe, systemy rozmyte, algorytmy genetyczne, systemy ekspertowe;
- diagnostyka energetyczna systemów technicznych;
- diagnostyka systemów mechatronicznych i antropotechnicznych;
- diagnostyka procesów przemysłowych;
- diagnostyczne systemy utrzymania ruchu maszyn;
- ekonomiczne aspekty zastosowania diagnostyki technicznej;
- analiza i przetwarzanie sygnałów.

Topics discussed in the journal:

- General theory of the technical diagnostics,
- Experimental diagnostic research of processes, objects and systems,
- Analytical, symptom and simulation models of technical objects,
- Algorithms, methods and devices for diagnosing, prognosis and genesis of condition of technical objects,
- Methods for detection, localization and identification of damages of technical objects,
- Artificial intelligence in diagnostics, neural nets, fuzzy systems, genetic algorithms, expert systems,
- Power energy diagnostics of technical systems,
- Diagnostics of mechatronic and antropotechnic systems,
- Diagnostics of industrial processes,
- Diagnostic systems of machine maintenance,
- Economic aspects of technical diagnostics,
- Analysis and signal processing.

Wszystkie opublikowane artykuły uzyskały pozytywne recenzje wykonane przez niezależnych recenzentów.

All the published papers were reviewed positively by the independent reviewers.

Redaktorzy działówi:

dr hab. inż. Tomasz BARSZCZ
prof. dr hab. inż. Wojciech CHOLEWA
prof. dr hab. Wojciech MOCZULSKI
prof. dr hab. inż. Stanisław RADKOWSKI
prof. dr hab. inż. Wiesław TRAMPCZYŃSKI
prof. dr hab. inż. Tadeusz UHL

Kopia wszystkich artykułów opublikowanych w tym numerze dostępna jest na stronie www.diagnostyka.net.pl

Druk:

Centrum Graficzne „GRYF”, ul. Pieniężnego 13/2, 10-003 Olsztyn, tel. / fax: 89-527-24-30

Oprawa:

Zakład Poligraficzny, UWM Olsztyn, ul. Heweliusza 3, 10-724 Olsztyn
tel. 89-523-45-06, fax: 89-523-47-37

Cena 25 zł (w tym 5% VAT)



Międzynarodowy Kongres Diagnostyki Technicznej
03 – 05 Wrzesień 2012
pod honorowym patronatem JM Rektora Akademii Górniczo – Hutniczej
w Krakowie
prof. Antoniego Tajdusia

W imieniu Polskiego Towarzystwa Diagnostyki Technicznej i swoim własnym mam zaszczyt zaprosić Państwa do udziału w 5 Międzynarodowym Kongresie Diagnostyki Technicznej, który odbędzie się w Krakowie w Centrum Dydaktyki Akademii Górniczo – Hutniczej. Celem Kongresu jest prezentacja osiągnięć naukowych zespołów badawczych krajowych i zagranicznych pracujących w obszarze szeroko rozumianej problematyki diagnostyki obiektów technicznych. Kongres stanowi okazję do integracji środowisk naukowych, nawiązania współpracy z ośrodkami krajowymi i zagranicznymi oraz z firmami wykorzystującymi metody diagnostyki technicznej. Nowością organizowanego kongresu będzie prezentacja „na żywo” systemów diagnostyki na specjalnie zorganizowanej sesji oraz spotkania z firmami wykorzystującymi diagnostykę w eksploatacji swoich konstrukcji i urządzeń technicznych. Tematyka kongresu obejmuje zagadnienia teoretyczne, badania eksperymentalne oraz rozwiązania praktyczne systemów diagnostycznych oraz zagadnienia zastosowania tych systemów w praktyce eksploatacyjnej dla różnego rodzaju obiektów począwszy od konstrukcji budowlanych, poprzez instalacje przemysłowe i maszyny, a skończywszy na konstrukcjach lotniczych i kosmicznych. Kongresowi towarzyszyć będzie wystawa sprzętu i oprogramowania, które mają zastosowanie w rozwiązywaniu problemów naukowych i praktycznych w zakresie diagnostyki technicznej. Patronat naukowy nad konferencją objęły: Komitet Budowy Maszyn Polskiej Akademii Nauk, Akademia Górniczo – Hutnicza w Krakowie, Polskie Towarzystwo Diagnostyki Technicznej.

Prezes Polskiego Towarzystwa Diagnostyki Technicznej
Tadeusz Uhl

Więcej informacji na stronie internetowej; www.kdt2012.pl (aktywna od 15 grudnia 2011)

Wszystkie opublikowane w czasopiśmie artykuły uzyskały pozytywne recenzje, wykonane przez niezależnych recenzentów.

Redakcja zastrzega sobie prawo korekty nadesłanych artykułów.

Kolejność umieszczenia prac w czasopiśmie zależy od terminu ich nadesłania i otrzymania ostatecznej, pozytywnej recenzji.

Wytyczne do publikowania w DIAGNOSTYCE można znaleźć na stronie internetowej:

<http://www.diagnostyka.net.pl>

Redakcja informuje, że istnieje możliwość zamieszczania w DIAGNOSTYCE ogłoszeń i reklam.

Jednocześnie prosimy czytelników o nadsyłanie uwag i propozycji dotyczących formy i treści naszego czasopisma.

Zachęcamy również wszystkich do czynnego udziału w jego kształtowaniu poprzez nadsyłanie własnych opracowań związanych z problematyką diagnostyki technicznej. Zwracamy się z prośbą o nadsyłanie informacji o wydanych własnych pracach nt. diagnostyki technicznej oraz innych pracach wartych przeczytania, dostępnych zarówno w kraju jak i zagranicą.